REPORT DOCUMENTATION PAGE

Form Approved OMB NO. 0704-0188

1. REPORT DATE (DD-MM-YYYY)	2. REPORT TYPE	3. DATES COVERED (From - To)
15-04-2015	Ph.D. Dissertation	-

4. TITLE AND SUBTITLE

Dynamic modulation of sensory cortex by top-down spatial attention

5a. CONTRACT NUMBER
W911NF-08-1-0148

5b. GRANT NUMBER

5c. PROGRAM ELEMENT NUMBER
611103

6. AUTHORS
Samuel Thorpe

5d. PROJECT NUMBER

5e. TASK NUMBER

5f. WORK UNIT NUMBER

7. PERFORMING ORGANIZATION NAMES AND ADDRESSES
University of California - Irvine
5171 California Avenue, Suite 150

Irvine, CA 92697 -7600

8. PERFORMING ORGANIZATION REPORT NUMBER

9. SPONSORING/MONITORING AGENCY NAME(S) AND ADDRESS (ES)

U.S. Army Research Office
P.O. Box 12211
Research Triangle Park, NC 27709-2211

10. SPONSOR/MONITOR'S ACRONYM(S)
ARO

11. SPONSOR/MONITOR'S REPORT NUMBER(S)
54228-LS-MUR.49

12. DISTRIBUTION AVAILIBILITY STATEMENT

Approved for public release; distribution is unlimited.

13. SUPPLEMENTARY NOTES

The views, opinions and/or findings contained in this report are those of the author(s) and should not contrued as an official Department of the Army position, policy or decision, unless so designated by other documentation.

14. ABSTRACT

The concept of attention provides a compelling bridge between the descriptions of higher cognitive processes at the mental and neural levels. We are all intuitively aware of the state of attending- it's psychological quality and associated behavioral benefits, yet only in recent decades has the neural basis for these benefits begun to be studied. The studies presented here use EEG and MEG to identify patterns of neural activity related to the deployment of attention in extrapersonal space, and examine the temporal dynamics of these signals as they evolve in response to attentional cues. In our first experiment, we use cued attention to auditory stimuli with similar spectral features to

15. SUBJECT TERMS

EEG attention vision lateralization audition

16. SECURITY CLASSIFICATION OF:			17. LIMITATION OF ABSTRACT	15. NUMBER OF PAGES	19a. NAME OF RESPONSIBLE PERSON
a. REPORT	b. ABSTRACT	c. THIS PAGE			Thomas D'Zmura
UU	UU	UU	UU		19b. TELEPHONE NUMBER 949-824-4055

Report Title

Dynamic modulation of sensory cortex by top-down spatial attention

ABSTRACT

The concept of attention provides a compelling bridge between the descriptions of higher cognitive processes at the mental and neural levels. We are all intuitively aware of the state of attending- it's psychological quality and associated behavioral benefits, yet only in recent decades has the neural basis for these benefits begun to be studied. The studies presented here use EEG and MEG to identify patterns of neural activity related to the deployment of attention in extrapersonal space, and examine the temporal dynamics of these signals as they evolve in response to attentional cues. In our first experiment, we use cued attention to auditory stimuli with similar spectral features to characterize the spatio-temporal and frequency structure of attention-related EEG signals. In a second experiment we use simultaneously recorded EEG/MEG to examine the interaction of these top-down signals with neural responses evoked by attended and unattended visual stimuli, tagged using gamma-band SSVEP. Finally, we present a physiologically motivated cortical population model capable of treating these interactions, and test its predictions against the effects observed in our data. Together, these studies suggest a picture of spatial attention signals originating in distributed fronto-parietal networks which operate via modulations of endogenous low-frequency activity.

UNIVERSITY OF CALIFORNIA, IRVINE

Dynamic modulation of sensory cortex by top-down spatial attention

DISSERTATION

Submitted in partial satisfaction of the requirements for the degree of

DOCTOR OF PHILOSOPHY

in Mathematical Behavioral Science

by Samuel Thorpe

Dissertation Committee:
Professor Ramesh Srinivasan, Chair
Professor Michael D'Zmura
Professor Michael Lee

2012

TABLE OF CONTENTS

Abstract: The concept of attention provides a compelling bridge between the descriptions of higher cognitive processes at the mental and neural levels. We are all intuitively aware of the state of attending- it's psychological quality and associated behavioral benefits, yet only in recent decades has the neural basis for these benefits begun to be studied. The studies presented here use EEG and MEG to identify patterns of neural activity related to the deployment of attention in extrapersonal space, and examine the temporal dynamics of these signals as they evolve in response to attentional cues. In our first experiment, we use cued attention to auditory stimuli with similar spectral features to characterize the spatio-temporal and frequency structure of attention-related EEG signals. In a second experiment we use simultaneously recorded EEG/MEG to examine the interaction of these top-down signals with neural responses evoked by attended and unattended visual stimuli, tagged using gamma-band SSVEP. Finally, we present a physiologically motivated cortical population model capable of treating these interactions, and test its predictions against the effects observed in our data. Together, these studies suggest a picture of spatial attention signals originating in distributed fronto-parietal networks which operate via modulations of endogenous low-frequency activity.

Chapter 1. Introduction

Much of the appeal in studying attention lies in its unique position as an aspect of higher cognition, seemingly under voluntary control, which has a direct, and substantial impact on the way we experience events in the external world. We are all familiar with the ways in which our attentive state dictates our sensory experiences. From missing a salient point in a lecture due to not "paying" attention, to the daily routine of directed search for one's keys, wallet and cell phone, the "top-down" psychological quality of attention is palpable, as its focus seems to be directed from within us. A bit of reflection on this notion alerts us to the fact that this is not always the case, however, as when our attentional resources are hijacked by overhearing one's name, or catching the unexpected glimpse of a familiar face. Nonetheless, attention is also top-down in a second, neuro-anatomical sense. That is, attention is thought to result as a consequence of feedback projections— from areas at the top of an information processing hierarchy, back down to areas at the bottom, which process mainly sensory data. Posner & Peterson (1990) refer to three different but interrelated components of attention which encompass the examples mentioned above. They refer to these as *orienting* (towards relevant sensory stimuli), *detecting* (signals or stimuli for conscious processing), and *alerting* (maintenance of an alert or vigilant state). Of these, the concept of orienting has an implicit relation to spatial reasoning, as we must necessarily orient towards a location in space. It is this notion of orienting, in both overt and covert fashions (discussed further below), which is commonly referred to by the general term "spatial attention".

1.1 Motor origins of covert spatial attention. Spatial attentional orientation is most commonly deployed overtly, that is, shifts in the focus of attention are accompanied by physical movements which allow us to process attended information as efficiently as possible. In the context of visual studies this usually means foveation of (making an eye movement directed towards) an attended visual stimulus (Posner 1988). In real world examples, foveation of an attended stimulus often necessarily requires the coordination of eye movement saccades with associated head and body movements. Although it is true that such head, eye, and body orientation are the clearest indicators of attentional orientation, human and monkey observers are demonstrably capable of attention to regions of space other than those to which the head and eyes are directly fixated. My personal favorite example of this phenomenon, referred to as *covert* attention (Desimone and Duncan 1995; Egeth and Yantis 1997; Kastner and Ungerleider 2000), comes from Moore et al. (2003), who point out that, for many social primate groups, direct eye contact is often interpreted as a sign of aggression. As a result, subdominant animals have need to monitor other animals for potential threats, while actively avoiding meeting their direct gaze.

While covertly attending to stimuli in such a manner, humans and monkeys are afforded similar behavioral advantages as during overt attention, i.e. increased accuracy at low threshold target detection (Shaw & Shaw 1977), and decreased reaction times (Eriksen & Hoffman 1972). Moreover, covertly attended stimuli also give rise to enhanced evoked responses in human EEG studies (Mangun & Hillyard, 1987; Hillyard and Anllo-Vento 1998). Evidence suggests that the effects of covert spatial attention extend to multiple sensory modalities including vision, somato-sensation, and audition

(Spence et al. 2000; Spence and Driver 1996). Studies involving covert attention provide an important experimental paradigm for a very simple reason—they afford us the opportunity to study the neural correlates of attention independently from those of the orienting movements which would naturally accompany them when attention is overt.

Mechanisms which selectively monitor environmental stimuli are essential to guide body, head and eye movements. Likewise, mechanisms which guide these movements would appear well situated to communicate top-down enhancement signals to sensory cortices which monitor stimuli at these locations. This reciprocal relationship between attention and movement orientation is supported by many experimental studies and theoretical models which suggest that motor programming plays a strong role in the top-down guidance of attention (Rizzolatti et al. 1987, Moore et al. 2003, Sheliga et al. 2004). Specifically, the *premotor theory* of attention put forth by Rizzolatti and colleagues contends that spatial attention operates via facilitation of neurons organized in "spatial pragmatic maps", and that such facilitation depends on preparations to perform goal-directed movements. Compelling evidence for this idea comes from monkey studies in which microstimulation currents were delivered to the cortical Frontal Eye Fields (FEF). At fixed thresholds, such stimulation will, with stable probability, evoke saccades to identifiable locations in visual space. Below threshold, these microstimulations do not evoke saccades, but Moore and colleagues (2003) showed that such subthreshold stimulation *does* increase the monkey's ability to detect visual targets. Importantly, the gains afforded target detection by microstimulation were specific to the location in space to which suprathreshold stimulations evoke saccades. Thus it would seem that by

directly manipulating the probability of an eye movement to a known location, these experimenters induced attentional gains at those same locations.

Further support for this link between spatial attention and motor programming is offered by fMRI studies which have identified a specific network of brain areas which become activated in response to both covert attentional shifts as well as the planning and execution of delayed eye movements (Corbetta et al. 1998, Gitelman et al. 1999). Specifically, these include the Frontal Eye Fields (FEF), and areas in the Intra Parietal sulcus (IPS). Corbetta et al. (2002) concluded that bilateral FEF and IPS form one of two fronto-parietal networks which together accomplish attentional tasks. This “dorsal”, or “goal-oriented” network becomes active in response to attentional cueing, and is thought to be responsible for the deployment and maintenance of attentional orientation in space. In particular, the frontal eye fields (FEF), located at the junction of the pre-central sulcus and the superior frontal sulcus, are thought to be involved in preparation of exploratory eye movements, whereas areas along the intraparietal sulcus (IPS) have been hypothesized to provide various sensorimotor maps of global extrapersonal space (Mesulam 1981).

1.2 Hemispheric lateralization of band-specific EEG/MEG activity as a neural correlate of top-down spatial attention.

Several studies have tried to extract information about a subject's attentional orientation in space from single EEG/MEG trials using this proposed link between attention and motor programming (Wolpaw et al. 2003; Wolpaw and McFarland 2004; Fabiani et al. 2004). Wang and Makeig (2009) achieved roughly 80% success in

distinguishing two directions on single trials in a delayed motor task, using independent components analysis (ICA) of event-related potentials (ERP) over lateralized posterior parietal scalp areas. Attempts to classify the location of attentional orientation using occipital-parietal alpha-rhythms have also met with success in MEG studies using visual stimuli (van Gerven and Jensen 2009; Bahramisharif et al. 2010). The Wadsworth EEG-based Brain-computer Interface (BCI) developed by Wolpaw and colleagues utilizes sensorimotor mu (10-16 Hz) and beta (16-25 Hz)- rhythms which subjects typically modulate using motor imagery. Moreover, Wolpaw and MacFarland (2004) successfully taught subjects to manipulate these rhythms, using a lateralization index for channels situated over sensorimotor cortex, to control the horizontal movement of a cursor on a screen. These studies demonstrate that motor programming related signals lateralize over symmetric scalp areas according to the direction of intended motor activity, with greater power over motor and parietal areas ipsilateral to the direction of intended movement. Moreover, the fact that this lateralization occurs over symmetric scalp areas which are consistent with the bilateral attention/motor-programming network described above suggest the intriguing possibility that signals related to spatial attention, which may also have motor origins, might lateralize similarly according to the direction of attentional orientation.

Worden and colleagues (2000) provided evidence for precisely this type of hemispheric lateralization of attention-related EEG activity, suggesting that occipital-parietal alpha-rhythms (8 – 12 Hz) may serve as an index of attentional orientation in visual tasks. Analogous to the motor studies mentioned above, these studies have shown an enhancement of ipsilateral parietal alpha-power when attention is selectively cued to

one side of visual space (Worden et al. 2000; Kelly et al. 2006; Rihs et al. 2007). Interestingly, additional studies using similar cueing paradigms have reported complimentary decreases over contralateral areas (Sauseng et al. 2005; Thut et al. 2006; Yamagishi et al. 2005). Both signals- contralateral decreases in alpha, as well as ipsilateral increases- have been proposed as candidate mechanisms for effecting modulations of sensory cortical responses. In the case of contralateral alpha, these signals are thought to reflect desynchronizations which enhance cortical excitability, and thus the effective response to a sensory stimulus. In contrast, the ipsilateral signals have been argued to suppress the response to unattended visual stimuli, thereby biasing against them in the competition for neural resources. The specific roles of these signals, if any, in facilitating effects of attention remains an open question, one which our second experiment addresses explicitly. Additionally, we have conducted a related study (described in detail in chapter 1) designed to investigate whether hemispheric lateralization of spatial attention-related EEG signals extends to other frequency bands outside of alpha, such as the mu and beta bands implicated in the motor and attention studies referenced above.

1.3 Interaction of top-down spatial attention signals with the sensory cortical response to attended/unattended stimuli.

In recent years, gamma-band (20 – 90 Hz) signals in EEG, EcoG, and animal LFP studies have been identified as a signature of information processing in human and animal visual systems (Basar 1999, Tallon-Baudry 1997, Eckhorn et al 1988). These gamma-band rhythms have generated widespread interest due to the hypothesis that they

reflect the binding of disparate aspects of a visual scene, processed independently within proximate neural populations, into coherent unified percepts (Singer 1993, 1995). In addition, computational models of local neural networks (those in which interactions between connected neurons occur with negligible delay) suggest that such networks characteristically oscillate at higher frequencies, above 20 Hz , and as such gamma-band activity may reflect natural resonance frequencies of sensory cortical populations. (Bush & Sejnowski, 1996; Lumer et al., 1997; Whittington & Traub 2003; Traub et al., 2005; Izhikevich 2003; Izhikevich 2006).

Attention is thought to modulate temporal firing patterns in these populations in a top-down manner, via signals originating outside of sensory cortex (Engel et al. 2001). Examples include Von Stein et al (2000), who made simultaneous recording of primary visual cortex and parietal visual areas in cats performing a visuomotor task, and observed that synchrony between these areas at lower frequencies in the theta and alpha range (4–12 Hz) depended strongly on task expectancy conditions. That notion that spatial attention effects the patterning of gamma-band activity is further supported by studies which have shown that spatial attention increases gamma-band synchrony in neural populations processing visual (Fries et al. 2001), auditory (Tiitinen et al. 1993), and somatosensory (Bauer et al. 2006) target stimuli. In the EEG literature, Müller at al. (2000), and Gruber et al. (1999) have demonstrated that attention to a visual stimulus results in increased levels of induced gamma-band power over occipito-parietal electrodes. Fries et al. (2001) showed that increased gamma-band synchrony in local populations processing an attended visual stimulus was accompanied by a complementary decrease in low frequency (<17 Hz) synchrony in these same

populations, in both pre- and post-stimulus intervals. This finding lead the authors to conclude that low frequency desynchronization might act to enhance post-synaptic efficacy of stimulus-related gamma-band oscillations.

The proposal that low-frequency desynchronization facilitates processing of behaviorally relevant stimuli has an interesting parallel in the EEG literature. As alluded to above, numerous studies have shown that the deployment of spatial attention to the left/right side of visual space results in a lateralization of alpha-band EEG power over occipito-parietal scalp areas (Worden et al. 2000; Kelly et al. 2006; Rihs et al. 2007). In these studies alpha-band power was seen to be enhanced over the hemisphere ipsilateral to the attended hemifield. but other related MEG/EEG studies using similar cueing paradigms report primarily alpha desynchronization over contralateral parietal sites (Sauseng et al. 2005; Thut et al. 2006; Yamagishi et al. 2005). In the studies in which ipsilateral increases were observed, authors have been lead to propose these parieto-occipital alpha rhythms as a candidate mechanism for suppressing unattended visual information. Where contralateral decreases have been reported, authors have tended to interpret this as evidence for the increased excitability of these areas- an interpretation consistent with the results from the animal literature cited above. Thus the state of affairs is such that, on one hand, observed *decreases* in low-frequency synchronization have been proposed to *enhance* the visual response to an attended stimulus. On the other, observed *increases* in low-frequency power have been proposed to *suppress* visual information which is to be ignored in unattended regions. These findings underline the importance of gaining a functional understanding of the causal relationship, if any, between low-frequency signals modulated by attention, and high frequency activity

evoked by a sensory stimulus. Our experiment number 2 has been designed to address such issues, and our conclusions about the relative timing of these attention-related signals are directly relevant to this open question.

Goals and outline of the research program. The goal of this research is to characterize the structure of spatial attention signals measurable in human EEG/MEG, and gain an understanding of the dynamical interaction of these signals with local neural populations in sensory cortex, which presumably have resonant frequencies in the gamma-band. To this end we have conducted a pair of attention experiments using spatial cueing. In the first, we cued attention to auditory stimuli with similar spectral features, but which originated at spatially distinct locations, to characterize the spatio-temporal and frequency structure of attention-related EEG signals. In a second experiment we examine the interaction of these top-down signals with gamma-band neural responses evoked by attended and unattended visual stimuli. For these purposes we used simultaneously recorded EEG/MEG to measure neural responses tagged using gamma-band SSVEP. Finally, we test the predictions of a physiologically motivated cortical population model capable of treating these interactions against the effects observed in our data. Our results provide evidence that top-down spatial attention signals arise in distributed fronto-parietal networks, which operate via modulation of endogenous band-specific low-frequency activity. Moreover, these attention-related modulations of endogenous rhythms display patterns of lateralization consistent with a role for these signals in motor programming. Finally, we identify the mechanism by which these networks effect attentional gains of sensory cortical responses as the active desynchronization of

endogenous alpha and mu-band activity within populations processing the attended stimulus.

References

Bahramisharif, A., van Gerven, M., Heskes, T., & Jensen, O. (2010). Covert attention allows for continuous control of brain-computer interfaces. *The European journal of neuroscience*, *31*(8), 1501-8. doi:10.1111/j.1460-9568.2010.07174.x

Basar, E., Basar-Eroglu, C., Karakas, S., & Schürmann, M. (1999). Oscillatory brain theory: a new trend in neuroscience. *IEEE engineering in medicine and biology magazine : the quarterly magazine of the Engineering in Medicine & Biology Society*, *18*(3), 56-66. Retrieved from http://www.ncbi.nlm.nih.gov/pubmed/10337564

Bauer, M., Oostenveld, R., Peeters, M., & Fries, P. (2006). Tactile spatial attention enhances gamma-band activity in somatosensory cortex and reduces low-frequency activity in parieto-occipital areas. *The Journal of neuroscience : the official journal of the Society for Neuroscience*, *26*(2), 490-501. doi:10.1523/JNEUROSCI.5228-04.2006

Bush, P., & Sejnowski, T. (1996). Inhibition synchronizes sparsely connected cortical neurons within and between columns in realistic network models. *Journal of computational neuroscience*, *3*(2), 91-110. Retrieved from http://www.ncbi.nlm.nih.gov/pubmed/8840227

Corbetta, M, Akbudak, E., Conturo, T. E., Snyder, a Z., Ollinger, J. M., Drury, H. a, Linenweber, M. R., et al. (1998). A common network of functional areas for attention and eye movements. *Neuron*, *21*(4), 761-73. Retrieved from http://www.ncbi.nlm.nih.gov/pubmed/9808463

Corbetta, Maurizio, & Shulman, G. L. (2002). Control of goal-directed and stimulus-driven attention in the brain. *Nature reviews. Neuroscience*, *3*(3), 201-15. doi:10.1038/nrn755

Desimone, R., & Duncan, J. (1995). Neural mechanisms of selective visual attention. *Annual review of neuroscience*, *18*, 193-222. Annual Reviews 4139 El Camino Way, P.O. Box 10139, Palo Alto, CA 94303-0139, USA. doi:10.1146/annurev.ne.18.030195.001205

Eckhorn, R., Bauer, R., Jordan, W., Brosch, M., Kruse, W., Munk, M., & Reitboeck, H. J. (1988). Coherent oscillations: A mechanism of feature linking in the visual cortex? *Biological Cybernetics*, *60*(2), 121-130. doi:10.1007/BF00202899

Egeth, H. E., & Yantis, S. (1997). Visual attention: control, representation, and time course. *Annual review of psychology*, *48*, 269-97. doi:10.1146/annurev.psych.48.1.269

Engel, a K., Fries, P., & Singer, W. (2001). Dynamic predictions: oscillations and synchrony in top-down processing. *Nature reviews. Neuroscience*, *2*(10), 704-16. doi:10.1038/35094565

Eriksen, C. W., & Hoffman, J. E. (1972). Temporal and spatial characteristics of selective encoding from visual displays. *Perception & Psychophysics*, *12*(2), 201-204. doi:10.3758/BF03212870

Fabiani, G. E., McFarland, D. J., Wolpaw, J. R., & Pfurtscheller, G. (2004). *Conversion of EEG activity into cursor movement by a brain-computer interface (BCI). IEEE Transactions on Neural and Rehabilitation Systems Engineering* (Vol. 12, pp. 331-338). Retrieved from http://www.ncbi.nlm.nih.gov/pubmed/15473195

Fries, P. (2001). Modulation of Oscillatory Neuronal Synchronization by Selective Visual Attention. *Science*, *291*(5508), 1560-1563. doi:10.1126/science.1055465

Gitelman, D. R., Nobre, a C., Parrish, T. B., LaBar, K. S., Kim, Y. H., Meyer, J. R., & Mesulam, M. (1999). A large-scale distributed network for covert spatial attention: further anatomical delineation based on stringent behavioural and cognitive controls. *Brain : a journal of neurology*, *122 (Pt 6*, 1093-106. Retrieved from http://www.ncbi.nlm.nih.gov/pubmed/10356062

Gruber, T., Müller, M. M., Keil, a, & Elbert, T. (1999). Selective visual-spatial attention alters induced gamma band responses in the human EEG. *Clinical neurophysiology : official journal of the International Federation of Clinical Neurophysiology*, *110*(12), 2074-85. Retrieved from http://www.ncbi.nlm.nih.gov/pubmed/10616112

Hillyard, S. A, & Lourdes Anllo-Vento. (1998). Event-related brain potentials in the study of visual selective attention. *Proceedings of the National Academy of Sciences*, *95*(3), 781-787. doi:10.1073/pnas.95.3.781

Izhikevich, E. M. (2006). Polychronization: computation with spikes. *Neural computation*, *18*(2), 245-82. doi:10.1162/089976606775093882

Izhikevich, E. M., Desai, N. S., Walcott, E. C., & Hoppensteadt, F. C. (2003). Bursts as a unit of neural information: selective communication via resonance. *Trends in Neurosciences*, *26*(3), 161-167. doi:10.1016/S0166-2236(03)00034-1

Kastner, S., & Ungerleider, L. G. (2000). Mechanisms of visual attention in the human cortex. *Annual review of neuroscience*, *23*, 315-341.

Kelly, S. P., Lalor, E. C., Reilly, R. B., & Foxe, J. J. (2006). Increases in alpha oscillatory power reflect an active retinotopic mechanism for distracter suppression during sustained visuospatial attention. *Journal of neurophysiology*, *95*(6), 3844-51. doi:10.1152/jn.01234.2005

Lumer, E. D., Edelman, G. M., & Tononi, G. (1997). Neural dynamics in a model of the thalamocortical system. I. Layers, loops and the emergence of fast synchronous rhythms. *Cerebral cortex (New York, N.Y. : 1991)*, *7*(3), 207-27. Retrieved from http://www.ncbi.nlm.nih.gov/pubmed/9143442

Mangun, G. R. R., & Hillyard, S. A. (1987). The Spatial Allocation of Visual Attention as Indexed by Event-Related Brain Potentials. *Human Factors: The Journal of the*

Human Factors and Ergonomics Society, *29*(2), 195-211. doi:10.1177/001872088702900207

Mesulam, M. M. (1981). A cortical network for directed attention and unilateral neglect. *Annals of neurology*, *10*(4), 309-25. doi:10.1002/ana.410100402

Moore, T., Armstrong, K. M., & Fallah, M. (2003). Visuomotor origins of covert spatial attention. *Neuron*, *40*(4), 671-83. Retrieved from http://www.ncbi.nlm.nih.gov/pubmed/14622573

Müller, M. M., Gruber, T., & Keil, a. (2000). Modulation of induced gamma band activity in the human EEG by attention and visual information processing. *International journal of psychophysiology : official journal of the International Organization of Psychophysiology*, *38*(3), 283-99. Retrieved from http://www.ncbi.nlm.nih.gov/pubmed/11102668

Posner, M. I., & Petersen, S. E. (1990). The attention system of the human brain. *Annual review of neuroscience*, *13*, 25-42.

Posner, M., Petersen, S., Fox, P., & Raichle, M. (1988). Localization of cognitive operations in the human brain. *Science*, *240*(4859), 1627-1631. doi:10.1126/science.3289116

Rihs, T. a, Michel, C. M., & Thut, G. (2007). Mechanisms of selective inhibition in visual spatial attention are indexed by alpha-band EEG synchronization. *The European journal of neuroscience*, *25*(2), 603-10. doi:10.1111/j.1460-9568.2007.05278.x

Rizzolatti, Giacomo, Riggio, L., & Sheliga, B. M. (1994). Space and selective attention. *Conscious and nonconscious information processing.Attention and performance series* (pp. 232-265).

Rizzolatti, Giacomo, Riggio, L., Dascola, I., & Umiltá, C. (1987). Reorienting attention across the horizontal and vertical meridians: Evidence in favor of a premotor theory of attention. *Neuropsychologia*, *25*(1), 31-40. doi:10.1016/0028-3932(87)90041-8

Sauseng, P., Klimesch, W., Stadler, W., Schabus, M., Doppelmayr, M., Hanslmayr, S., Gruber, W. R., et al. (2005). A shift of visual spatial attention is selectively associated with human EEG alpha activity. *The European journal of neuroscience*, *22*(11), 2917-26. doi:10.1111/j.1460-9568.2005.04482.x

Shaw, M. L., & Shaw, P. (1977). Optimal allocation of cognitive resources to spatial locations. *Journal of Experimental Psychology: Human Perception and Performance,, Vol 3*(2), 201-211.

Sheliga, B.M., Riggio, L., & Rizzolatti, G. (1994). Orienting of attention and eye movements. *Experimental Brain Research*, *98*(3). doi:10.1007/BF00233988

Singer, W. (1993). Synchronization of cortical activity and its putative role in information processing and learning. *Annual review of physiology*, *55*, 349-74. doi:10.1146/annurev.ph.55.030193.002025

Singer, W., & Gray, C. M. (1995). Visual feature integration and the temporal correlation hypothesis. *Annual review of neuroscience*, *18*, 555-86. doi:10.1146/annurev.ne.18.030195.003011

Spence, C., Pavani, F., & Driver, J. (n.d.). Crossmodal links between vision and touch in covert endogenous spatial attention.

Tallon-Baudry, C., Bertrand, O., Delpuech, C., & Pernier, J. (1997). Oscillatory gamma - Band (30-70 Hz) Activity Induced by a Visual Search Task in Humans. *J. Neurosci.*, *17*(2), 722-734. Retrieved from http://www.jneurosci.org/cgi/content/abstract/17/2/722

Thut, G., Nietzel, A., Brandt, S. a, & Pascual-Leone, A. (2006). Alpha-band electroencephalographic activity over occipital cortex indexes visuospatial attention bias and predicts visual target detection. *The Journal of neuroscience : the official journal of the Society for Neuroscience*, *26*(37), 9494-502. doi:10.1523/JNEUROSCI.0875-06.2006

Tiitinen, H., Sinkkonen, J., Reinikainen, K., Alho, K., Lavikainen, J., & Näätänen, R. (1993). Selective attention enhances the auditory 40-Hz transient response in humans. *Nature*, *364*(6432), 59-60. doi:10.1038/364059a0

Traub, Roger D, Bibbig, A., LeBeau, F. E. N., Cunningham, M. O., & Whittington, M. A. (2005). Persistent gamma oscillations in superficial layers of rat auditory neocortex: experiment and model. *The Journal of physiology*, *562*(Pt 1), 3-8. doi:10.1113/jphysiol.2004.074641

Wang, Y., & Makeig, S. (2009). Predicting Intended Movement Direction Using EEG from Human Posterior Parietal Cortex, 437-446.

Whittington, M. a, Traub, R. D., Kopell, N., Ermentrout, B., & Buhl, E. H. (2000). Inhibition-based rhythms: experimental and mathematical observations on network dynamics. *International journal of psychophysiology : official journal of the International Organization of Psychophysiology*, *38*(3), 315-36. Retrieved from http://www.ncbi.nlm.nih.gov/pubmed/11102670

Whittington, M. A., & Traub, R. D. (2003). Interneuron Diversity series: Inhibitory interneurons and network oscillations in vitro. *Trends in Neurosciences*, *26*(12), 676-682. doi:10.1016/j.tins.2003.09.016

Wolpaw, J. R., & McFarland, D. J. (2004). Control of a two-dimensional movement signal by a noninvasive brain-computer interface in humans. *Proceedings of the National Academy of Sciences of the United States of America*, *101*(51), 17849-54. doi:10.1073/pnas.0403504101

Wolpaw, J. R., McFarland, D. J., Vaughan, T. M., & Schalk, G. (2003). The Wadsworth Center brain-computer interface (BCI) research and development program. *IEEE transactions on neural systems and rehabilitation engineering : a publication of the IEEE Engineering in Medicine and Biology Society*, *11*(2), 204-7. doi:10.1109/TNSRE.2003.814442

Worden, M. S., Foxe, J. J., Wang, N., & Simpson, G. V. (2000). Anticipatory biasing of visuospatial attention indexed by retinotopically specific alpha-band

electroencephalography increases over occipital cortex. *The Journal of neuroscience : the official journal of the Society for Neuroscience*, *20*(6), RC63. Retrieved from http://www.ncbi.nlm.nih.gov/pubmed/10704517

Yamagishi, N., Goda, N., Callan, D. E., Anderson, S. J., & Kawato, M. (2005). Attentional shifts towards an expected visual target alter the level of alpha-band oscillatory activity in the human calcarine cortex. *Brain research. Cognitive brain research*, *25*(3), 799-809. doi:10.1016/j.cogbrainres.2005.09.006

van Gerven, M., & Jensen, O. (2009). Attention modulations of posterior alpha as a control signal for two-dimensional brain-computer interfaces. *Journal of neuroscience methods*, *179*(1), 78-84. doi:10.1016/j.jneumeth.2009.01.016

von Stein, a, Chiang, C., & König, P. (2000). Top-down processing mediated by interareal synchronization. *Proceedings of the National Academy of Sciences of the United States of America*, *97*(26), 14748-53. doi:10.1073/pnas.97.26.14748

Chapter 2. Lateralization of frequency-specific networks for covert spatial attention to auditory stimuli

Abstract: *We conducted a cued spatial attention experiment to investigate the time-frequency structure of human EEG induced by attentional orientation of an observer in external auditory space. Seven subjects participated in a task in which attention was cued to one of two spatial locations at left and right. Subjects were instructed to report the speech stimulus at the cued location and to ignore a simultaneous speech stream originating from the uncued location. EEG was recorded from the onset of the directional cue through the offset of the inter-stimulus interval (ISI), during which attention was directed toward the cued location. Using a wavelet spectrum, each frequency band was then normalized by the mean level of power observed in the early part of the cue interval to obtain a measure of induced power related to the deployment of attention. Topographies of band specific induced power during the cue and inter-stimulus intervals showed peaks over symmetric bilateral scalp areas. We used a bootstrap analysis of a lateralization measure defined for symmetric groups of channels in each band to identify specific lateralization events throughout the ISI. Our results suggest that the deployment and maintenance of spatially oriented attention throughout a period of 1100 ms is marked by distinct episodes of reliable hemispheric lateralization ipsilateral to the direction in which attention is oriented. An early theta lateralization was evident over posterior parietal electrodes and was sustained throughout the ISI. In the alpha and mu bands punctuated episodes of parietal power lateralization were observed roughly 500 ms after attentional deployment, consistent with previous studies of visual attention. In the beta band these episodes show similar patterns of lateralization over frontal motor areas. These results indicate that spatial attention involves similar mechanisms in the auditory and visual modalities.*

1. Background and Significance

Many previous EEG and fMRI studies have examined the effects of attentional orientation on the brain's response to sensory stimuli (e.g., Hillyard and Anllo-Vento 1998; Kastner et al. 1999). The primary effect observed in these studies is that larger responses are evoked by a stimulus when it is attended. Our present goal is to identify the neural events which occur when one orients attention in a single direction, even when there is no stimulus at that location. This would be the case if one were to use attentional signals to designate an *intended direction* for movement or exploration. Our focus is on

the top-down orientation of attention in a single direction or location rather than on the bottom-up orienting elicited by a salient stimulus.

The most obvious indicators of attentional orientation are head and eye orientation. Yet even when head and eyes are oriented in a fixed direction, an observer can still attend to other directions. In experimental psychology, this is referred to as covert attention (Desimone and Duncan 1995; Egeth and Yantis 1997; Kastner and Ungerleider 2000). Covert attention involves all the spatial senses including vision, somato-sensation, and audition (Spence et al. 2000; Spence and Driver 1998). Mechanisms which selectively monitor environmental stimuli are essential to guide body, head and eye movements. Moreover, mechanisms which guide these movements are likely well suited to communicate top-down enhancement signals to sensory cortices which monitor stimuli at these locations. This reciprocal relationship between attention and movement orientation is supported by many experimental studies and theoretical models which suggest that motor programming plays a strong role in the top-down guidance of attention (Moore et al. 2003; Sheliga et al. 1994).

Several recent studies have tried to extract information on intended direction from single EEG trials by using this proposed link between attentional selection and motor programming (Wolpaw et al. 2003; Wolpaw and McFarland 2004; Fabiani et al. 2004; Wang and Makeig 2009). Several methods have been used to extract this information, and the search for novel functional methods is still underway. Wang and Makeig (2009) achieved roughly 80% success in distinguishing two directions on single trials in a delayed motor task, using independent components analysis (ICA) of event-related potentials (ERP) over lateralized posterior parietal scalp areas. The Wadsworth EEG-

based Brain-computer Interface (BCI) developed by Wolpaw and colleagues utilizes sensorimotor μ and β- rhythms which subjects typically modulate using motor imagery. Moreover, Wolpaw and MacFarland (2004) successfully taught subjects to manipulate these rhythms, using a lateralization index for channels situated over sensorimotor cortex, to control the horizontal movement of a cursor on a screen.

Worden and colleagues proposed that occipital-parietal alpha rhythms may serve as an index of attentional orientation in visual tasks (Worden et al. 2000). These studies have shown a lateralization of parietal alpha rhythms when attention is selectively cued to one side of visual space, with alpha power enhanced over posterior sites ipsilateral to the cued hemifield relative to contralateral sites (Worden et al. 2000; Thut et al. 2006; Rihs et al. 2007). Attempts to classify the location of attentional orientation using occipital-parietal alpha rhythms have also met with success in MEG studies using visual stimuli (van Gerven and Jensen 2009; Bahramisharif et al. 2010). The question remains as to whether these principles extend to spatial attention in general, i.e. to what degree the networks which give rise to these lateralized rhythms are engaged during attentional selection in other modalities.

The purpose of this study is to investigate the temporal, spectral, and spatial structure of EEG while the subject orients attention toward some location in extrapersonal space. Attention in the auditory domain is particularly attractive because the auditory system can localize sources which lie outside the visual scene, including to the side of, behind, and above the observer. In the experiment described in this paper, subjects are cued verbally to anticipate a speech stimulus at one of two competing locations. An initial analysis of data from this experiment using spectral analysis of the

inter-stimulus interval showed that one may decode intended direction on single trials from top-down attentional signals (Thorpe et al 2009; Srinivasan et al 2009). This initial analysis showed that, for some subjects, sufficient information exists in EEG data to classify intended direction correctly on over 80% of trials using auditory spatial orientation. However, no simple lateralization of EEG rhythms was apparent in the spectral structure which allowed for this successful classification of single trials.

The present work provides a deeper analysis of these data. We use wavelet analysis to investigate whether attention-related modulation not obvious in a simple spectral analysis of single trials is evident in the EEG. The wavelet analysis reveals that the neural signatures of attentional orienting are organized temporally into a sequence of discrete events. These events include lateralized activity in the θ (4 - 6 Hz), α (7 - 10 Hz), μ (11 - 14 Hz), and β (16 - 28 Hz) frequency ranges. Similar rhythms have been observed in previous BCI studies (Wolpaw and McFarland 2004), as well as electrophysiological studies of attending cats (Rougel-Buser and Buser 1997; Buser and Rougel-Buser 2005). Patterns of scalp activity found in the present experiment on intended direction show band specific foci over bilateral occipital, parietal and sensorimotor areas, consistent with earlier results on classification of intended direction from motor imagery (Wolpaw and McFarland 2004; Pfurtscheller at al. 2006), and fMRI studies of attentional orientation (Corbetta and Shulman 2002; Gitelman et al. 1999). Moreover, these scalp patterns show systematic lateralization which depends on the direction of attentional orientation.

2. Materials and Methods

Procedure. Seven subjects (6 male, 0 left-handed, 6 native English speaking) participated in the experiment. Each subject sat in a dimly lit room with two speakers. The speakers were placed at a distance of one meter from the subject's head and were positioned 45 deg to the left or 45 deg to the right, respectively (see Figure 1). The subject was instructed to fixate on a point directly ahead, in the direction bisecting the directions to the speakers.

There were two experimental conditions: attend left and attend right. The subject was presented the spoken cue "Ready left" or "Ready right" at the onset of each trial through both speakers. After a variable interstimulus interval (ISI) of duration 500, 700, 900, 1100, 1300 or 1500 ms, two different sentences were presented simultaneously: one sentence per speaker. The subjects' task was to report words in the sentence from the speaker in the cued direction. This task was made difficult by adjusting the ratio of the volumes of the cued and uncued speakers. An adaptive staircase procedure, described below, was used to set speaker volumes in a way that ensured subjects' attention to the sentence from the speaker in the cued direction. Additionally, the staircase procedure ensured that subjects performed the task at similar levels of accuracy.

The sentence stimuli were all spoken by the same male voice (cepstral David; http://cepstral.com). The

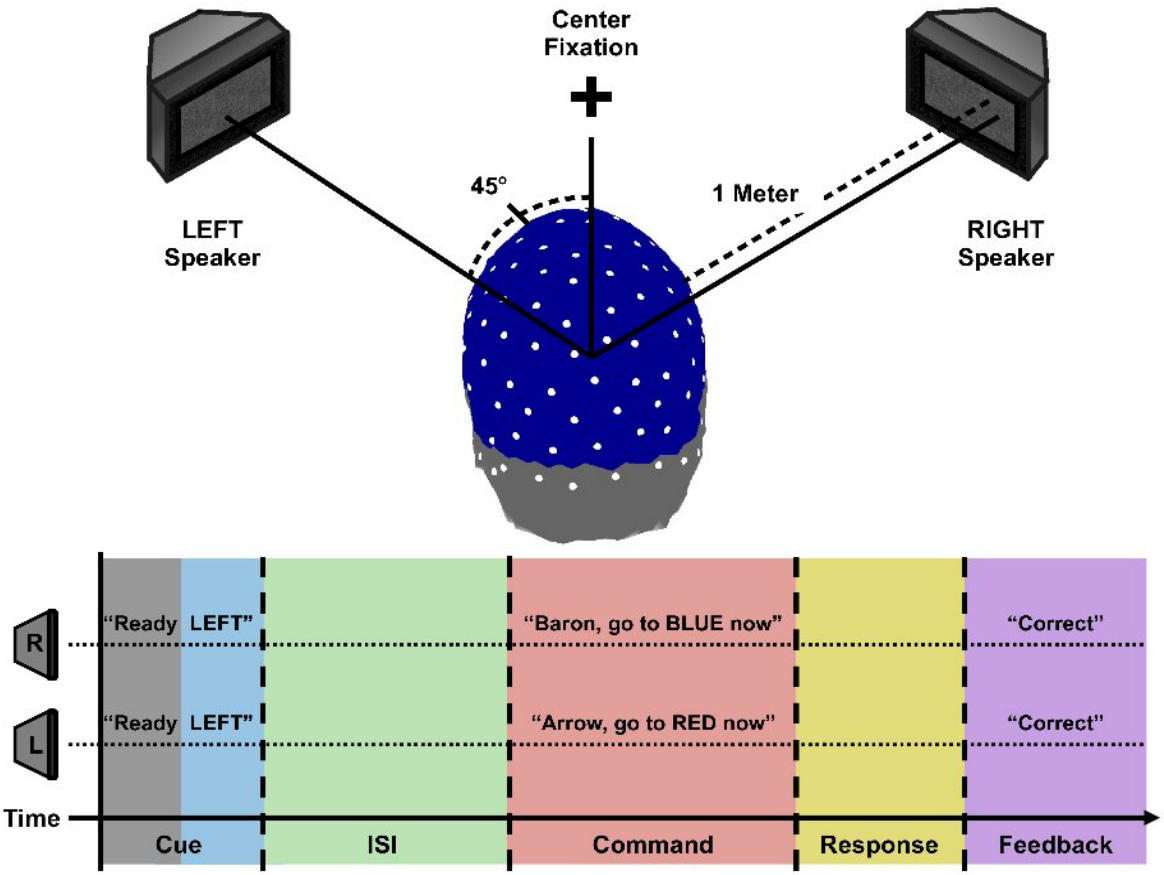

Fig. 1. The experimental setup. (a) The physical layout of the experiment. Note that each speaker was 45 degrees away from fixation and could not be seen by observer without moving the eyes. (b) The time course of each trial in the experiment. In the example shown the subject is cued to attend to the left speaker (indicted in blue/gray). Data from the interval in which the word "Ready" was played (indicated in gray) was used to normalize wavelet spectra for each trial. After a variable ISI (500-1500 ms, shown in green), two distinct sentences are played through each speaker (interval shown in red); the subject's task is to indicate the codeword and color played from the cued speaker (response interval shown in yellow). In the example shown, the subject responds "Arrow" and "Red", and received feedback indicating a correct response (feedback interval indicated in purple).

sentences were based on a simplified version of sentences drawn from the Coordinate Response Measure corpus (Moore 1981). The sentences have the structure "[callsign] go to [color] now", where possible callsign words included Arrow, Baron, Eagle and Tiger and possible color words included Blue, Green, Red, or White. The subjects' task was to identify the callsign and color words in the sentence played through the speaker in the cued direction; responses were made using a keyboard. A subject's response to a trial

was judged correct if the subject indicated the callsign correctly. Choosing the response to the initial callsign word as the performance measure helped ensure that the subject directed attention to the cued speaker before the speech stimulus was played. Otherwise, the subject would miss the first word in the sentence: the callsign. The variable ISI ensured that the observer quickly deployed and maintained attention to the cued speaker at left or at right.

An adaptive staircase procedure was used to control subject performance. When the subject responded correctly to the callsign word, the volume was reduced by 5% (-0.45 dB) on the cued speaker and increased by 5% (+0.42 dB) on the uncued speaker on the next trial. When the subject responded incorrectly to the callsign word, the volume was increased by 10% (+0.83 dB) on the attended speaker and decreased by 10% (-0.92 dB) on the unattended speaker. With this procedure, subjects identified the cued callsign word correctly about 70% of the time. The amplitude of the speaker in the cued direction was typically 14 dB below that in the uncued direction. A single experimental session comprised 200 trials, presented in two 100 trial blocks with a break between. Each subject participated in three such sessions, each lasting around one hour, for a total 600 trials per subject.

EEG recording. EEG was recorded using a 128-channel Geodesic Sensor Net (Electrical Geodesics, Inc.) in combination with an amplifier and acquisition software (Advanced Neuro Technology, Inc.). The EEG was sampled at 1024 Hz and on-line average referenced. Artifact editing was performed through a combination of automatic editing using an amplitude threshold and manual editing to check the results. Trials with excessive bad channels (>15%) were first discarded; channels with excessive bad trials

were then discarded. Across subjects this yielded around 100 common usable EEG channels (out of 128), and for each subject roughly 550 usable trials (out of 600).

Normalized Wavelet Analysis. EEG data were low pass filtered (50 Hz) and down sampled from 1024 to 192 samples per second. A complex Morlet wavelet transform with frequencies centered on 4, 5, 6, 7, 8, 9, 10, 11, 12, 14, 16, 18, 20, 24, 28, 32, 36, 40 and 48 Hz was then applied to the data. This provided a time-frequency spectrum for each of 128 channels on each trial. The time-frequency spectra started at the onset of the trials' cue interval and terminated at the offset of the ISI.

In order to examine changes in the wavelet time-frequency spectra associated specifically with the onset of cued attention, the wavelet spectra for each channel of each trial were normalized by a frequency-dependent baseline power level. We used as baseline the mean wavelet power in a given frequency band over a 250 ms interval which began at the onset of the cue period. We chose this interval because it coincided with the time in which the subject heard the word “Ready”, but before the cued direction was announced, thus the normalization interval contained no information concerning attentional orientation. Moreover, the interval length of 250 ms allowed us to include a full cycle of the lowest frequency included in our analysis (4 Hz).

In order to allow a sufficient amount of time for the temporal structure of attention to unfold while still retaining a single common pool of trials for group averaging/bootstrapping, we ignored data from trials with ISI duration less than 1100 ms, thus retaining approximately 50% of the data for each subject. Data from each attention condition was then pooled across six of our seven subjects. Due to anomalies explained in the results section below, we excluded our non-native English speaker from the group

analysis. The remaining trials were aligned from the onset of the cue interval to the end of the common 1100 ms ISI and averaged across attention condition to obtain the induced time-frequency power spectrum ($P_C(f,t)$) for each channel (C) for left correct and right correct trials respectively.

Band Specific Lateralization Index. We proceeded to analyze our data with respect to five frequency bands of interest. These were the theta (θ : 4 – 6 Hz), alpha (α : 7 – 10 Hz), mu (μ : 11 – 14 Hz), beta (β : 16 - 28), and gamma (γ : 32 – 48 Hz) bands. For each of the five frequency bands (B) a measure of induced band power was computed for each channel by averaging induced power for each condition over each frequency within the respective band. Scalp topographies were then computed for each band by averaging induced band power spectra over each time point of the cue and inter-stimulus intervals. In each band the resultant topographies showed clear maxima of power in pairs of bilateral channel groups which were approximately symmetric over left and right scalp hemispheres. The number and precise location on the scalp of these paired symmetric groups was band specific, but symmetric groups over left and right hemispheres (LG, RG) were always chosen to have the same number of channels. For each channel group pair in each frequency band, we defined a lateralization index ($LI(t)$) as the ratio of induced band power averaged over the left group and induced band power averaged over the right group:

1. $$LI(t) = 20\log_{10}\left[\frac{\sum_{C\in LG}\sum_{f\in B} P_C(f,t)}{\sum_{C\in RG}\sum_{f\in B} P_C(f,t)}\right]$$

Bootstrap distributions. Empirical lateralization index bootstrap distributions were computed in order to test the null hypothesis that the lateralization index for each channel

group was constant throughout the cue interval and ISI regardless of attention condition. For each time point in the interval from the beginning of the directional cue to 1100 ms into the ISI (312 total time samples) a bootstrap sample was obtained by sampling with replacement from all trials taken from all six subjects included in our group analysis. For each bootstrap sample the lateralization index was then calculated as described above. This process was repeated 500 times for each time-point/channel-group to create lateralization index distributions with 500 elements. These distributions were then pooled across time points, and a 95% confidence interval was computed by taking the values in the resultant distribution which corresponded to the 2.5^{th} and 97.5^{th} percentiles. For each attention condition, time points for which the actual lateralization index was less than the 2.5^{th} percentile or greater than the 97.5^{th} of the empirical distribution were deemed significant (two-tailed $p<0.05$, see Efron and Tibshirani 1993). In order to account for the problem of multiple comparisons we performed a post-hoc analysis of the number of significant time-points obtained for each lateralization index. If the null hypothesis holds, then the lateralization indices at each time point still have a 5% chance of attaining significance. If we assume that these false positives are binomially distributed with an underlying probability of 5%, this allows us to compute the probability of observing a given number of significant samples (N) using a binomial distribution B(312,0.05). Thus the probability that an effect consisting of N or more false positives are observed for a given condition is given by:

2. $$1-\sum_{i=1}^{N-1}\binom{312}{i}0.05^{i}\left(1-0.05\right)^{312-i}$$

We also applied this test to the entire set of statistical tests to determine the probability of the number of significant effects observed across all frequency bands and

channel groups. Taken together, we performed a total of 4368 total tests. For three frequency bands we had a single channel group, each with two attention conditions which tested 312 time points; for the remaining two frequency bands we had two channel groups each with two attention conditions testing 312 time points – [3 x 2 x 312] + [2 x 2 x 2 x 312] = 4368. Thus we tested the null hypothesis that all significant effects observed throughout the experiment were due to chance using a binomial distribution B(4368,0.05).

3. Results

Behavioral Results. The staircase procedure used to set sentence volume from the speakers at left and right resulted in a remarkably consistent level of performance across most subjects, with accuracy hovering around 69 percent correct for the reported callsign (68.7%, 68.4%, 69.5%, 69.2%, 68.9% and 68.8% for subjects S1, S3, S4, S5, S6 and S7, respectively). Subjects were generally less accurate (mean 48.4%) and showed greater variability (standard deviation 9.8%) in performance for color words, suggesting that sustaining attention in one direction in the presence of a loud competing stimulus from the other direction was difficult. For these subjects, we observed in each session a consistent volume ratio (decibel difference) between cued and uncued speakers of around -13.87 dB (with an average across sessions of -12.40, -16.52, -18.55, -14.69, -9.33, and -11.76 dB for subjects S1, S3, S4, S5, S6 and S7, respectively). The one exception to this was our nonnative English speaker S2, who was less accurate (61.8% for callsigns, 27.7% for colors) and who stabilized at a dB offset of +26.88, indicating a substantial increase in required signal relative to distracter volume required for correct identification

of the cued callsign word. For these reasons we chose to exclude S2's data from the subsequent group analysis. On average, subjects performed similarly across all ISI conditions, which suggests that the shortest ISI duration, 500 ms, provides a sufficient window in which to orient attention fully. No obvious behavioral benefit, assessed by cued callsign word identification, was gained by letting the subject maintain attention over longer intervals.

Band Specific Time-Frequency Structure. Figure 2 shows the time-frequency structure of induced power in each band found by averaging data from all subjects across channels. Induced power time-frequency spectra for each attention condition were found by averaging across left correct (LC, Fig. 2a) and right correct (RC, Fig. 2b) trials respectively. The interval from -770 to zero ms corresponds to the cue interval in which the subjects were given the attention instruction ("Ready Left/Right"). The subset of this interval from -770 to -520 is the interval over which the mean wavelet power for each frequency band was normalized on each trial. This interval was chosen because it corresponds to the time at which the subject heard the word "Ready", but before the announcement of the cued direction. Log induced power values during this interval are very near zero due to the fact that the mean of this interval was used as the normalization baseline. Solid gray lines indicate the offset of the normalization interval, and the onset of the interval in which the cued direction was announced. Thus the normalization interval contains no directional information. In both attention conditions the cue evoked a large response primarily in the theta, alpha, and mu frequency bands which lasted roughly 100 ms into the ISI. Solid black lines at zero ms indicate the offset of the cue interval and the onset of the ISI. Induced power in the alpha and mu bands increases

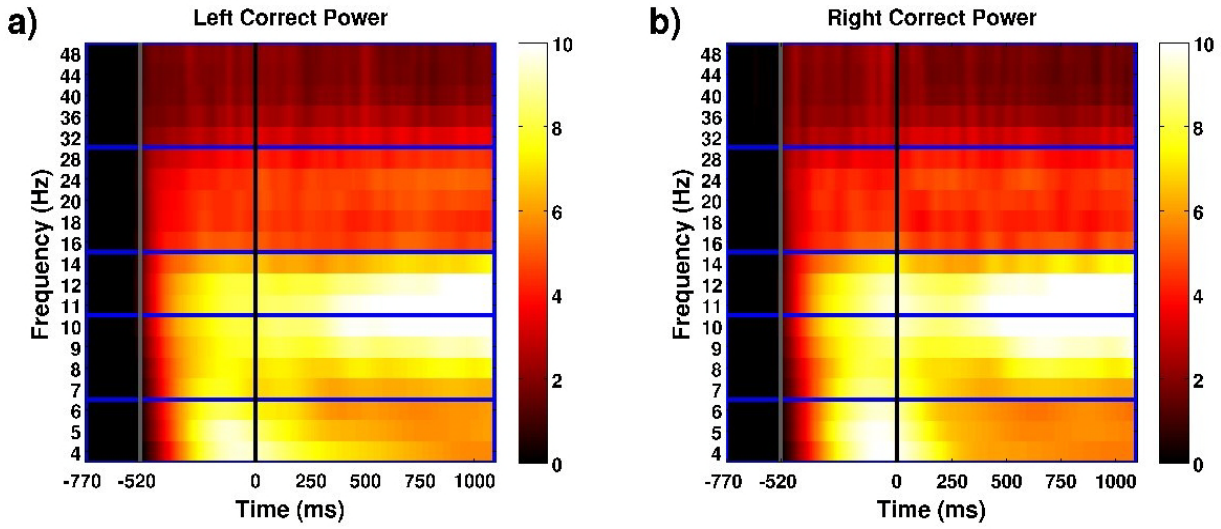

Fig 2. Induced power time-frequency spectra are shown in decibel units for left correct (a) and right correct (b) trials respectively. Horizontal blue lines indicate the partitioning of the 5 frequency bands: θ (4 - 6 Hz), α (7 - 10 Hz), μ (11 - 14 Hz), and β (16 - 28 Hz), and γ (32 - 48 Hz). The interval from -770 to zero ms corresponds to the cue interval in which the subjects were given the attention instruction ("Ready Left/Right"). The subset of this interval from -770 to -520 (corresponding to the word "Ready") is the interval over which the mean wavelet power for each frequency band was normalized on each trial. Solid gray lines indicate the offset of the normalization interval, and the onset of the interval in which the cued direction ("Left" or "Right") was announced. Solid black lines at zero ms indicate the offset of the cue interval and the onset of the ISI. Induced power in the alpha and mu bands increases markedly in both attentional conditions around 300 ms after the onset of the ISI and rises steadily until the ISI offset at 1100 ms.

markedly in both attentional conditions around 300 ms after the onset of the ISI and rises steadily until the ISI offset at 1100 ms.

Band specific lateralization within attentional conditions. Figures 3 - 8 depict the temporal development of topographic lateralization patterns for LC and RC trials throughout the cue and inter-stimulus intervals for the various frequency bands. Topographies for each band were computed by averaging LC and RC induced band power spectra over all time points in the cue and inter-stimulus intervals. Both LC (Figs. 3-8, a) and RC (Figs. 3-8, b) topographies in each band show clear bilateral foci in channel groups situated over approximately symmetrical scalp areas in the left and right hemispheres. These channel groups are indicated by pink and blue dots on the left and

right hemispheres respectively. In the alpha and mu bands additional magenta and cyan dots indicate a second pair of groupings over parietal areas. Lateralization indices for each attention condition are shown as a function of time for each of the various band specific channel groups (Figs. 3-8, c; Figs. 4d, 5d). For each channel group, green dashed lines represent the upper and lower bounds of lateralization index values which could be expected to occur given the null hypothesis that the lateralization index is constant throughout the cue and inter-stimulus intervals regardless of the direction of attentional orientation.

In order to address the problem of multiple comparisons across frequency bands and channel groupings we tested the hypothesis that all of the significant effects we observed throughout the entire experiment were due to chance. As described above in methods, we performed a total of 4368 total tests . Of these tests a total of 309 came out significant. Assuming again that false positives are binomially distributed, the probability that these 309 significances were attained by chance is vanishingly small (p<10e-8).

Development of topographic lateralization in the α – band. Figure 3 shows induced alpha band power averaged over the cue and ISI intervals for LC (Fig. 3a) and RC (Fig. 3b) attention conditions respectively. Two groups of approximately symmetric channels appear as maxima in the resultant topographies. The first of these, situated over motor areas (C3/C4 in the 10/20 system), are indicated in the left hemisphere by pink dots and in the right by blue. The temporal structure of the lateralization index for this pair of groups is shown in figure 3c for both LC (pink) and RC (blue) attention conditions. The lateralization index in this band shows an early negativity during the cue interval for both directions that persists throughout the initial part of the ISI. This suggests that in both

conditions, less alpha band power was induced over the left hemisphere by the initial cue. However, at no point throughout the entirety of the cue or ISI intervals does the lateralization index for this group reach significant levels for either attention condition.

The second pair of channel groups apparent in this band lie over bilateral parietal areas which are indicated by magenta and cyan dots over the left and right hemispheres respectively. Figure 3d shows the temporal development of lateralization within this group for both attention conditions. Throughout the cue and initial part of the ISI, parietal lateralization for both conditions hovers near the expected mean obtained from our bootstrap. However, around 400 ms into the ISI a divergence is evident between the direction of lateralization for each condition. At around 400 ms a sharp increase in lateralization index begins for Left Correct trials, reaching significance at around 700 ms, before falling back toward the mean again towards the end of the ISI. Lateralization for Right Correct trials show an opposite pattern, nearly reaching significant negative values at around 650 ms, then showing a distinct significant negative peak at the end of the ISI around 1000 ms. While the number of significant samples observed for LC trials (19, p = 0.15) cannot be ruled out as chance, the complimentary effect observed for RC trials (30 time samples, p<0.01) cannot reasonably be attributed to chance. Between these two conditions it is evident that induced alpha band power clearly lateralizes over parietal areas. The direction of the observed lateralization corresponds to greater power over the hemisphere ipsilateral to the direction of attentional orientation. This result is in agreement with previous studies which have shown that alpha band power induced by spatial attention to visual stimuli lateralizes over posterior parietal areas with the same relation to the direction of orientation (Worden et al. 2000; Thut et al. 2006; Rihs et al.

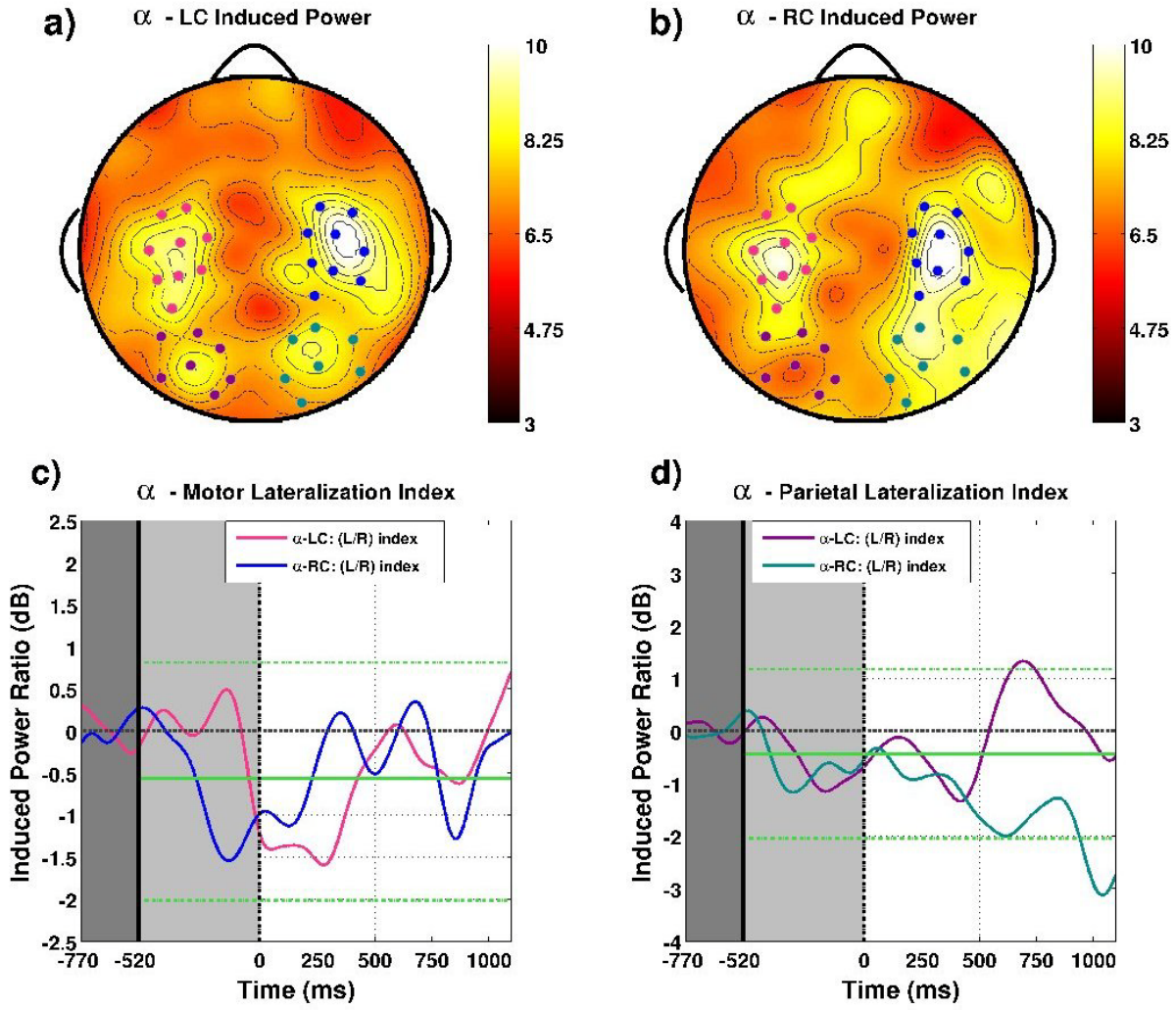

Fig 3. Induced alpha band power is shown averaged over the cue and ISI intervals for LC (a) and RC (b) attention conditions respectively. Two pairs of symmetric channel groups appear as peaks in the resultant band power topographies. These are situated over bilateral motor (indicated by pink/blue dots for left/right respectively), and parietal areas (indicated by magenta/cyan dots for left/right respectively). Lateralization indices for both attention conditions are shown as functions of time for the motor and parietal groups in (c) and (d) respectively. Parietal lateralization (d) for both conditions hovers near the expected mean obtained from our bootstrap (indicated by solid green lines). Around 400 ms into the ISI a divergence is evident in the direction of lateralization for each condition, indicating greater induced power over the channel group ipsilateral to attentional orientation, with positive values for LC trials and negative values for RC trials both reaching bootstrap significant levels (indicated by dashed green lines).

2007). Moreover, the 400 ms interval we observed between cue offset and the onset of our alpha band effect matches the 400 ms observed by Rihs and colleagues and is in the range of the 500 ms observed by Worden and colleagues as well.

Development of topographic lateralization in the μ – band. Figure 4 shows induced band power by attention condition for the mu band (11-14 Hz) averaged over the cue and inter-stimulus intervals. Similar to the alpha band, topographies for LC (Fig. 4a) and RC (Fig. 4b) trials in this band also showed two pairs of symmetric channel groups over bilateral motor and parietal areas. Lateralization indices for the μ - motor group are shown in figure 4c. We observed no significant lateralization for these channels throughout the cue and inter-stimulus intervals. However, we did find significant parietal lateralization (Fig. 4d) with temporal structure for both attention conditions similar to that observed in the alpha band. For LC trials a positive peak reaches significance around 600 ms into the ISI (22 time samples, $p<0.05$). The lateralization index then falls back to the mean before returning to near significant positive levels towards the end of the ISI. This pattern is mirrored by complimentary negative peaks for RC trials, the larger of which reaches significance at the end of the ISI around 1000 ms (although at only 12 significant samples the effect size cannot be ruled out as chance).

Taken together the mu and alpha bands tell similar stories. Directing attention towards a cued speaker results in increased power over parietal areas ipsilateral to the cued direction. For both bands the patterns of lateralization are much the same throughout the cue interval and first few hundred milliseconds of the ISI. However, a marked divergence between attentional conditions occurs beginning around 400 ms into the ISI. For the mu band this divergence takes the form of two distinct episodes of lateralization which occur roughly 400-500 ms apart and have opposite sign for each attention condition.

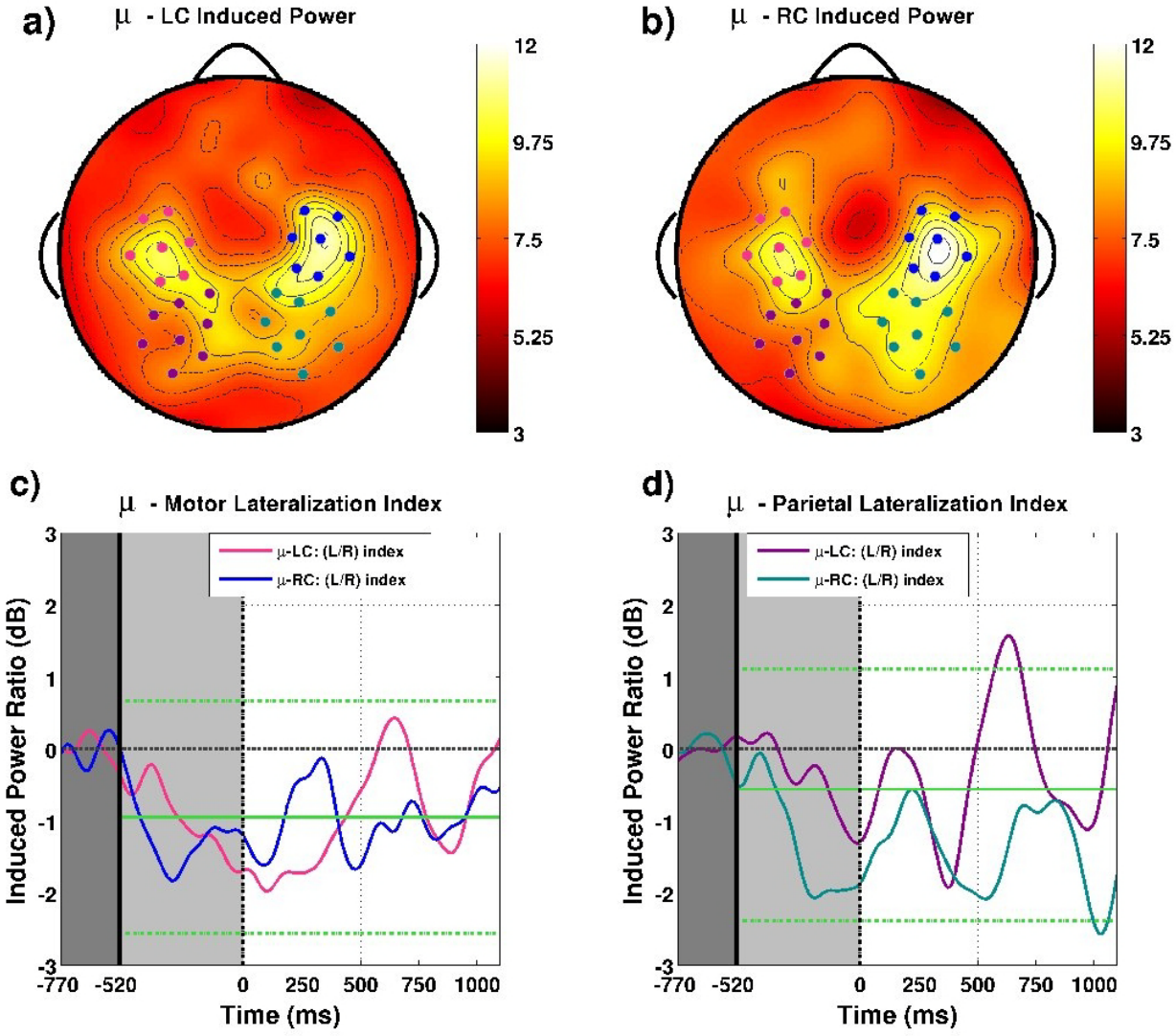

Fig 4. Induced band power by attention condition for the mu band (11-14 Hz) averaged over the cue and inter-stimulus intervals. Similar to the alpha band, topographies for LC (a) and RC (b) show pwo pairs of symmetric channel groups over bilateral motor (pink/blue for left/right) and parietal areas (magenta/cyan for left/right). Lateralization indices for the μ - motor group (c) show no significant lateralization throughout the cue and inter-stimulus intervals. However, parietal lateralization (d) within this band does reach significance and displays temporal structure for both attention conditions similar to that observed in the alpha band. Divergence between attentional conditions occurs around 400 ms into the ISI in the form of two distinct episodes of lateralization which occur roughly 400-500 ms apart and have opposite sign for each attention condition.

Development of topographic lateralization in the β – band. Induced beta band power for both LC and RC trials throughout the cue and ISI show a single pair of bilateral foci over motor areas (Fig. 5a,b). For both attention conditions, significant negative

lateralizations were observed during the cue interval (Fig. 5c). This trend was also present in the time courses for alpha and mu lateralization as well, but did not reach significance in those bands. This result is consistent with multiple interpretations. First is the possibility that directional information presented during the cue interval is associated with left hemisphere motor desynchronization regardless of the cued direction. This could be due to the inherent hemispheric asymmetry of the cortex with regards to speech processing during the cue interval (Alho et al. 1998; Poeppel 2003). Another interpretation would be that directional information present in the cue results in synchronization of beta activity over right hemisphere motor areas regardless of the cued direction, perhaps reflecting a right hemisphere cortical asymmetry associated with spatial orienting in global extrapersonal space (Fink et al. 1996; Martinez et al. 1997; Arrington et al. 2000).

Around 500 ms into the ISI the lateralization indices for attentional conditions within the β - motor group begin to diverge (Fig. 5c). For LC trials the index shows a brief significant positive peak (27 significant samples, $p<0.01$) just before 750 ms then returns to near zero towards the end of the ISI. For RC trials a significant negative peak is observed around 600 ms, after which the lateralization index stays negative throughout the remainder of the ISI, reaching significance again around 750 and 1050 ms (the total number significant samples in these three peaks is 42, $p<<0.01$). The direction of this lateralization event is the same as that observed in the alpha and mu bands, with greater induced power over areas ipsilateral to the direction of attentional deployment. This result is similar to that obtained by Wolpaw and MacFarland in the mu band, where

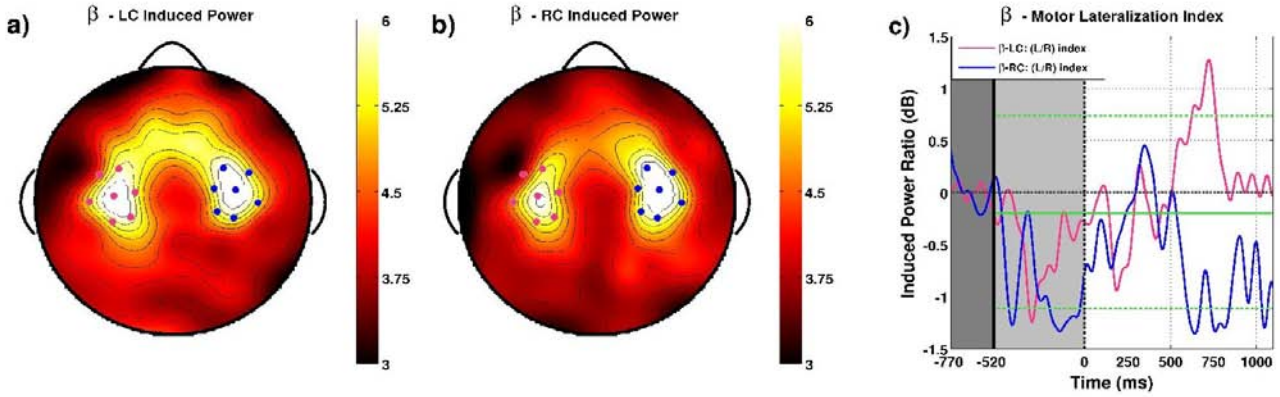

Fig 5. Induced beta band power for both LC (a) and RC (b) trials averaged over the cue and inter-stimulus intervals show a single pair of bilateral foci over motor areas (pink/blue for left/right). Significant negative lateralizations were observed during the cue interval for both attention conditions, possibly reflecting hemispheric asymmetries involved in speech processing or spatial orientation. Around 500 ms into the ISI the lateralization indices for attentional conditions within the β - motor group begin to diverge (c). The direction of this lateralization event is the same as that observed in the alpha and mu bands, with greater induced power over areas ipsilateral to the direction of attentional deployment.

subjects learned to make use of mu rhythms originating from similar motor areas which lateralized with the same relationship toward intended direction.

Development of topographic lateralization in the θ – band. Induced theta band power topographies reveal a pair of channel groups situated over posterior parietal areas. For left correct (LC) trials one finds a clear peak over a group of left posterior parietal areas (Fig. 6a), while for right correct (RC) trials a similar group of left hemisphere channels is accompanied by an approximately symmetrical group over the right hemisphere (Fig. 6b). The time course of the lateralization index for these groups differs from that found for previous groups in two specific ways. First, the lateralization indices do not show a general trend toward negativity for both attention conditions during the cue interval. If the negative trend observed during the cue interval for previous bands are indeed associated with specific hemispheric asymmetries, then this suggests that theta band EEG is functionally distinct from activity in these other bands. Second, the temporal

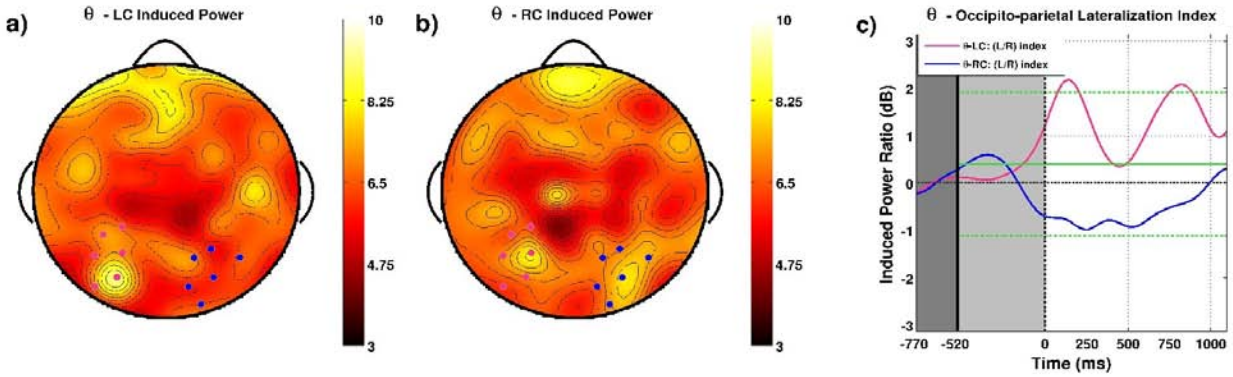

Fig 6. Induced theta band power topographies for left correct trials (a) show a clear peak over a group of left posterior parietal areas (indicated in pink), while for right correct trials (b) a similar group of left hemisphere channels is accompanied by a group over the right hemisphere (indicated in blue). The lateralization indices in this band show early and sustained divergence, having opposite sign for LC and RC trails for nearly the entire ISI (c). Although the negative values observed for RC trials (shown in blue) fail to reach significance, positive peaks observed for LC trials attain significance in two distinct episodes. The first of these occurs around 100-200 ms and precedes all lateralization events in other bands.

development of lateralization in this band shows early and sustained divergence. Lateralization indices for LC and RC trials are of opposite sign for nearly the entire ISI. Although the negative values observed for RC trials (shown in blue) fail to reach significance, this is not the case for the positive peaks observed for LC trials, which attain significance in two distinct episodes. The first of these occurs early in the ISI around 100-200 ms (25 significant samples, $p<0.01$), at a time when lateralization had yet to develop in any other band; the second occurring just after 750 ms (27 significant samples, $p<0.01$).

Development of topographic lateralization in the γ – band. The lowest levels of induced power that we observed were in the gamma band, which were typically less than 3 dB as opposed to between 6 and 13 dB for other bands. Yet induced power in this band shows bilateral peaks over frontal areas that were unique with regard to all other bands (Fig. 7 a,b), being situated over more anterior areas than the motor peaks observed in the alpha, mu, and beta bands. However, the lateralization indices for these groups show

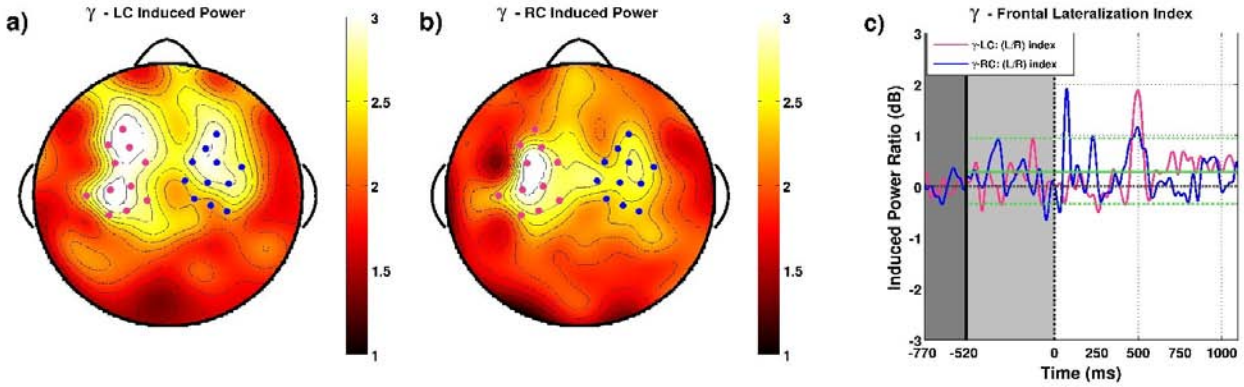

Fig 7. Induced power averaged over the cue and inter-stimulus intervals in the gamma band peaked at less than 3 dB as opposed to between 6 and 13 dB for other bands. Induced power in this band does show bilateral peaks for both LC (a) and RC (b) trials over frontal areas that were unique relative to all other bands. However, the lateralization indices for these groups show little systematic evidence for specific lateralization events. Instances of lateralization which reach bootstrap significance are small and unassociated with clear instances of lateralization in the opposite direction for the opposite attention condition, making the observed gamma band lateralization data hard to interpret.

little systematic evidence for specific lateralization events. The largest instance of induced power for both attention conditions comes around 500 ms into the ISI and is isolated primarily to a single channel over left frontal areas. At 13 and 8 significant samples for LC and RC trials respectively, neither peak can confidently be ruled out as chance. For RC trials, two positive peaks reach significance within the first 250 ms of the ISI. Both of these effects are small and brief and neither is associated with clear instances of lateralization in the opposite direction for LC trials. The nature of these effects and the generally low level of induced power in this band suggest there is little evidence for gamma band lateralization.

Summary of lateralization effects across bands. A concise summary of the time-frequency structure of lateralization events observed in our study is given in figures 8 and 9. Topographies for each of the time intervals indicated in these figures were computed for each attention condition by averaging induced band power over all time samples

within the indicated interval. For each band an interval was chosen that best coincides with significant lateralization effects of opposite sign in each attention condition. For the theta band the minimum length of the chosen interval was set at 250 ms in order to contain at least one entire cycle of the lowest frequency contained in that band (4 Hz), whereas for the remaining bands the chosen interval length of 150 ms satisfies the same requirement.

The earliest lateralization effect is found in the theta band during the interval 1-250 ms in the ISI. Topographies associated with this effect are shown for LC and RC trials in figure 8a, and 8b respectively. The primary effect is driven by a group of posterior parietal channels over the left hemisphere which display elevated induced theta band power for LC trials during this interval; a similar, smaller effect is seen in the right hemisphere for LC trials. The next effects occur in the adjacent alpha and mu bands over parietal areas during identical 550-700 ms intervals (Fig. 8c-f). Note that for both attentional conditions induced band power over the bilateral motor foci in both frequency bands is nearly the same over left and right hemispheres, while induced band power over parietal areas is lateralized, coinciding with greater power over the hemisphere ipsilateral to the attentional cue. Finally, the effects in the alpha and mu bands are trailed very closely by a beta band effect which is lateralized over motor areas (Fig. 8g,h), and displays the same relationship between lateralization and attentional orientation as observed in the previous lower frequency bands.

A second series of effects with a similar time-frequency relationships begins with another theta band effect (700-950 ms; Fig. 9 a,b). Here topographies for both LC and RC trials display foci of induced band power over posterior parietal electrode groups

Early Effects

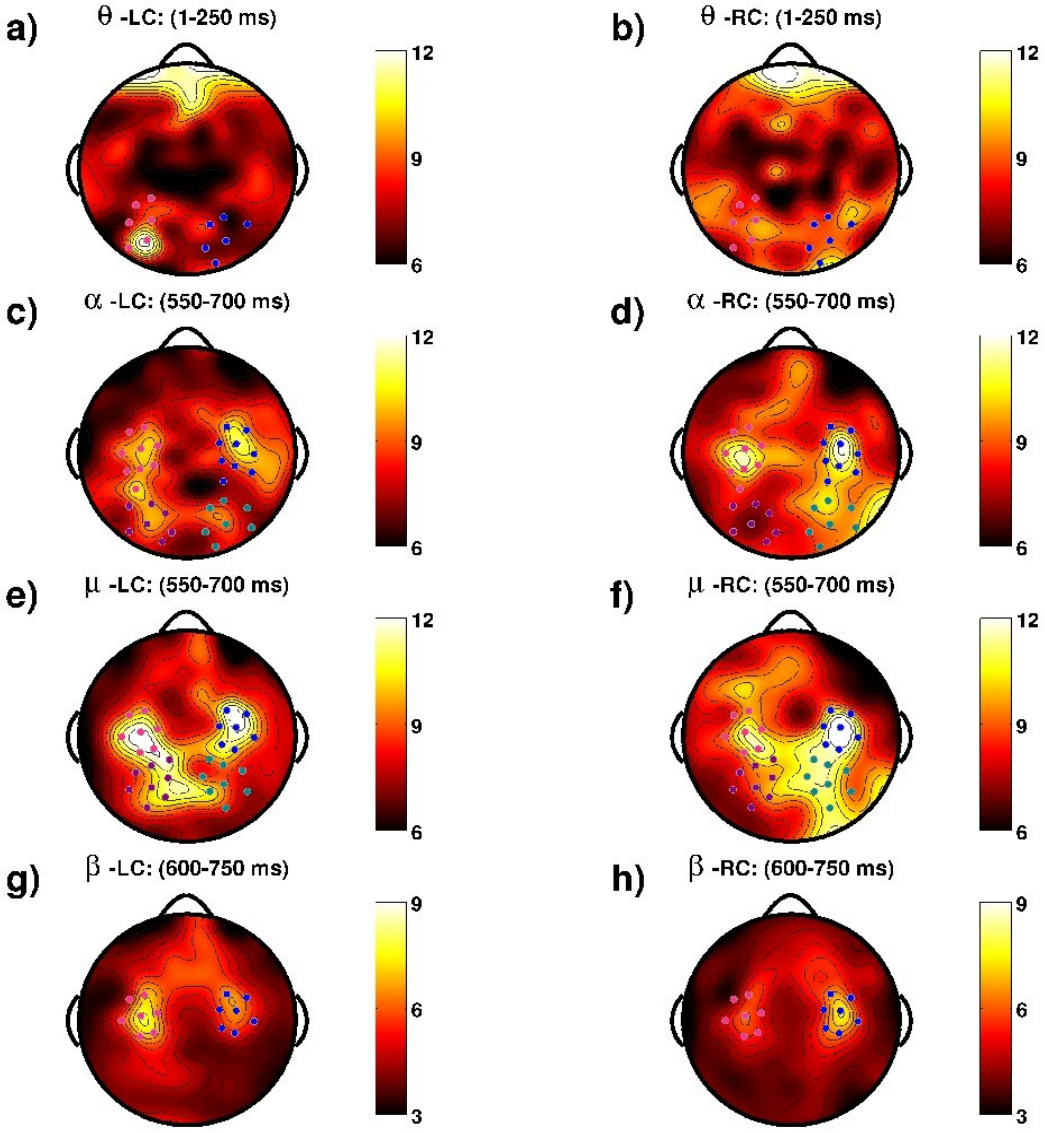

Fig 8. A summary of the early lateralization events observed in each band. For each band topographies are shown for the interval that best coincides with significant lateralization effects of opposite sign in each attention condition. The earliest effect is found in the theta band from 1-250 ms in the ISI, for which topographies are shown for LC and RC trials in (a) and (b) respectively. A group of posterior parietal channels drives this effect over the left hemisphere while a similar, smaller effect is seen in the right hemisphere. The next effects occur in the adjacent alpha (c,d) and mu (e,f) bands over parietal areas during identical 550-750 ms intervals. For both attentional conditions induced band power over the bilateral motor areas in both frequency bands is nearly the same over left and right hemispheres, while induced band power over parietal areas is lateralized with greater power over the hemisphere ipsilateral to the attentional cue. These effects are trailed closely in time by a beta band effect which shows opposite lateralizations over motor areas for LC (g) and RC (h) trials, again with greater power over the hemisphere ipsilateral to the attentional cue.

Late Effects

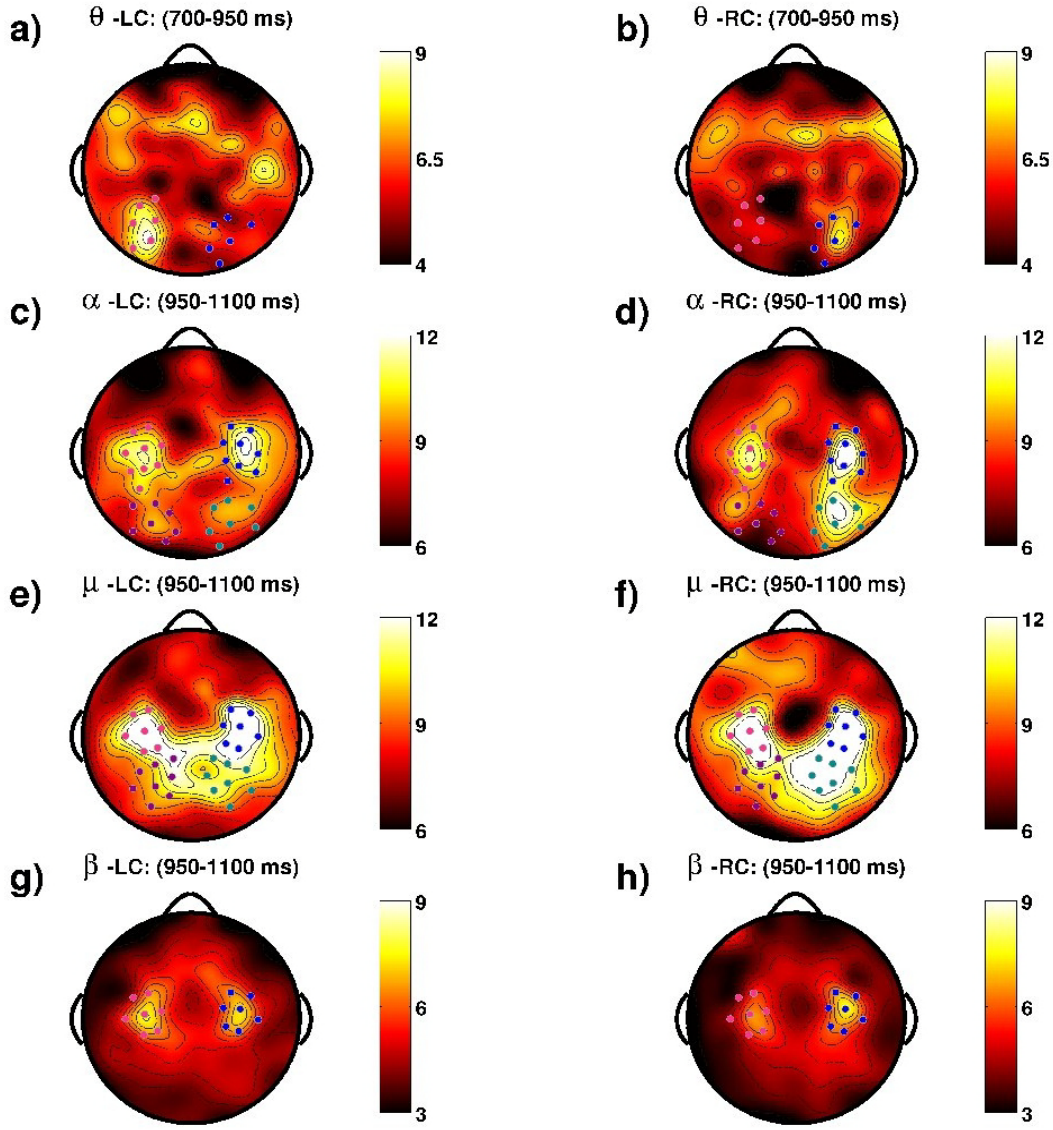

Fig 9. A second series of effects with a similar time-frequency relationships begins with another theta band effect around 700 ms. Topographies for both LC (a) and RC (b) trials display foci of induced band power over posterior parietal electrode groups ipsilateral to the attended direction. As in figure 8, this effect trailed by simultaneous effects in the alpha (c,d) and mu (e,f) bands, this time during the interval from 950-1100 ms. Induced band power in both attention conditions shows lateralizes over parietal areas with the same familiar pattern: greater power induced over areas ipsilateral to attentional orientation. The final beta band effect in this same interval shows a small degree of lateralization for LC trials (g), but for RC trials the lateralization is more pronounced (h). Together figures 8 and 9 suggest that hemispheric lateralization unfolds in punctuated events throughout the attention interval, and that the direction of the lateralization consistently reflects the direction in which attention is orientated.

ipsilateral to the attended direction. This theta band effect is again trailed by simultaneous effects in the alpha and mu bands during the interval from 950-1100 ms (Fig. 9,c-f). Induced band power shows a large degree of lateralization over parietal areas with the same familiar pattern of lateralization: greater power induced over areas ipsilateral to the cued direction. The final beta band effect in this same interval (Fig. 9g,h) shows only a small degree of lateralization for LC trials, but for RC trials the same general pattern is clear. Taken together these results suggest that hemispheric lateralization with specific time-frequency structure unfolds throughout the attention interval in punctuated events, and that the direction of the lateralization is critically dependent upon the direction of attentional orientation. Interestingly, the specific time-frequency structure of the lateralization events we observed suggest that early theta band events in posterior parietal areas are trailed by events in higher frequency bands situated over more anterior scalp areas.

4. Discussion

The results of the experiment concern the dynamic structure of covert spatial attention. The results bear on three aspects of this structure: (1) the spatial organization of attentional networks within the brain; (2) the time course of attentional deployment, and (3) the hemispheric lateralization of attention-related activity.

Spatial organization of attentional networks within the brain. Several neuroimaging studies undertaken during the past two decades provide compelling evidence for the involvement of specific premotor, parietal and inferior frontal cortical areas in visual spatial attention (Mesulam 1981; Posner and Peterson 1990; Pardo et al. 1991; Corbetta

et al. 1998; Gittleman et al. 1999). The frontal eye fields (FEF), located at the junction of the pre-central sulcus and the superior frontal sulcus, are thought to be involved in preparation of exploratory eye movements. Areas along the intraparietal sulcus (IPS) have been hypothesized to provide various sensorimotor maps of global extrapersonal space. Regions of inferior frontal cortex, finally, are thought to provide information on the motivational relevance of expected target stimuli (Mesulam 1981).

Several more recent studies have used event-related fMRI techniques to distinguish attentional control signals from the effects of these signals on subsequent target stimulus processing (Corbetta et al 2000; Hopfinger 2000). From such studies, a model of visual spatial attention has emerged in which attentional orienting is carried out by two anatomically independent but overlapping frontoparietal networks: the dorsal (goal-oriented) and ventral (stimulus-driven) attention systems (Corbetta et al. 2002; Corbetta et al. 2006). The dorsal system is bilateral and includes the FEF and IPS areas. This system becomes activated in response to attentional cueing and is thought to control top-down orienting of attention. The ventral system is highly right lateralized and includes primarily regions of temporo-parietal and inferior frontal cortex. This system is excited by behaviorally relevant targets, especially by those which appear in unexpected locations, and is thought to act as a "circuit breaker" for the dorsal system: capturing attention and directing it to relevant stimuli in a bottom-up fashion.

Although the Corbetta model was proposed to account for findings concerning visual attention, a growing body of work which suggests that this framework may be extended in a natural way to auditory attention (Krumbholz et al. 2009; Wu et al. 2007; Salmi et al. 2009; Smith et al. 2009). While covert visual attention primarily involves

preparation of intended eye movements, so that an object of interest may be foveated, we suggest that covert auditory attention involves preparation for intended head and body movements, so that a sound source of interest may be located directly in front of a listener, where auditory acuity is highest (Blauert 2001). This idea is supported by recent fMRI studies which show similar activation patterns are elicited when subjects are cued to make spatial judgements about stimuli in analogous auditory and visual tasks (Smith et al. 2009; Krumbholz et al. 2009). Moreover, the activated areas in these studies include all the primary areas implicated in Corbetta's dorsal network. We believe our results support the emerging idea that top-down spatial orienting of both visual and auditory attention is accomplished by a supramodal attention network including bilateral parietal and motor areas.

The results of this study are consistent with a picture in which spatial attention is accomplished by the dorsal top-down attention network. While we acknowledge that precise anatomical information concerning the brain networks underlying our effects is impossible to determine from observed scalp topographies alone, the topographies associated with the time-frequency events identified in figures 3-9 are at least consistent with activity arising in a bilateral network of frontal, motor, and parietal areas, possibly including FEF and areas along the intraparietal sulcus. If this could be shown to be the case, then our results suggest that the deployment of spatial attention within this network may manifest in episodic bursts of band specific activity which lateralize according to the direction of attentional orientation.

The time course of attentional deployment. An abundance of studies have probed the temporal characteristics with which humans deploy, maintain, and switch attentional

focus (see Egeth and Yantis 1997 for review). These studies suggest that there are two types of attentional cueing effects which differ in their temporal response properties. Paradigms which compare peripheral to central cueing (Müller and Rabbitt 1989, Nakayama and Mackeben 1989) show that peripheral cueing *at* a to-be-attended location captures attention automatically and results in a fast, transient increase in performance accuracy, while central cueing *to* a target location provokes deliberate shifts in attention for which benefits in performance are much slower. Similar experiments performed using the rapid visual serial presentation (RSVP) paradigm have estimated the time shift for top-down goal-directed attention to lie between 300-500 ms (Reeves and Sperling 1986).

Weichselgartner and Sperling (1995) proposed an episodic theory of spatial attention to account for data from several types of visual attention experiments in which the focus of attention was switched from one location to another. The episodic theory suggests that spatial attention occurs in discrete space-time separable events. Attention at one location in space is likened to a spotlight which becomes active at a single location with simple exponential rise time, like a spotlight warming up. When attention is shifted to another location, the spotlight at the previous location decays (cools down) with a similar time course while the next location heats up. The spotlight analogy is useful in comparing the episodic theory to the competing analog theory, in which the spotlight moves continuously to follow the action on the stage. The episodic theory holds that attentional shifts require a fixed deployment time of around 400 msec which is independent of the distance jumped, a finding shared by numerous other studies (Sagi and Julesz 1985, Kwak et al. 1991). The 400 ms required for subjects to shift attention in

space, according to the episodic theory, matches nicely the duration of the interval we observed between the offset of the directional cue and the initial α, μ, and β – frequency events (Figs. 3d, 4d, 5c). The present results suggest that the emergent lateralization evident in these frequency bands after 400-500 ms may reflect the successful deployment of spatial attention.

Hemispheric Lateralization of attention-related activity. Compelling evidence exists which suggests that top-down modulation of sensory processing is achieved through the biasing of temporal firing patterns in sensory cortices by areas higher up in the functional attention hierarchy (see Engel 2001 for review). In particular, spatial attention has been shown to increase gamma band synchrony in neural populations processing visual (Fries et al. 2001), auditory (Tiitininen et al. 1993), and somatosensory (Bauer et al. 2006) target stimuli. Fries and colleagues (2001) showed that individual neurons in area V4 of occipital cortex increase the synchrony of their firing with gamma band local field potentials in response to an attended stimulus. This same study also showed a complementary decrease in low frequency (<17 Hz) synchrony in both pre- and post-stimulus intervals within the same populations for which gamma synchrony was enhanced, leading the authors to conclude that low frequency desynchronization might act to enhance post-synaptic efficacy of high frequency oscillations.

A number of studies in the EEG/MEG literature have corroborated this picture and propose parieto-occipital alpha rhythms as a candidate mechanism for suppressing unattended visual information (Foxe et al. 1998; Fu et al. 2001). These studies show that parieto-occipital alpha rhythms are significantly greater when subjects are cued to attend to an upcoming auditory stimulus than when cued to attend to visual stimuli, and attribute

the source of the rhythms underlying this effect to parietal regions which are part of the attention networks described above. In addition, related studies have demonstrated a lateralization of the alpha biasing signals in experiments where attention is selectively cued to one side of visual space, with alpha power most diminished in electrodes over posterior sites contralateral to the cued hemifield (Worden et al. 2000; Thut et al. 2006; Rihs et al. 2007). In this study we found clear evidence of such lateralization. Our results suggest that α-lateralization over parieto-occipital electrodes is not a phenomenon particular to visual spatial attention, but one which extends at least to spatial attention in the auditory domain as well.

Other studies suggest that neural signatures of top-down attention involve additional frequency-specific oscillations. Rougel-Buser and Buser (1997) recorded electrocorticographic (ECoG) activity from behaving cats in sensorimotor, parietal, and occipital cortex. They observed what they termed an “expectancy rhythm” over sensorimotor cortex in the range of 10-14 Hz. These rhythms dominated periods when the animal was actively attending to an area where a mouse was expected to appear, and dissipated immediately upon arrival of the stimulus. These prototypical μ-rhythms have traditionally been thought to reflect suppression or idling of motor networks, although recent studies have challenged these assumptions (Pineda 2005). Rougel-Buser and Buser also found that periods of μ-rhythm during the expectancy period were followed immediately by brief bursts of activity in the range of 20 Hz, which the authors took to mark a transition between a passive waiting and a kind of “active or intense monitoring". Interestingly, we observed a similar sequence of activity in these same bands (Figure 7, 8). Moreover, the induced activity that we observed was greater over scalp areas

ipsilateral to the direction of attentional orientation, specifically over parietal areas in the mu band and motor areas in the beta band. Taken together, these results suggest that relative timing of activity in the μ and β - bands provides information about the temporal structure of attentional deployment, and that the hemispheric lateralization of these rhythms over specific attentionally relevant scalp areas provides information about the direction of attentional orientation.

A final note of interest involves the interpretation of the theta band lateralization effect observed in our study. Recent studies have suggested a role for theta rhythms in the mediation of synchrony between distal neural populations distributed throughout the brain (Schak et al. 2002; Conolty et al. 2006). Sauseng and colleagues (2008) showed that attentional shifts to a cued hemifield facilitated theta-gamma band phase synchronization in response to validly cued targets over posterior scalp areas contralateral to the cue. Doesburg and colleagues (2008) carried out a study where attention was cued to one side of visual space and measured lateralized gamma-band synchrony between widespread cortical areas and posterior sites contralateral to the attended hemifield. They showed that gamma synchrony increased in punctuated bursts whose timing coincided with activity in the theta band (4-7 Hz). The authors concluded that this timing reflects the maintenance or refinement of spatial attention networks by distributed theta band activity. Although we did not observe lateralized gamma band activity over sensory cortical areas, the lateralized theta activity we did observe may well reflect a similar top-down signal which mediates the formation and maintenance of transitory attentional networks via the modulation of high frequency synchrony, which is difficult to observe in scalp recordings (Nunez and Srinivasan 2010).

Conclusions. Our results suggest that the deployment and maintenance of spatial attention in a cued direction induces hemispheric lateralization events in specific frequency bands, and that the direction of the lateralization consistently reflects the direction of attentional orientation. The specific time-frequency structure of events we observed are consistent with the notion that early theta band lateralization in posterior parietal areas facilitate shifts of attention to the cued location. Later lateralization events in α, μ frequency bands over parietal areas beginning roughly 400 ms after the directional cue and beta lateralization over motor areas may reflect successful deployment of top-down oriented spatial attention.

Acknowledgements

We thank Tom Lappas, Siyi Deng, Cort Horton, and Bill Winter for their contributions to this work. This work was supported by ARO 54228-LS-MUR, and R01-MH68004.

References

Alho K, Connolly JF, Cheour M, Lehtokoski A, Huotilainen M, Virtanen J, Aulanko R, Ilmoniemi, RJ (1998) Hemispheric lateralization in preattentive processing of speech sounds. Neuroscience Letters. 258:9-12

Arrington CM, Carr TH, Mayer AR, Rao SM (2000) Neural mechanisms of visual attention: object-based selection of a region in space. Journal of Cognitive Neuroscience. 12(Supplement 2): 106-117

Bahramisharif A, van Gerven M, Heskes T, Jensen O (2010) Covert attention allows for continuous control of brain-computer interfaces. The European Journal of Neuroscience. 31(8): 1501-1508

Bauer M, Oostenveld R, Peeters M, Fries P (2006) Tactile spatial attention enhances gamma-band activity in somatosensory cortex and reduces low-frequency activity in parieto-occipital areas. The Journal of Neuroscience. 26(2):490-501

Blauert J (2001) *Spatial Hearing. The Psychophysics of Human Sound Localization. Rev. Ed.* Cambridge: MIT

Buser P, Rougeul-Buser A, (2005) Visual attention in behaving cats: Attention shifts and sustained attention episodes are accompanied by distinct electrocortical activities. Behavioural Brain Research. 164(1): 42-51

Canolty RT, Edwards E, Dalal SS, Soltani M, Nagarjan SS, Kirsch HE, Berger MS, Barbaro NM, Knight RT (2006) High gamma power is phase-locked to theta oscillations in human neocortex. Science. 313:1626-1628

Corbetta M, Akbudak E, Conturo TE, Synder AZ, Ollinger JM, Drury HA, Linenweber HR, Petersen SE, Raichle ME, Van Essen DC, Shulman GL (1998) A common network of functional areas for attention and eye movements. Neuron. 21(4):761-773

Corbetta M, Kinkade JM, Ollinger JM, McAvoy MP, Shulman GL (2000) Voluntary orienting is dissociated from target detection in human posterior parietal cortex. Nature Neuroscience. 3(3):292-297

Corbetta M, Shulman GL (2002) Control of goal- and stimulus-driven attention in the brain. Nature Reviews Neuroscience. 31:201-215

Desimone R, Duncan J (1995) Neural mechanisms of selective visual attention. Annu Rev Neurosci. 18:193-222

Doesburg SM, Roggeveen AB, Kitajo K, Ward LM (2008) Large scale gamma band phase synchronization and selective attention. Cerebral Cortex. 18:386-396

Efron B., Tibshirani R (1993) *An Introduction to the Bootstrap*. Boca Raton, FL: Chapman & Hall/CRC

Egeth HE, Yantis S (1997) Visual attention: control, representation, and time course. Annual Reviews in Psychology. 48:269-297

Engel AK, Fries P, Singer W (2001) Dynamic predictions: oscillations and synchrony in top-down processing. Nature Reviews Neuroscience. 2(10):704-716

Fabiani GE, McFarland DJ, Wolpaw JR, Pfurtscheller G (2004) Conversion of EEG activity into cursor movement by a brain-computer interface (BCI). IEEE transactions on neural systems and rehabilitation engineering, 12(3): 331-338

Farwell LA, Donchin E (1988) Talking off the top of your head: toward a mental prosthesis utilizing event-related brain potentials. Electroencephalography and Clinical Neurophysiology. 70(6): 510-523

Fink GR, Halligan PW, Marshall JC, Firth CD, Frackowiak RSJ, Dolan RJ (1996) Where in the brain does visual attention select the forest and the trees? Nature. 382:626-628

Fox MD, Corbetta M, Snyder AZ, Vincent JL, Raichle ME (2006) Spontaneous neuronal activity distinguishes human dorsal and ventral attention systems. Proceedings of the National Academy of Sciences of the United States of America. 103(26):10046-10051

Foxe J, Simpson G, Ahlfors S (1998) Parieto-occipital ~10 Hz activity reflects anticipatory state of visual attention mechanisms. NeuroReport 9:3929–3933

Fries P, Reynolds JH, Rorie AE, Desimone R (2001) Modulation of Oscillatory Neuronal Synchronization by Selective Visual Attention. *Science.* **291**(5508):1560-1563

Fu K, Foxe J, Murray M, Higgins B, Javitt D, Schroeder C (2001) Attention-dependent suppression of distracter visual input can be cross-modally cued as indexed by anticipatory parieto –occipital alpha-band oscillations. Cognitive Brain Research. 12:145–152

Gitelman D, Nobre A, Parrish T, LaBar K, Kim Y, Meyer M, Mesulam M (1999) A large-scale distributed network for covert spatial attention, Further anatomical delineation based on stringent behavioral and cognitive controls. Brain. 122(6):1093-1106

Hillyard SA, Anllo-Vento L (1998) Event-related brain potentials in the study of visual selective attention. Proceedings of the National Academy of Sciences of the

United States of America. 95:781-787
Hopfinger JB, Buonocore MH, Mangun GR (2000). The neural mechanisms of top-down attentional control. Nature Neuroscience. 3(3):284-291
Kastner S, Pinsk M, De Weerd P, Desimone R, Ungerleider L (1999) Increased activity in human visual cortex during directed attention in the absence of visual stimulation. Neuron 22:751-761
Kastner S, Ungerleider LG (2000) Mechanisms of visual attention in the human cortex. Annual Review of Neuroscience. 23:315-341
Krumbholz K, Nobis EA, Weatheritt RJ, Fink GR (2009) Executive control of spatial attention shifts in the auditory as opposed to the visual modality. Human Brain Mapping. 30:1457-1469
Kwak H, DagenBach D, Egeth H, (1991) Further evidence for a time-independent shift of the focus of attention. Perception and Psychophysics. 49(5):473-480
Martinez A, Moses P, Frank L, Buxton R, Wong E, Stiles J (1997) Hemispheric asymmetries in global and local processing: evidence from fMRI. NeuroReport. 8:1685-1689
Mesulam MM (1981). A cortical network for directed attention and unilateral neglect. Annals of neurology. 10(4):309-325
Moore T, Armstrong KM, Fallah M (2003) Visuomotor origins of covert spatial attention. Neuron. 40:671-683
Moore TJ (1981) Voice communication jamming research. AGARD Conference Proceedings 331: Aural Communication in Aviation. 2:1-6
Müller HJ, Rabbitt PM (1989) Reflexive and voluntary orienting of visual attention: Time course of activation and resistance to interruption. Journal of Experimental Psychology: Human Perception and Performance. 15(2):315-330
Nakayama K, Mackeben M (1989) Sustained and transient components of focal visual attention. Vision Research. 29(11):1631-47
Nunez PL, Srinivasan R (2006) *Electric Fields of the Brain: The Neurophysics of EEG*, 2nd Ed. New York, NY: Oxford University Press
Nunez PL, Srinivasan R (2010) Scale and frequency chauvinism in brain dynamics: too much emphasis on gamma band oscillations. Brain Structure and Function. 215:67-71
Pardo JV, Fox PT, Raichle ME (1991) Localization of a human system for sustained attention by positron emission tomography. Nature 349:61-64
Pfurtscheller G, Brunner, C, Schlogl A, Lopes da Silva FH (2006) Mu rhythm (de) synchronization and EEG single-trial classification of different motor imagery tasks. NeuroImage. 31(1): 153-159
Pineda JA (2005) The functional significance of mu rhythms: Translating. Brain Research Reviews. 50(1):57-68
Pineda JA, Allison PZ, Vankov A (2000). The effects of self-movement, observation, and imagination on rhythms and readiness potentials (RP's): Toward a brain–computer interface (BCI). IEEE transactions on rehabilitation engineering. 8(2):219-222
Poeppel D (2003) The analysis of speech in different temporal integration windows: cerebral lateralization as 'asymmetric sampling in time'. Speech Communication. 41:245-255

Posner M, Petersen S (1990) The attention system of the human brain. Annual Review of Neuroscience. 13:25-42

Reeves A, Sperling G (1986) Attention gating in short-term visual memory. Psychological Review. 93(2):180-206

Rihs TA, Michel CM, Thut G (2007) Mechanisms of selective inhibition in visual spatial attention are indexed by α – band EEG synchronization. European Journal of Neuroscience. 23:603-610

Rougeul-Buser A, Buser P (1997) Rhythms in the alpha band in cats and their behavioural correlates. International Journal of Psychophysiology. 26(1-3): 191-203

Sagi D, Julez B (1985) Fast noninertial shifts of attention. Spatial vision. 1(2):141-149

Salmi J, Rinne T, Koistinen S, Salonen O, Alho K (2009) Brain networks of bottom-up triggered and top-down controlled shifting of auditory attention. Brain Research. 1286: 155-164

Sauseng P, Klimesch W, Gruber WR, Birbaumer N (2008) Cross frequency phase synchronization: a brain mechanism of memory matching and attention. NeuroImage. 40:308-317

Schack B, Vath N, Petsche H, Geissler HG, Moller E (2002) Phase-coupling of theta-gamma EEG rhythms during short-term memory processing. International Journal od Psychophysiology. 44:143-163

Sheliga BM, Riggio L, Rizzolatti G (1994) Orienting of attention and eye movements. Experimental Brain Research. 98:507-522

Smith DV, Davis B, Niu K, Healy EW, Bonilha L, Fridriksson J, Morgan PS, Rorden C (2009) Spatial attention evokes similar activation patterns for visual and auditory stimuli. Journal of Cognitive Neuroscience. 22(2): 347-361

Spence C, Driver J (1998) Crossmodal attention. Current Opinion in Neurobiology. 8:245-253

Spence C, Pavani F, Driver J (2000) Crossmodal links between vision and touch in covert endogeneous spatial attention. Journal of Experimental Psychology: Human Perception and Peformance. 26:1298-1319

Srinivasan R, Thorpe S, Deng S, Lappas T, Dzmura M (2009) Decoding Attentional Orientation from EEG Spectra. Human-Computer Interaction: New Trends. 5610:176-183

Thorpe S, Srinivasan R, Deng S, Lappas T, D'Zmura M. Decoding attentional orientation from EEG spectra. Poster presented at the annual meeting of the Society for Neuroscience; 2009, Chicago, IL.

Thut G, Nietzel A, Brandt SA, Pascual-Leone A (2006) Alpha-**Band Electroencephalographic Activity over Occipital Cortex Indexes Visuospatial Attention Bias and Predicts Visual Target Detection. Journal of Neuroscience**. 26(37):9494-950

Tiitinen HT, Sinkkonen J, Reinikainen K, Alho H, Lavikainen J, Naatanen B (1993) Selective attention enhances the auditory 40-Hz transient response in humans. Nature. 364(6432):59-60

van Gerven M, Jensen O (2009) Attention modulations of posterior alpha as a control signal for two-dimensional brain-computer interfaces. Journal of Neuroscience Methods. 179(1): 78-84

Wang Y, Makeig S (2009) Predicting intended movement direction using EEG from human posterior parietal cortex. Foundations of Augmented Cognition: Neuroergonomics and Operational Neuroscience. 5638: 437-446

Weichselgartner E, Sperling G (1987) Dynamics of automatic and controlled visual attention. *Science. 238:*778-780

Wolpaw JR, McFarland DJ, Vaughan TM, Schalk G (2003) The Wadsworth Center brain-computer interface (BCI) research and development program. IEEE Transactions on Neural Systems and Rehabilitation Engineering. 11(2): 204-207

Wolpaw JR, McFarland DJ (2004) Control of a two-dimensional movement signal by a noninvasive brain-computer interface in humans. Proceedings of the National Academy of Sciences of the United States of America. 101(51): 17849-17854

Worden M, Foxe J, Wang N, Simpson G (2000) Anticipatory Biasing of Visuospatial Attention Indexed by Retinotopically Specific alpha band Electroencephalography Increases over Occipital Cortex. The Journal of Neuroscience. 20(63): 1-6

Wu CT, Weissman DH, Roberts KC, Woldorff MG (2007) The neural circuitry underlying the executive control of auditory spatial attention. Brain Research. 1134:187-198

Chapter 3. Effects of Top-Down Spatial Attention signals on gamma-band steady-state evoked responses.

Abstract. *Studies in animal models suggest that spatial attention increases gamma-band (>20 Hz) synchronization in local neural assemblies processing visual stimuli at the attended location, thereby facilitating binding of information into coherent percepts. In parallel, Studies in human have shown that deployment of attention to one side of visual space results in lateralization of band-specific EEG activity over symmetric parietal and occipital areas. Our goal was to determine how these lateralized attention-related signals interact with local populations processing visual stimuli, which presumably have resonant frequencies in the gamma band methods to simultaneously localize gamma-band sensory responses to attended and unattended visual stimuli, recorded using simultaneous EEG/MEG. The subject observed a pair of dynamic flickering stimuli presented in symmetric left/right visual hemifields, one which flickered at 20 Hz, the other at 30 Hz. The stimulus in each hemifield consisted of a circular region containing a field of randomly oriented bars- a novel bar-field was presented on each flicker cycle . Subjects were asked to detect targets in the attended fields, which were bounded by a green annulus, and ignore false targets in the unattended field which were bound by a red annulus. The bounding annuli switched colors at random intervals, prompting the subject to switch attention to the opposite hemifield. The flickering stimuli evoked steady-state responses which localized to occipital areas showed increased magnitude when attended. We also observed attention-related lateralization of alpha-band power in response to attentional switches. The time course of these effects, analyzed using wavelets, suggest that decreases in alpha, and mu-band power, over areas contralateral to the attended location, precede attentional modulations of the stimulus evoked steady-state response. Moreover, both of these modulations precede the complimentary increases in alpha and mu-band power over corresponding ipsilateral areas. These results suggest that attention-dependent decreases in contralateral power facilitate gains in the attended repsonse, whereas increases in ipsilateral activity may not play an active role in suppression unattended information.*

1. Background and Significance

In recent years, gamma-band (20 – 90 Hz) signals in EEG, EcoG, and animal LFP studies have been identified as a signature of information processing in the human and animal visual systems (Basar 1999, Tallon-Baudry 1997, Eckhorn et al 1988). These gamma-band rhythms have generated widespread interest due to the hypothesis that they reflect the binding of disparate aspects of a visual scene, processed independently within proximate neural populations, into unified coherent percepts (Singer 1993, 1995). In

addition, computational models of local neural networks suggest that such networks characteristically typically exhibit oscillations at these higher frequencies, above 20 Hz , and as such gamma-band activity may reflect natural resonance frequencies of sensory cortical populations. (Bush & Sejnowski, 1996; Lumer et al., 1997; Whittington and Traub 2003; Traub et al., 2005; Izhikevich 2003; Izhikevich 2006).

Attention is thought to modulate temporal firing patterns in these populations in a top-down manner, via signals originating outside of sensory cortex (Engel et al. 2001). von Stein et al. (2000), for example, made simultaneous recoding of primary visual cortex and parietal visual areas in cats performing a visuomotor task, and showed that synchrony between these areas at lower frequencies in the theta and alpha range (4–12 Hz) was observed to depend strongly on task expectancy conditions. The impact of spatial attention on gamma-band rhythms is supported by studies which have shown that spatial attention increases gamma-band synchrony in neural populations processing visual (Fries et al. 2001), auditory (Tiitinen et al. 1993), and somatosensory (Bauer et al. 2006) target stimuli. In the EEG literature, Müller at al. (2000), and Gruber et al. (1999) have demonstrated that attention to a visual stimulus results in increased levels of induced gamma-band power over occipito-parietal electrodes. Fries et al. (2001) showed that increased gamma-band synchrony in local populations processing an attended visual stimulus was accompanied by a complementary decrease in low frequency (<17 Hz) synchrony in these same populations, in both pre- and post-stimulus intervals. This finding lead the authors to conclude that low frequency desynchronization might act to enhance post-synaptic efficacy of stimulus-related gamma-band oscillations.

The proposal that low-frequency desynchronization may act causally to enhance the neural response to a sensory stimulus has an interesting parallel in the EEG literature. Numerous studies have shown that the deployment of spatial attention to the left/right side of visual space results in a lateralization of alpha-band EEG power over occipito-parietal scalp areas (Worden et al. 2000; Kelly et al. 2006; Rihs et al. 2007). In these studies alpha-band power is always enhanced over the hemisphere ipsilateral to the attended hemifield. These findings lead the authors to propose parieto-occipital alpha rhythms as a candidate mechanism for suppressing unattended visual information. Other related MEG/EEG studies using similar cueing paradigms report primarily alpha desynchronization over contralateral parietal sites (Sauseng et al. 2005; Thut et al. 2006; Yamagishi et al. 2005), and interpret this as evidence for increased cortical excitability of these areas- an interpretation consistent with the results from the animal literature cited above. Thus it appears that different scholars have independently developed complementary explanations for seemingly related phenomenon. On one hand, observed *decreases* in low-frequency synchronization have been proposed to *enhance* the visual response to an attended stimulus. On the other, observed *increases* in low-frequency power have been proposed to *suppress* visual information which is to be ignored in unattended regions. These findings further underline the importance of gaining a functional understanding of the causal relationship, if any, between low-frequency signals modulated by attention, and high frequency activity evoked by a sensory stimulus.

The EEG studies described above did a good job of describing the temporal evolution of attention-related alpha-band activity in response to cueing, but they were not likewise designed to investigate the temporal dynamics of the neural response to the

visual stimuli themselves. This is because the stimuli in their experimental designs were not displayed continuously, but discretely in time. As such the only available measure of the neural response to their visual stimuli were event-related potentials (ERP). Analysis of such potentials must necessarily take the form of comparing differences between attended/unattended ERP waveforms at the specific latencies corresponding their standard maxima/minima. In contrast, Müller at al. (1998) designed a study comparing steady-state evoked potentials (SSVEP) evoked by attended/unattended arrays of light emitting diodes (LED's) which flickered continuously at gamma-band frequencies (20.8 and 27.8 Hz). In addition to a number of other advantages (discussed in more detail below), the resultant gamma-band SSVEP unfold continuously over time. Müller was able to show that when attention was cued to a given flicker the SSVEP subsequently increased after a delay of 600-800 ms. Unfortunately, at the time his experiment was run, the results concerning attention related lateralization of alpha-band EEG signals were largely unknown.

In this study we use a steady-state design to analyze the temporal evolution of *both* the gamma-band response to attended/unattended visual stimuli, as well as lower frequency attention-related signals, in a single unified framework. Though most of the EEG/MEG studies cited above have focused exclusively on changes in levels of alpha-rhythm, we recently conducted an auditory attention study which suggests that attention-related lateralizations extend to other bands as well (Thorpe et al. 2011). We therefore chose to include in this study analyses of mu (12 - 16 Hz), and theta (5 - 7 Hz) band activity as well. Our results indicate that, after an attentional switch, desynchronization of alpha and mu band power over occipito-parietal areas contralateral to the attended

location precedes the gain in the response to the attended stimuli. Conversely, the decrease in the response to the unattended flicker precedes observed increases in low-frequency power over ipsilateral areas. These results suggest that contralateral desynchronization facilitates the gain in attended responses, whereas increases in ipsilateral activity may not have an active role.

2. Materials and Methods

Steady-State Visual Evoked Potentials/Fields (SSVEP/F). Recent studies have shown that the recording of authentic gamma-band EEG activity can be problematic due to contamination by muscle (Whitham et al. 2008) and oculomotor (Yuval-Greenberg 2008) activity which overlap in frequency. One way to get around this problem is to make use of steady-state or "frequency-tagging" methods which are uniquely robust to this type of broad-band artifact. In the frequency tagging experimental design subjects are presented with task related visual stimuli which flicker at a fixed frequency (Srinivasan, 1999). The resultant steady state visual evoked potentials (SSVEP) or magnetic fields (SSVEF) are measured in the narrow band centered on the stimulus frequency, thereby allowing the experimenter to isolate the response to the visual stimulus with relative immunity to broad-band artifact. In this way the signal to noise ratio can be made very large (Regan 1977, 1989).

Simultaneously recorded EEG/MEG. Recall that we seek to understand interactions between endogenous attention signals which originate in globally distributed (fronto-parietal) source configurations, and sensory signals which originate locally in occipital cortex. Since EEG is preferentially sensitive to sources oriented radially with respect to the scalp, and MEG preferentially sensitive to tangential sources, each methodology also

has different sensitivity to these global/local source configurations. This is due to the columnar structure of human neocortex, in which sources oriented radially with respect to the scalp tend to be found on cortical gyri, while tangential sources are typically found in the cortical sulci. As a result, globally distributed source configurations that are coherent and in-phase across large portions of the cortical surface tend to sum across the gyri and cancel across the sulci, and thus drive large EEG but small MEG responses. MEG, however, is highly sensitive to localized tangential dipole sources in cortical sulci, which are not always readily observable in the EEG. Thus it is advantageous for our purposes to compare EEG and MEG recorded simultaneously (Nunez 1995; Nunez and Srinivasan 2006). For our experiment, ***s***imultaneous MEG/EEG signals were measured with an Elekta/Neuromag whole head neuromagnetometer at USCD Radiology Department in La Jolla, California. This system records field fluctuations using two planar gradiometers and one scalar magnetometer at each of 102 locations. In this study we analyze data exclusively from the 102 magnetometers. 128 channels of EEG were also simultaneously recorded. Both signals were sampled at 1000 Hz. The locations of the EEG electrodes and MEG magnetometers were coregistered with respect to anatomical features of the subjects head using a Polhemus FastTrack 3-D digitizer.

Procedure. Seven subjects (6 male, 0 left-handed) participated in the experiment. On each trial the subject observed a pair of flickering stimuli presented symetrically in each visual hemifield (eccentricity from center was 2.275 degrees of visual angle). The stimulus in each field consisted of a circular region (6.5 dva) containing randomly oriented bars (unit length for each of 0.56 dva) which appeared for a single frame (refreshed at 60 Hz). After a fixed period corresponding to the given flicker frequency, a

new array was presented. The subject was instructed to always attend to the stimulus region bounded by a green annulus, and to ignore the opposite sie region bounded by a red annulus. At random intervals (between 6-12 seconds) throughout the 100 second trial, the colors of the annuli in the respective hemispheres switched, prompting the subject to switch attention to the opposite hemifield.

The subject's task was to maintain center fixation (indicated by a gray fixation square) while simultaneously detecting targets in the attended hemifield and ignoring targets in the unattended hemifield. A target consisted of a 250 ms interval in which each field of randomly oriented bars contained an iso-oriented subset. The fraction of this subset as a percentage of the whole field was determined by a psychophysical staircasing procedure for each subject. On a previous day, subjects completed a psychophysical version of the experiment in which they were asked to detect the presence of a target in the cued hemifield within a three second interval. Subjects completed 100 such trials for each of four stimulus types (20/30 Hz Left/Right, attend Left/Right). Each time the subject responded correctly the fraction of iso-oriented bars on the successive target trial decreased by 1%, whereas the fraction increased 3% on incorrect trials. In order to facilitate accuracy on the more difficult task of sustained attention, the target level for each stimulus type was defined as that of the 95^{th} percentile of all incorrect responses on each respective staircase.

An example of a target frame in which the subjects attention was directed left is shown in figure 1. Note that for convenience in the source analysis we placed the pair of stimuli in the lower visual field in order to stimulate local networks along the dorsal surface of visual cortex. A total of 24 100 second trials were collected over two sessions,

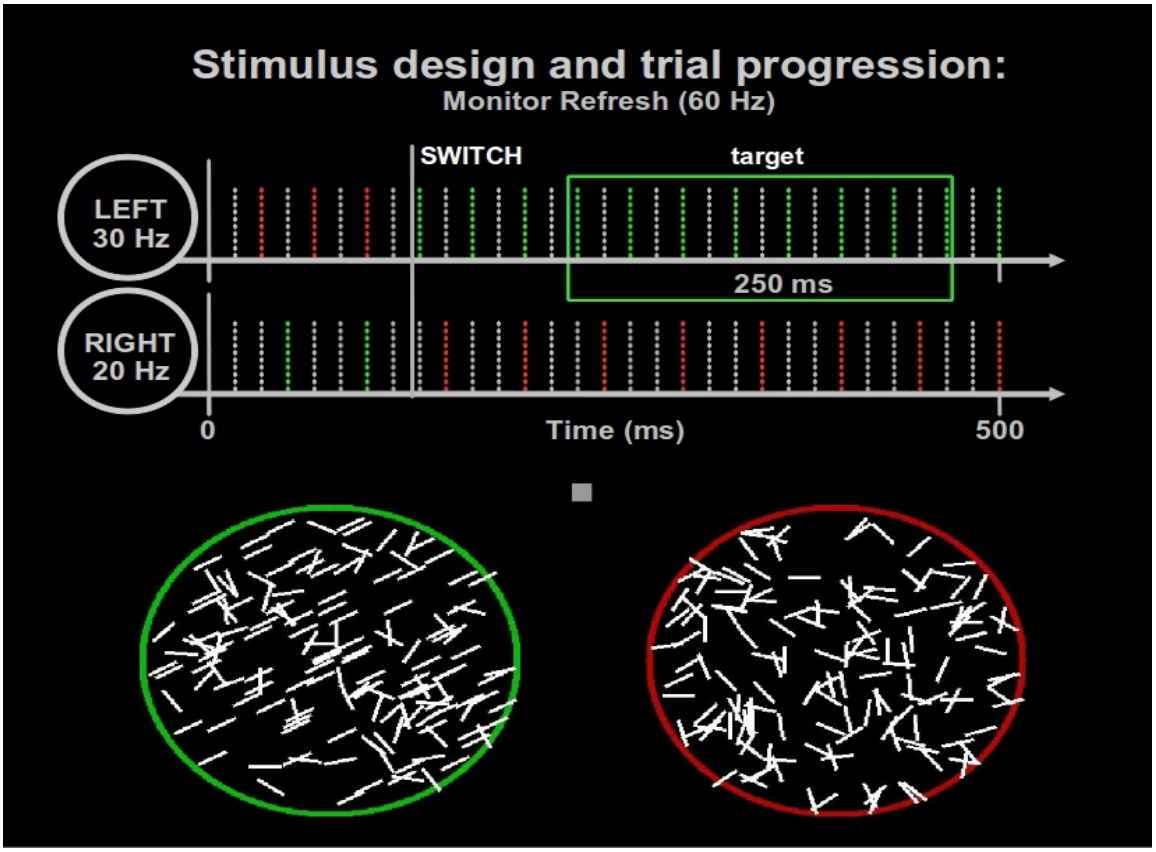

Figure 1. ***The stimulus display and trial progression.*** Seated in front of a monitor, the subject is asked to fixate while detecting targets in the green annulus. New randomly oriented bar fields are flickered on each side with fixed periodicity. In the example above this occurs at 20 Hz (every third frame) for the right flicker, and 30 Hz for the left (every other frame). Targets occur at random intervals (roughly every 3-6 seconds). Targets occur when, for a 250 ms window, the randomly oriented bar field contains an iso-oriented subset. In the example above, roughly two thirds of the total field is oriented uniformly at 30 degrees. False targets also occur at random intervals in the opposite (red) annulus, which the subject is askted to ignore. Additionally, the left/right annuli switch colors roughly every 6-12 seconds, indicating to the subject to switch their attentional focus and detect targets at the new location.

corresponding to a single pair of flicker frequencies (20 and 30 Hz) presented in each of two visual hemispheres (Left/Right), with each trial type repeated twelve times throughout the experiment in random order. This resulted in an average of approximately 240 switches per subject, roughly 210 of which were kept after artifact editing.

Artifact and editing and Independent Components Analysis (ICA). EEG/MEG data were band-pass filtered from 2-50 Hz, and aligned on the switches. For each switch the interval spanning 4.5 seconds prior to 4.5 seconds post-switch was included for analysis.

A subset of these epochs containing excessive movement artifact were identified and excluded. For each subject, a subset of channels/sensors that showed high amplitude drift across many trials due to either poor contact with the scalp (EEG) or poor tuning (MEG) were identified and their data excluded. Separate Independent Components Analyses (ICA) were then run for EEG and MEG data for each recording session on the concatenated set of good epochs using the FastICA algorithm developed for Matlab by Aapo Hyvarinen et al. (2000).

For both EEG and MEG data, 50 Independent Components were obtained. For each session, one obvious component containing the eye blink waveform was removed. For the remaining components we computed the Fourier spectra corresponding to each epoch by aligning the data on the last common frame of the 20 & 30 Hz flicker before the switch occured, and computing the FFT of the interval spanning two seconds prior to four seconds after this frame. This was done in order to ensure an exact integer number of cycles of each flicker were included in the FFT, thereby optimizing our estimation of the SSVEP/F at each flicker frequency. With the aim of eliminating all components related to muscle and movement artifact, the activity of which typically occurs in broad high-frequency bands overlapping our SSVEP/F signal, we instituted the following ranking scheme. First, to assess each component's contribution to the total SSVEP/F, we averaged each component's complex Fourier coefficients across epochs, and computed the resultant power spectrum, which we then ranked by power separately for each of our flicker frequencies (20 & 30 Hz). Here we average the complex coefficients because we desire to estimate the nonzero, constant-phase signal that is common across trials- a procedure which is common for estimating steady-state evoked responses (Nunez & Srinivasan,

2005). Next, to assess each component's contribution to the classic alpha-band activity which dominates spontaneous human EEG, we computed the variance of each component's Fourier spectrum across epochs, and ranked them by summed variance from 8-12. Since EEG and MEG are nonstationary signals, this procedure of computing the variance has the effect of removing the nonzero mean of the signal accross trials (Nunez & Srinivasan, 2005).

Upon reviewing the contributions of each component, we found that for both the low-frequency signal, as well as the SSVEP, a small number of components captured a large fraction of the total signal, while a majority contributed very little. By including only components which contributed at least 2% or more of the total signal, we compiled overlapping lists of components specific to the low-frequency bands, and the 20 & 30 Hz SSVEP/F signals respectively. Finally, we reconstituted the data back into channel/sensor space from the union of these lists. For each subject, this scheme resulted in keeping approximately half of the 50 total components, which accounted for roughly 90% of the total 20 & 30 Hz SSVEP/F signal, and roughly 70% of the alpha variance.

Wavelet Analysis. The resultant cleaned EEG/MEG data werethen aligned on the last common frame of the 20 & 30 Hz flicker before the switch occured, and a complex Morlet wavelet transform, with frequencies (*f*) centered on 4, 5, 6, 7, 8, 10, 12, 14, 16, 20, 24, 30, and 36 Hz, was applied to the interval spanning the period from two seconds prior to four seconds after this common frame. As noted above, this alignment was done in order to ensure an exact integer number of cycles of each flicker were included in the wavelet, and thereby optimize our estimation of the SSVEP/F at each flicker frequency. In order to optimize the trade off between our ability to resolve our 20 & 30 Hz signals

independently, while still maintaining adequate temporal sensitivity, we chose Morlet center frequency and frequency bandwidth parameters of 5 and 1, respectively, after extensive simulations with simulated 10, 20 and 30 Hz signals. To avoid distortion by the wavelet at the tails of the time series, only the interval from one second prior to three seconds post-switch was included for further analysis. This resulted in a time-frequency spectrum of complex wavelet coefficients, $W_{c,j}(f,t)$, for each good channel (c), for each trial (j), for each subject. Finally, the resultant wavelet coefficients were down sampled from 1000 to 144 samples per second.

Alpha, mu, and theta-band wavelet time series estimation. In the low-frequency bands, we computed the variance for each frequency's wavelet time series coefficient across all trials in each switching condition, resulting in a pair of time series representations for each frequency/channel corresponding to LR and RL trials. In order to examine changes specifically associated with the switch, we then performed a normalization of each time series, denoted WN(f,t) below, taking the 20*log ratio (dB units) of the time series and its mean power in the second prior to the last common frame before the switch. Next, we obtained a single time series representation of band-specific power for each channel by averaging wavelet time series over [4-7], [8-12], and [14-16] Hz bands for theta, alpha, and mu, respectively.

Our goal was to obtain wavelet time series measures which capture the dynamics of attentional modulation for each switching condition, i.e. from Left-to-Right (LR), and from Right-to-Left (RL). From the previous alpha-lateralization results cited above, we had reason to suspect these dynamics would differ across the left/right cerebral hemispheres depending on whether the hemisphere was contralateral or ipsilateral to the

direction of the switch. Towards this aim we obtained average wavelet time series measures in each band for two groups of EEG/MEG channels over Left/Right regions of interest. We defined these left/right channel groups for each band by looking at subject averaged scalp patterns of normalized wavelet modulation, choosing symmetric groups for each band corresponding to the peaks in positive/negative modulation averaged across the entire post-switch interval (see figures 3 – 8). In order to perform the subject averaging, we interpolated time series' for the subset of excluded bad channels for each subject, and averaged the complete set of channels across subjects. Due to our normalization procedure, negative peaks indicated areas which were suppressed relative to the pre-switch interval, whereas positive peaks indicated areas where power increased after the switch. This resulted in symmetric left/right occipito-parietal channel groups which were largely overlapping across bands. For LR trials, the left/right channel groups constituted the contra/ipsilateral signals, respectively, whereas for RL trials, the contra/ipsilateral signals were determined by the right/left channels.

SSVEP/F wavelet time series estimation. For our SSVEP/F signals, we first partitioned the trials according to *both* direction of the switch, as well as which flicker frequency appeared on which side. We designate these trial types with the names L20R30, L30R20, R20L30, and R30L20- where L20R30 indicates trials for which the subject switched attention *from* the 20 Hz flicker located on the left *to* the 30 Hz flicker located on the right. For each of these trial types, we computed a phase locking index (PLI) for each flicker frequency by normalizing the wavelet time series by its squared modulus, and averaging across trials:

$$\mathrm{PLI}_c(f,t) = \left| \sum_j \frac{\mathrm{W}_{c,j}(f,t)}{\left|\mathrm{W}_{c,j}(f,t)\right|^2} \right|^2$$

The procedure for computing phase-locking is nearly identical to the complex-domain average of Fourier coefficients which is commonly used to estimate constant phase SSVEP signals, but with one important feature. With this measure, the amplitude information contributing to the complex-domain average for each trial is normalized out. Thus PLI is purely a measure of the degree to which phase is consistent across trials. Signals with perfect phase consistency (such as a pure sinusoid) will show PLI values of 1, whereas signals with random phase across trials (such as random noise) will show PLI near zero.

Next, for each switch condition we averaged these phase locking indices over flicker frequencies depending on whether they were switched-to, or switched-from. So, for example, for LR trials we computed switch-to phase locking index by averaging phase locking indices at 30 Hz from L20R30 trial, and at 20 Hz from L30R20. Finally, for each subject we interpolated time series' for the subset of excluded bad channels, and averaged the complete set of channels across subjects. Upon examining the scalp topographies of these signals, computed for each switch condition by averaging the time series across the post-switch interval, we observed the clear patterns with distinct focal maxima over parieto-occipital electrodes depending on whether the flicker was presented in the Left or Right visual hemifield (see figures 10-11). This allowed us to define two channel groups corresponding to the left flicker, and right flicker respectively. Averaging our phase locking power time series over channels in each group, we obtained a single pair of SSVEP/F time series measures characterizing the attentional modulation of the

steady-state response for comparison across switching conditions. In the LR switch condition, responses evoked by the flicker on the left/right constitute the “switched-to” and “switched-from” signals, respectively. Conversely for RL trials, responses evoked by the flicker on the left/right constitute the “switched-from” and “switched-to” signals.

Bootstrap Significance tests. The procedure detailed above resulted in our obtaining a pair of contralateral/ipsilateral signals in each band, as well as a pair of SSVEP/F signals corresponding to the flickers which were “switched-to”, and switched-from”. Together, these signals characterize the temporal modulation of low-frequency and steady-state responses for the switch conditions in our experiment. For the purposes of significance testing we computed bootstrapped distributions of each of our four signals in each switching condition. To accomplish this we repeated the same procedures detailed above a total of 1000 times, except that, instead of averaging over the full set of trials, for each repetition we randomly sampled the full set of trials with replacement and averaged our measures over these bootstrap samples. This procedure resulted in a set of distributions of bootstrapped time series which characterize the variability of each of our signals in each attention condition.

3. Results

Behavioral Results. For each subject, the staircase procedure we used to set target thresholds determined the fraction of bars within each target frame that shared the same orientation. Subjects had independent thresholds for each of four trial types (20/30Hz displayed on the Left/Right). Average target threshholds across trial types for each subject were 25%, 30%, 31%, 63%, 44%, 27%, and 64% for subjects 1-7, respectively. Subjects 1-3, and 5 had all been participants in previous attention experiments conducted

in our lab, and so were able to detect very subtle targets, whereas subjects 4, and 7 had not had previous experience with these types of stimuli, and so required targets have greater saliency in order to detect them. Subject 5 was participant in previous attention experiments, but fell between these two groups at 44%. This is because he was the only subject whos thresholds were biased for a specific trial type (standard deviation of thresholds across trial types for all other subjects was less than 5%). This subject was less able to detect the 30 Hz targets, with thresholds for Left/Right 30 Hz targets at 49 /56%, and for Left/right 20 Hz targets at 37, and 33%. The subject was thus able to detect 20 Hz targets at levels comparable to our other mastered subjects, but required more salient 30 Hz targets for detection.

Target detection rates during the actual experiment averaged 71% across subjects, with standard deviation of 12%. Average hit rates for individual subjects are summarized in table 1. Subject 5 was excluded from our behavioral analysis due to this subject's error in indicating his responses. Throughout the experiment, subjects had to keep their index finger in position on a response pad which blocked the path of a beam of light- momentarily lifting their finger from this default position indicated a response. The failure was the result of the subject not consistently returning their finger in position to interfere with the light sensor.

Subject	**Attend Left**	**Attend Right**	**Attend 20 Hz**	**Attend 30 Hz**	**Average**
S1	73.78%	52.74%	61.37%	65.15%	63.61%
S2	79.56%	79.86%	75.92%	83.50%	79.81%
S3	60.70%	71.80%	75.35%	57.15%	66.32%
S4	71.80%	58.99%	65.65%	64.36%	65.09%
S5*	N/A	N/A	N/A	N/A	N/A
S6	82.42%	92.22%	90.03%	84.61%	86.96%

S7	86.41%	78.05%	78.94%	85.52%	82.33%

Band-pecific baseline power. Figure 2 shows grand averaged EEG/MEG wavelet power in the alpha (2a,b), mu (2c,d) , and theta bands (2e,f). Wavelet power in each band was first averaged across all trials of both switching directions, and then averaged across all time points, resulting in a single estimate of power at each of our 128 electrodes/102 magnetometers. Throughtout the switching interval, baseline power was higher in the alpha and theta bands than in the mu-band. However, power topographies for all three bands were very similar. In each band we see symmetric bilateral foci over the back of the head. These foci sit over occipital parietal sensors in both the EEG/MEG. These patterns are important because it is primarily the activity over these foci which is modulated by the attentional switch. As such, they provide our baseline for normalization, allowing us to better illustrate the divergent temporal dynamics which occur over ipsilateral/contralateral hemispheres in response to an attentional switch.

Temporal structure of alpha-band lateralization. Figures 3 and 4 show alpha-band wavelet power

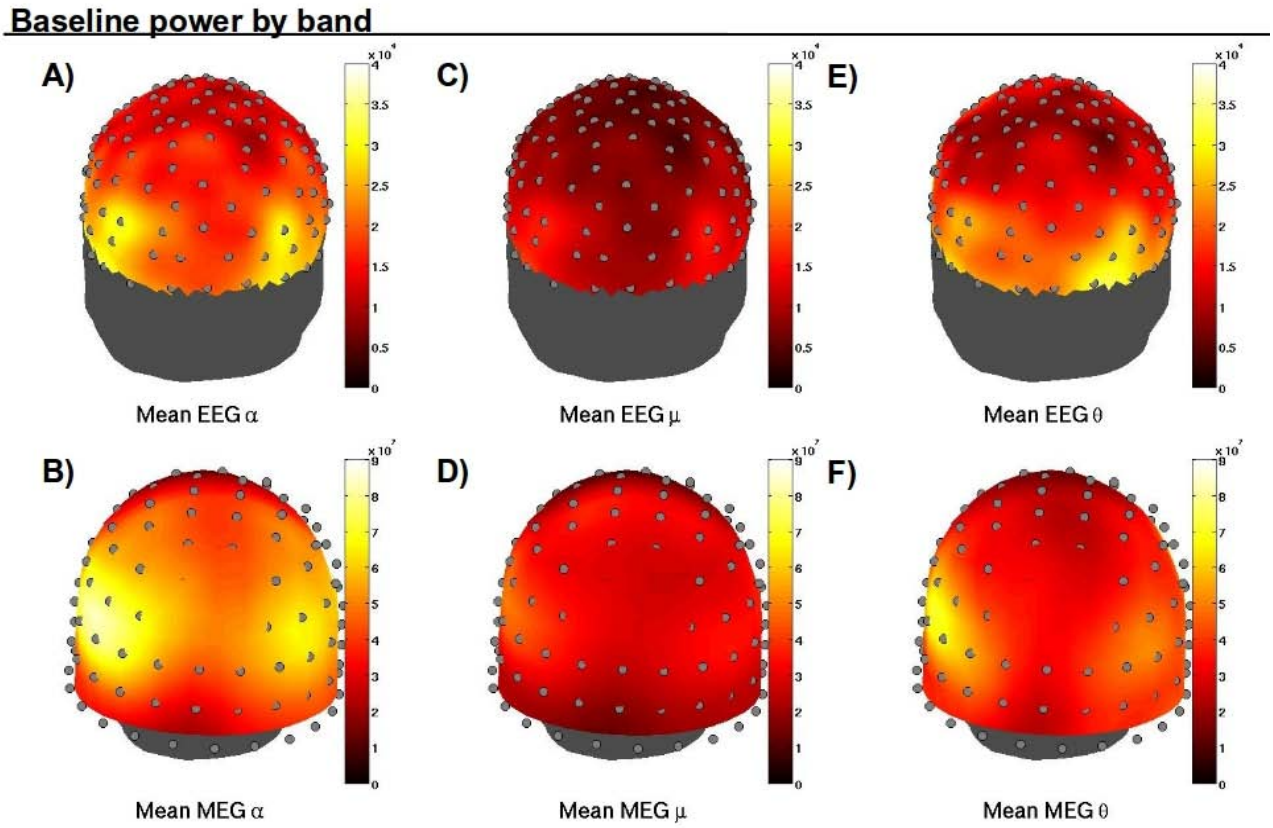

Figure 2. Baseline EEG/MEG wavelet power is shown for each band. Wavelet power in each band was grand averaged over all time points in the pre to post-switch interval. Topographies in each band, which show bilateral foci over occipito-pareital sensors, demonstrate the spatial structure of our normalization baseline. Band-specific power over these foci is modulated by attentional switches.

over Left/Right channel groups as it unfolds throughout the pre and post-switch interval for switch Left-to-Right (LR) and Right-to-Left (RL) conditions, respectively. Figures 3a,c and 4a,c show normalized wavelet power averaged over all time points in the post-switch interval. These topographies illustrate that after the switch, power over the cerebral hemisphere contralateral to the new attended location decreases with repsect to the baseline pre-switch. Likewise, power in the corresponding ipsilateral hemisphere increases in response to the switch. In the alpha-band, these lateralization patterns were more symmetrical, and the modulations slightly larger in magnitude for the EEG data than for the MEG. As described in our methods section, we identified sensors in

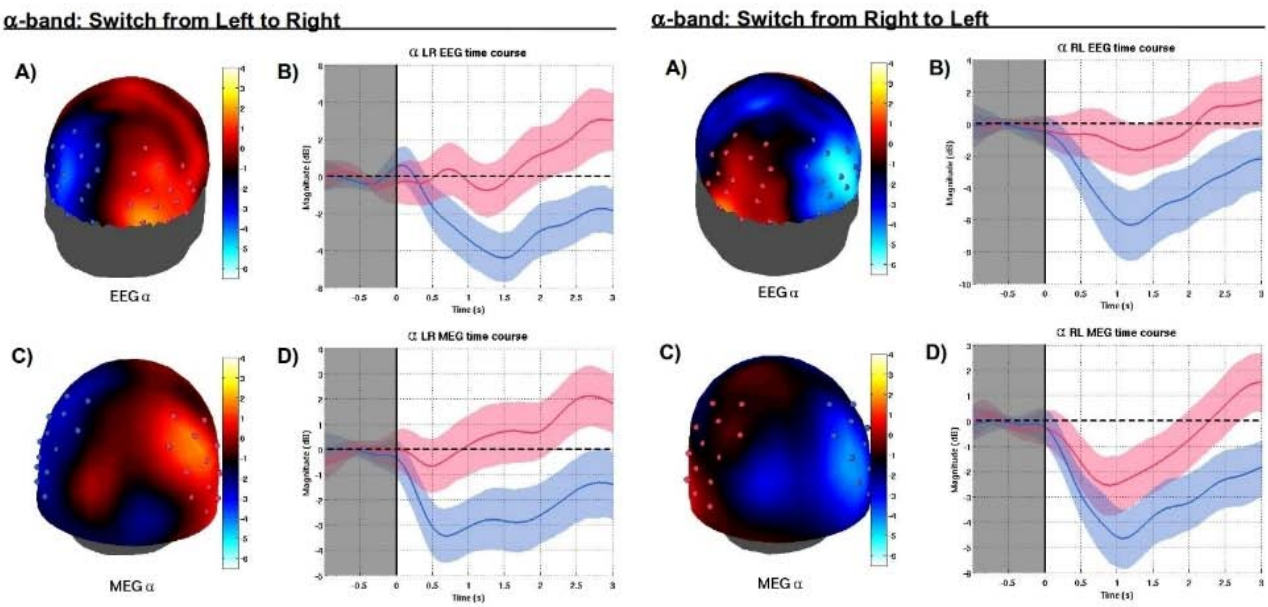

Figure 3 (left). and **Figure 4 (right).** Alpha-band wavelet power over Left/Right channel groups is shown throughout the pre and post-switch interval for LR (Figure 3), and RL (Figure 4) conditions, respectively. Figures 3a,c and 4a,c show normalized wavelet power averaged over all time points in the post-switch interval. After the switch, power over the cerebral hemisphere contralateral to the new attended location decreases with repsect to the baseline pre-switch. Power in the corresponding ipsilateral hemisphere increases in response to the switch. As described in methods, we identified sensors in symmetric groups over each hemisphere which showed maximal positive (pink dots) and negative (blue dots) modulations. The time course of normalized wavelet power is shown averaged over channels in each group in figures 3b,d, and 4b,d. Soon after the switch, contralateral alpha (shown in blue) begins to decrease, whereas ipsilateral alpha (shown in pink) begins its corresponding increase much later. Bootstrapped confdence intervals indicate that these effects all reach statistical significance during the post-switch interval.

symmetric groups over each hemisphere which showed maximal positive and negative modulations. By convention, these

sensors will always be indicated by blue dots for groups over the contralateral hemisphere, and by pink dots for ipsilateral groups. The time course of normalized wavelet power is shown averaged over channels in each group in figures 3b,d, and 4b,d. One clear pattern was observed for both EEG and MEG data in both switching conditions- very soon after the switch, contralateral alpha (shown in blue) begins to decrease, whereas ipsilateral alpha (shown in pink) begins its corresponding increase much later. Our bootstrapped confdence intervals indicate that the contralateral decrease

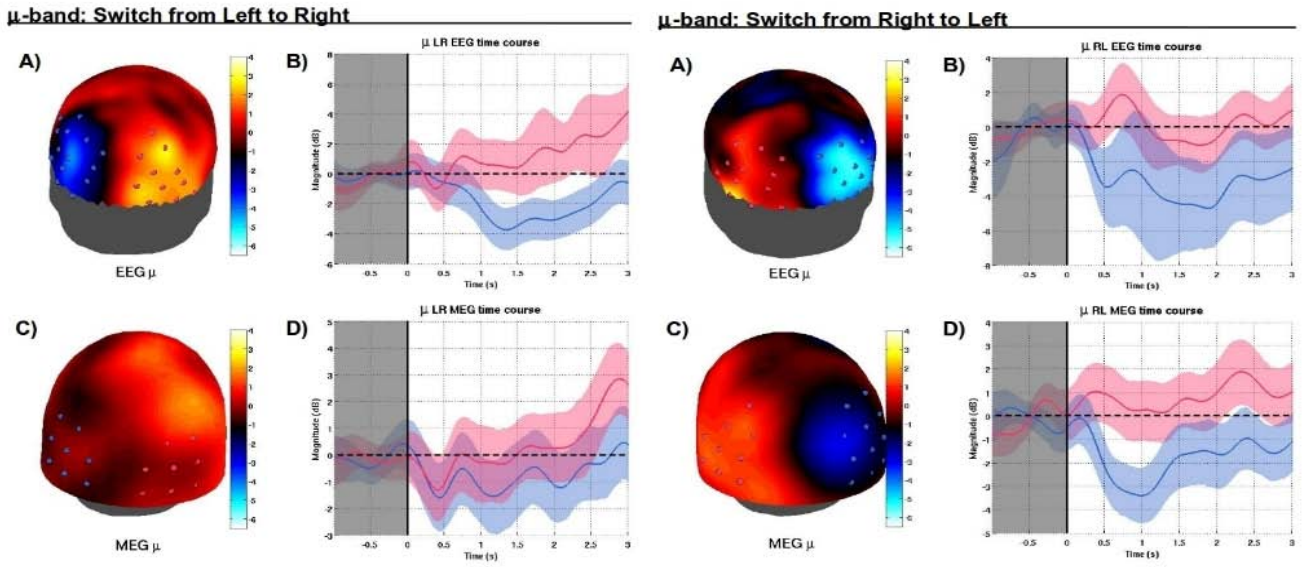

Figure 5 (left). and **Figure 6 (right).** Wavelet power in mu-band Left/Right channel groups shown as it unfolds throughout the switch interval. Comparison of data shown here with that shown for the adjacent alpha band (Figure 3,4) suggest that the dynamics underlying attentional modulation of the mu-band are likely the same as those underlying the alpha band.

reaches significance for both data types and switch conditions within the first half-second after the switch, and remain significantly diminished throughout the rest of the interval. Increases in ipsilateral alpha reach significance between 2-3 seconds after the switch for LR EEG/MEG (fig 3b,d), and RL MEG (fig 4d). For RL EEG the ipsilateral alpha increase does not technically reach significance in the post-switch interval, although it comes very close (fig 4b). Although not pictured in the figures, signicifance testing of the difference between the ipsilateral and contralateral curves reveals that the two become significantly different from one another in the first half-second after the switch. In the RL switch condition, this occurs at roughly the same time in the EEG and MEG (284/256 ms post-switch, respectively). In the LR condition, these times are not as similar (430, and 118 ms post-switch for EEG/MEG, respectively). In one condition, the RL MEG, we observed a highly significant decrease in ipsilateral MEG power which had similar temporal structure as that observed for contralateral power. We interpreted this as an

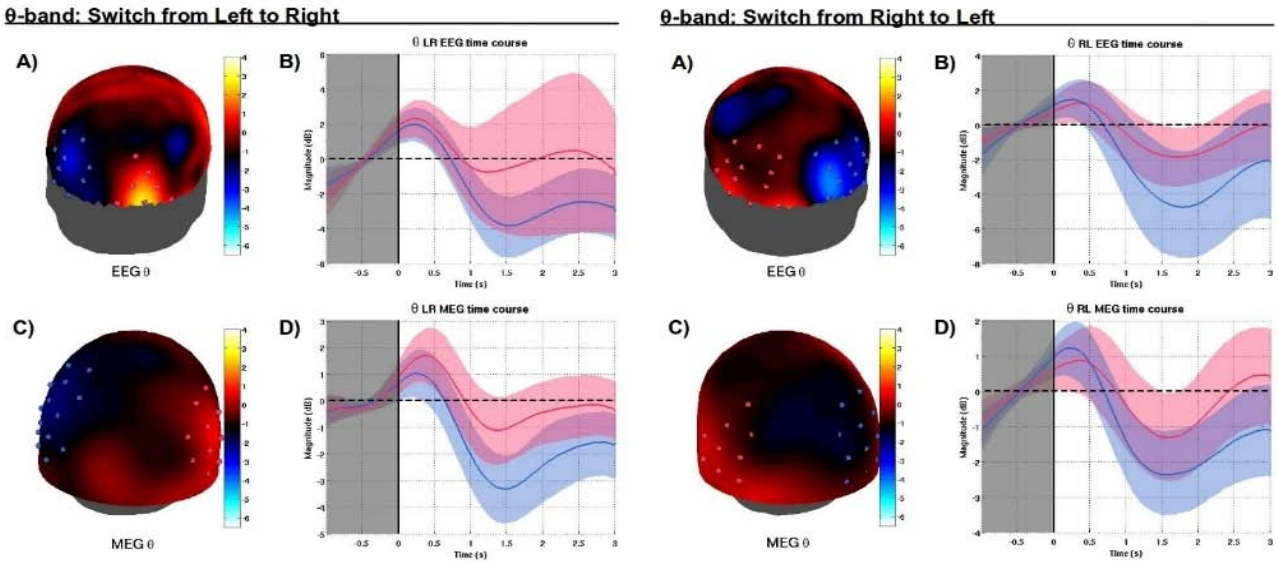

Figure 7 (left). and **Figure 8 (right).** Theta-band wavelet power over Left/Right channel groups as it unfolds throughout the switch interval. The dynamics of this bandare fundam entally different from those of the previous two, as in all cases, there is a significant increase in both ipsilateral and contralateral theta power which reaches significance within the first half-second after the switch. The uniformity of this pattern suggests a global response to the switch itself. These data suggest the possibility that two distinct attention related signals may overlap in the theta-band. One which results in sustained divergence between overall levels of contralateral and ipsilateral power, similer to that seen in previous bands, and another which is elicited globally by the switch.

indication of weak lateralization in this condition. Taken all together, these data clearly demonstrate that our experimental manipulation induced systematic modulations of alpha-band power in lateralized sensor groups which evolved with stable temporal structure after the switch.

Temporal structure of mu-band lateralization. Figures 5 and 6 show mu-band wavelet power over Left/Right channel groups as it unfolds throughout the switch interval. The evolution of contralateral/ipsilateral power in this band, though less pronounced in magnitude, is similar in structure as that observed for alpha. Contralateral mu-band power decreases significantly within the first half-second after the switch in three cases: the RL EEG/MEG, and the LR MEG (fig 6b,d and fig 5d). Contralateral power in the LR EEG take longer, but also become significantly decreased around 800 ms after the switch (fig 5b). Contralateral MEG in the LR condition reaches significance

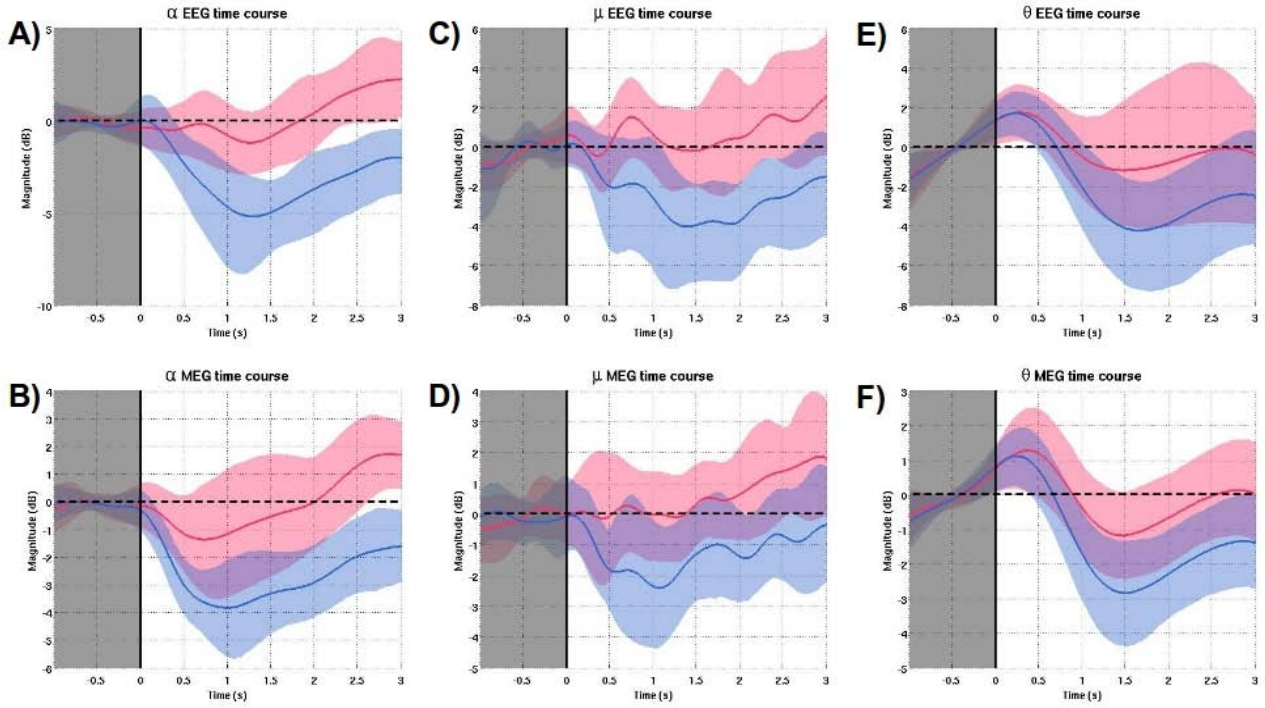

Figure 9. Trial averages for these contralateral (blue) and ipsilateral (pink) signals are shown collapsed across LR and RL switch conditions, along with corresponding condifence intervals obtained from the collapsed pool of trials from each attention condition. The gross features of our signals are faithfully represented in the pooled data. In the alpha and mu bands, decreases in contralateral power reach significance very soon after the switch, whereas rises in ipsilateral power occur much later. In the theta band, increases in both ipsilateral and contralateral power occur almost immediately after the switch.

only for two brief episodes after the switch (fig 5d). Scalp topography for this data confirms that MEG lateralization recorded across the hemispheres in this condition was very weak (fig 5c). Again we observe that increases in ipsilateral mu-power take much longer to emerge, eventually reaching significance in three cases (LR-EEG/MEG, and RL-MEG) between 2-3 seconds after the-switch. The magnitude of divergence between the two signals is also less pronounced, though it does reach significance in all cases. This occurs earlier in the RL condition (263 and 236 ms for EEG/MEG respectively) than it does for the LR condition (645 and 1090 ms for EEG/MEG, respectively). Our data suggest that the dynamics underlying attentional modulation of the mu-band are probably

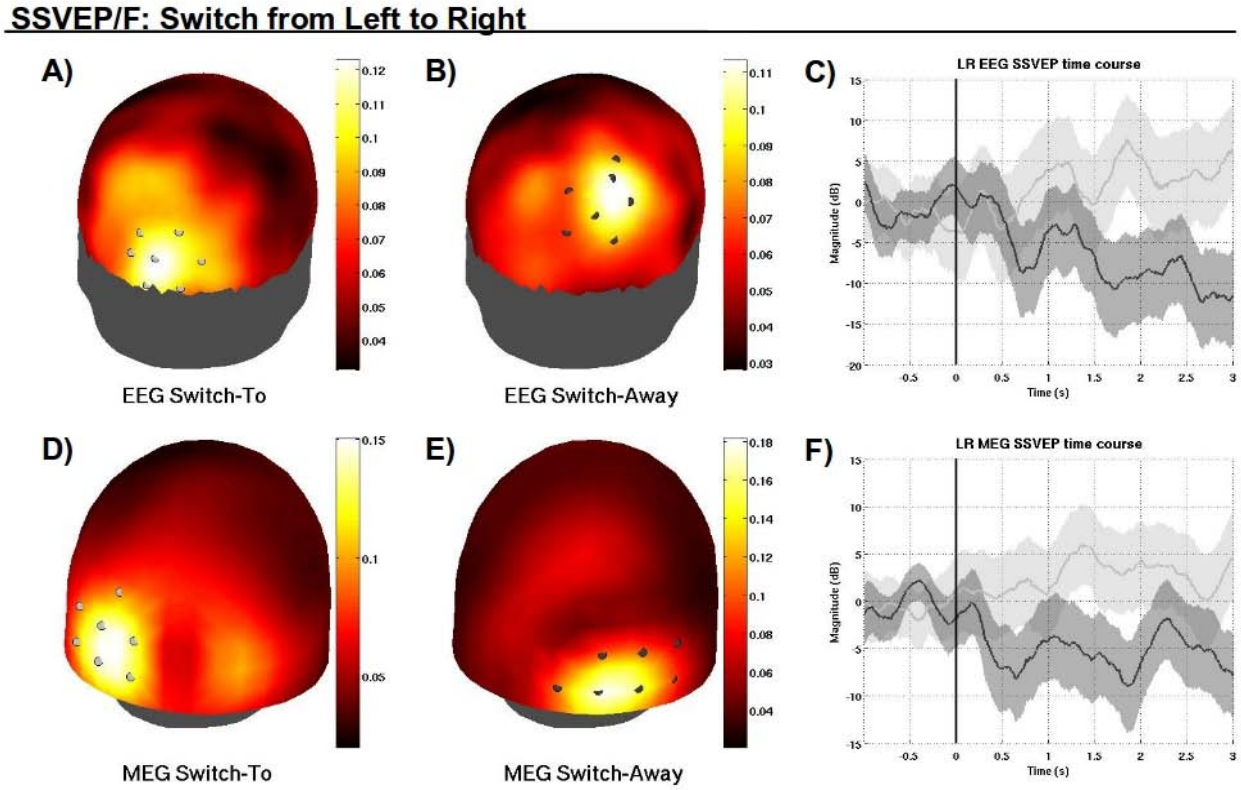

Figure 10. Topographic, and temporal structure of SSVEP/F wavelet power as it unfolds throughout the pre and post-switch interval for LR switch condition. SSVEP/F were analyzed in terms of whether it was "switched-to" or "switched-from". In all cases, the observed topographies showed a single major focus of activity over a small number of adjacent channels which, lateralized nicely to the hemisphere contralateral to the flicker, indicating that subjects were indeed maintaining fixation, and not foveating on the attended flicker. We averaged the switch-to/from responses over the sensors overlaying the peaks observed in the corresponding topographies (indicated by light grey dots for switch-to responses, and by dark-grey for switch-from). The temporal evolution of the SSVEP/F are shown throughout the switch interval for both of these averaged switch-to and switch-from responses (fig 10c,f), and show that switch-to and switch-from steady-state responses modulate in opposite directions after the switch, demonstrating that spatial attention facilitates gain in the attended SSVEP/F.

the same as those underlying the adjacent alpha band, but are simply less influential in effecting changes in this band.

Temporal structure of theta-band lateralization. Similar to figures 3-6 for the alpha and mu-bands, figures 7 and 8 show theta-band wavelet power over Left/Right channel groups as it unfolds throughout the switch interval. The dynamics of this band, however, are fundamentally different from those of the previous two. The most unique feature of this

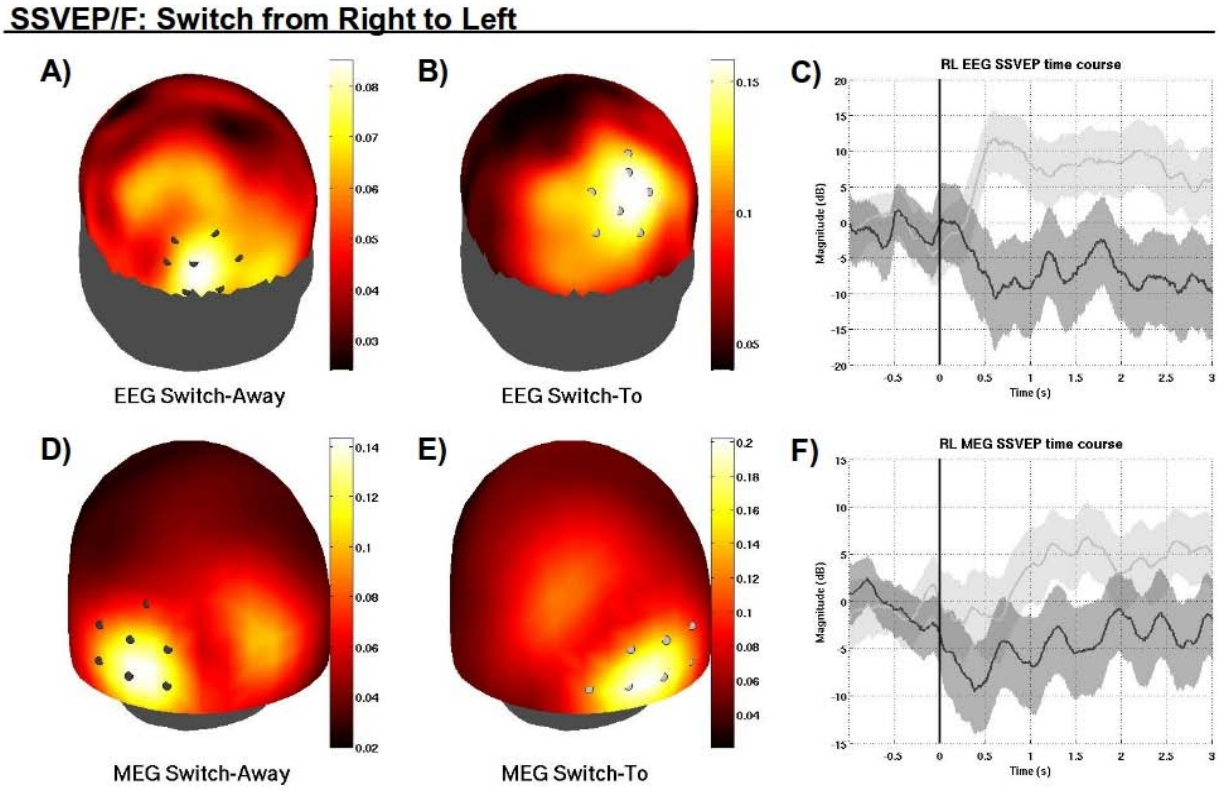

Figure 11. Topographic, and temporal structure of SSVEP/F wavelet power as it unfolds throughout the pre and post-switch interval for RL switch condition, illustate similar results as were observed for the oppsoite switch case in figure 10.

data is that, in all cases, there is a significant increase in both ipsilateral and contralateral theta power which reaches significance within the first half-second after the switch. The uniformity of this pattern suggests a global response to the switch itself. Soon after, a decrease in both ipsilateral and contralateral signals follows (which reaches significance in the RL data), followed again by steady-increases towards the end of the signal. However, unlike the alpha and mu-bands, after the first half-second of the switch interval, no theta signals show a significant increase. Significant divergences between the contralateral/ipsilateal signals do develop though, in most cases much later than observed for previous bands (1145 and 881 ms for RL EEG and MEG, respectively, 868 ms for LR EEG), though almost immediately for the LR MEG (48 ms). Taken together these data suggest the possibility that two distinct attention related signals may overlap in the theta-

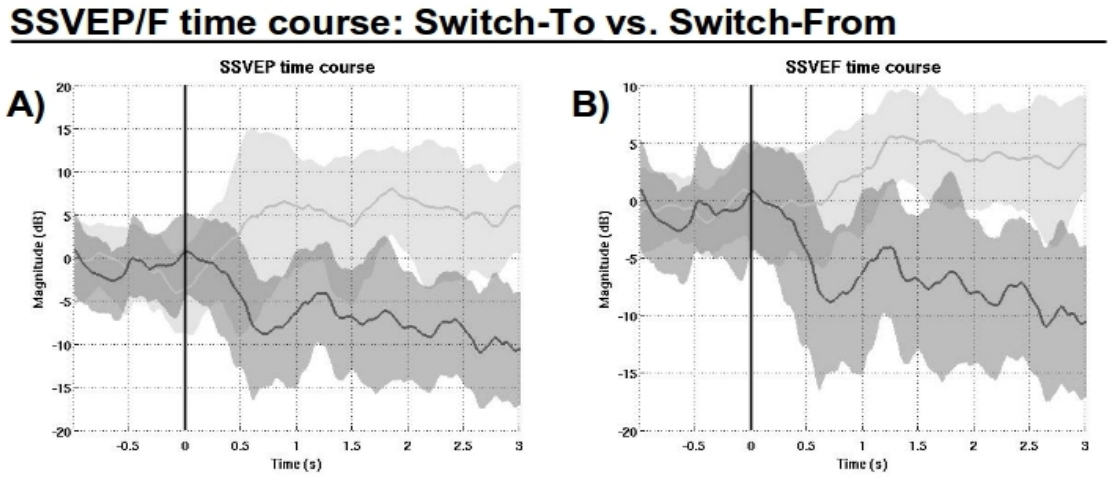

Figure 12. The time course of averaged switch-to/from SSVEP (A), and SSVEF (B) are shown along with bootstrapped confidence intervals based on trials pooled across attention conditions. In both the SSVEP/F, decreases in switch-from power reach significance in the first second post-switch (roughly 600 ms for both the SSVEP/F), whereas the corresponding increases in switch-to SSVEP reach significance noticeably later (around 1700, 1200 ms for the SSVEP/F respectively). Interestingly, for both the switch-to and switch-from responses, these modulation latencies are intermediate with respect to those observed for the contra/ipsilateral signals in the alpha and mu-bands, where contralateral decreases occurred within the first half-second, and ipsilateral increases occurred towards the end of the analyzed interval, between 2-3 seconds after the switch.

band. One which results in sustained divergence between overall levels of contralateral and ipsilateral power, similaer to that seen in previous bands, and another which is elicited globally by the switch itself.

Ipsilateral vs. Contalateral Signals. Having analyzed our switching conditions independently, we feel the resultant ipsilateral/contralateral signals are sufficiently similar in their gross characteristics to conduct a single analysis of the two, keeping in mind that in LR trials the ipsilateral/contralateral trials originate from group of sensors over the right/left sensors, and vice versa for the RL trials. Trial averages for these two signals are shown in figure 9, along with corresponding condifence intervals obtained from the collapsed pool of trials from each attention condition. The gross features of our signals are indeed faithfully represented in the pooled data. Namely, in the alpha and mu bands decreases in contralateral power reach significance very soon after the switch

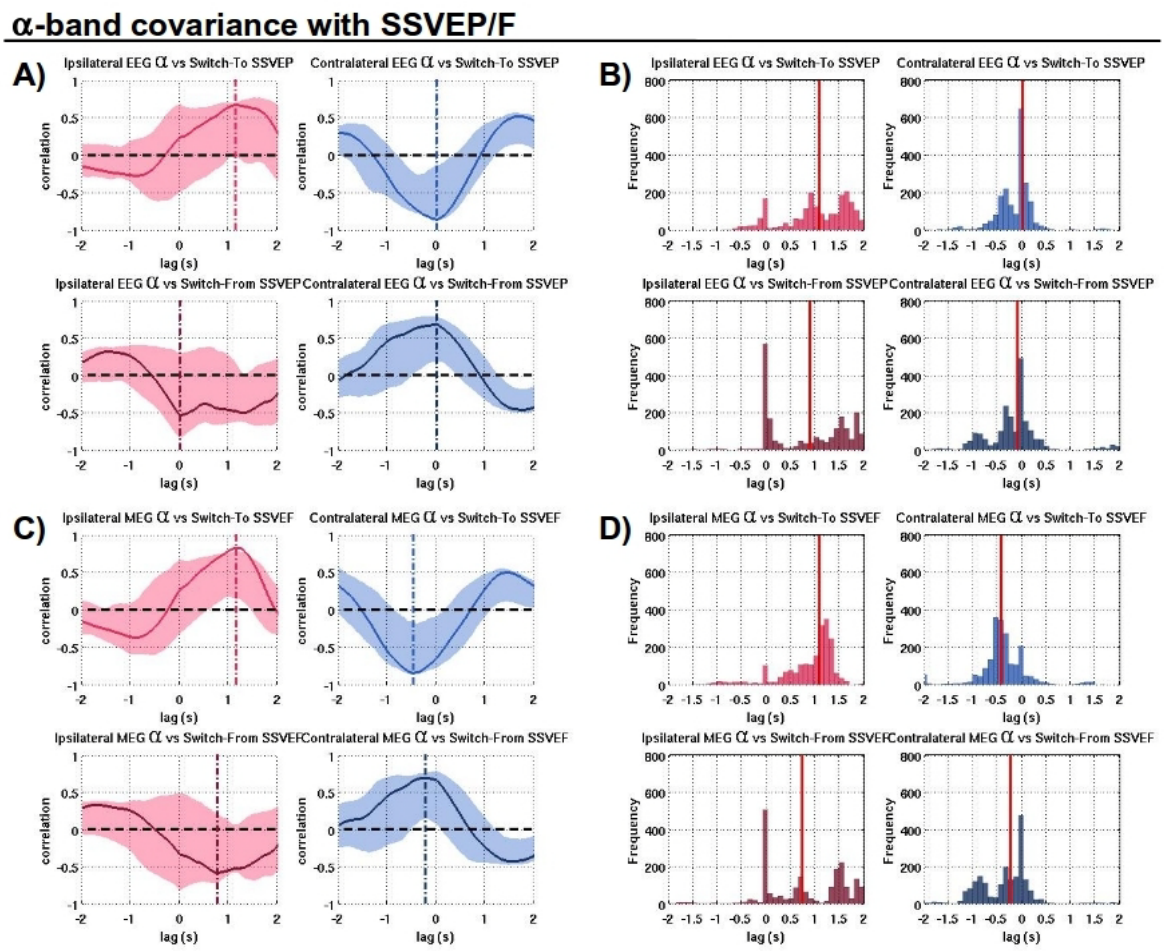

Figure 13. Cross-covariance estimates between the switch-to/from SSVEP/F, and contra/ipsilateral alpha band signals, as a function of lag. Lags represents the relative time shift between the two signals, positive or negative, at which covariance is computed. By convention, negative lags indicate the low-frequency signal leading the SSVEP/F, and vice versa for positive lags. Also shown are bootstrapped confidence intervals, obtained by computing cross-covariance between signals for each of our 1000 bootstrap samples. Contralateral alpha signals (blue) show negative covariance with the switch-to SSVEP/F, and positive covariance with the switch-from SSVEP/F. Conversely, ipsilateral alpha signals show significant positive correlations with the switch-to SSVEP/F, and corresponding negative covariance with the switch-from SSVEP/F. This general pattern reflects the fact that, after the switch, contralateral alpha and witch-from SSVEP/F decrease, whereas ipsilateral alpha and switch-to SSVEP/F increase. A pattern with respect to the relative timing of these covariances is also apparent. Contralateral covariance with both SSVEP/F signals peaks at or before zero, whereas ipsilateral covariance with the SSVEP/F generally peaks much later. To further quantify this effect we show histograms of the lags for which each bootstrap sample obtains its maximum covariance (right). For the contralateral EEG (fig 13B) these distributions are centered on zero (medians indicated in red), whereas for the contralateral MEG (Fig 13D) they are centered at roughly -350 and -500 ms for covariance with respect to the switch-to and switch-from SSVEF, respectively. In contrast, distributions for ipsilateral alpha are centered on larger positive lags. These results ullustrate that contralateral decreases in alpha band power precede attentional modulation of our gamma-band SSVEP/F, whereas the corresponding ipsilateral increases trail them.

(within the first 500 ms for all but the mu-band EEG), whereas rises in ipsilateral power occur much later. In the theta band, increases in both ipsilateral and contralateral power occur almost immediately after the switch. Finally, pooled bootstrapped estimates of time to divergence between the ipsilateral/contralateral signals indicates that significant divergence occurs within the first half second after the switch in the alpha band (402 and 215 ms for EEG/MEG respectively). This is followed by later divergence in the mu-band (611 and 1000 ms for EEG/MEG respectively), and theta-bands (1215 and 8403 ms for EEG/MEG respectively).

Temporal structure of the gamma-band SSVEP/F. Figures 10 and 11 show topographic, and temporal structure of SSVEP/F wavelet power as it unfolds throughout the pre and post-switch interval for LR (fig 10) and RL (fig 11) switch conditions. For each attention condition, SSVEP/F were analyzed in terms of whether it was "switched-to" or "switched-from". So, for example, for LR trials, the switch-to/from SSVEP/F correspond to the flicker that was presented on the right/left, respectively. In all cases, the observed topographies showed a single major focus of activity over a small number of adjacent channels. Naturally, these groups were the same for LR/RL switch-to/from, and LR/RL switch-from/to responses, as data in these corresponding conditions were evoked by the same flicker. Moreover, these grouping lateralized nicely to the hemisphere contralateral to the flicker, although this lateralization was more obvious for our MEG data (fig 10d,e, and fig 11d,e) than it was for our EEG data (fig 10d,e, and fig 11d,e) for which evoked responses were closer to midline. Such lateralized responses are what we would expect should be evoked by our peripheral stimuli, and indicates that subjects were indeed maintaining fixation, and not foveating on the attended flicker. As described in

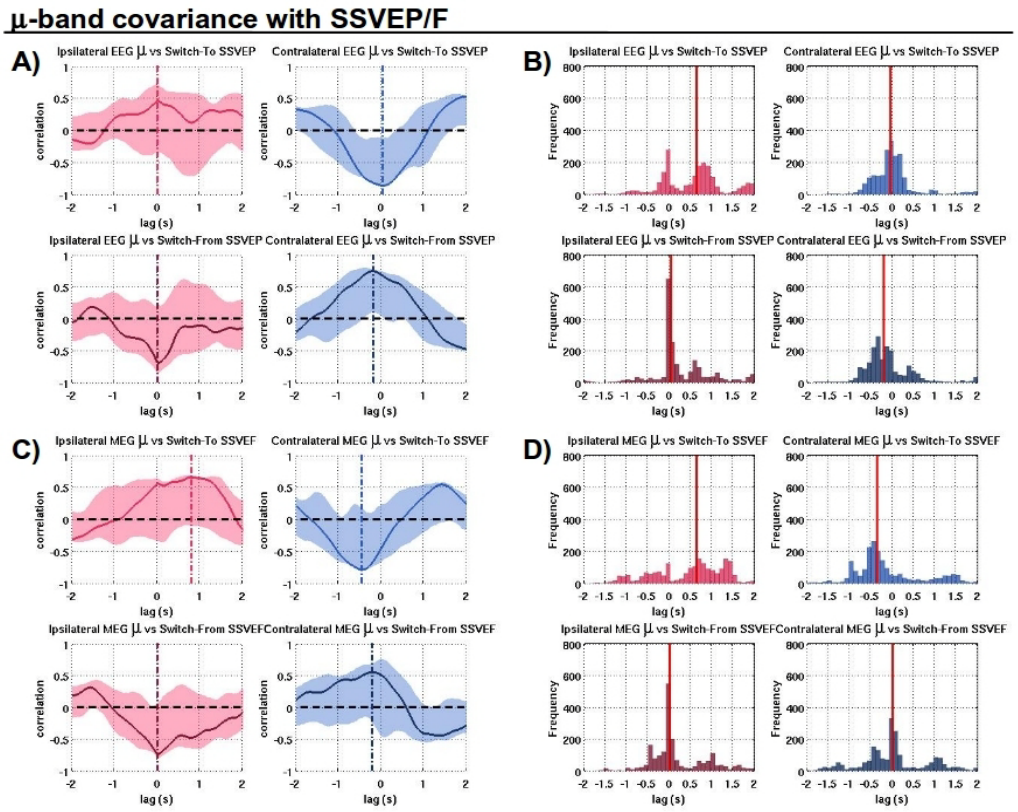

Figure 14. Similar patterns are apparent in the covariance between the SSVEP/F and our mu-band attention signals as were observed for the alpha-band. The primary difference observed between the mu and alpha band is that covariance rarely reaches significance. It does, however, reach significance between the contralateral EEG and both SSVEP/F responses. For the contralateral mu and switch-to SSVEP, covariance peaks at zero, whereas for the contralateral mu and switch-from SSVEP it peaks just before. Histograms of lags corresponding to maximal covariance for the bootstrap samples confirms these timings. Again, these data would seem to suggest that atttentional modulations of contralateral mu precede those of the stimulus evoked response.

methods, we averaged the switch-to/from responses over the sensors overlaying the peaks observed in the corresponding topographies. By convention, these sensors are always indicated by light grey for switch-to responses, and by dark-grey for switch-from. The temporal evolution of the SSVEP/F are shown throughout the switch interval for both of these averaged switch-to and switch-from responses (fig 10cf, and fig 11c,f). In most cases, significant decreases in the switch-from SSVEP/F generally precede significant increases in the switch-to SSVEP/F. This trend is clearest in the LR data, in which decreases in switch-from SSVEP occur within the first second post-switch (roughly 650

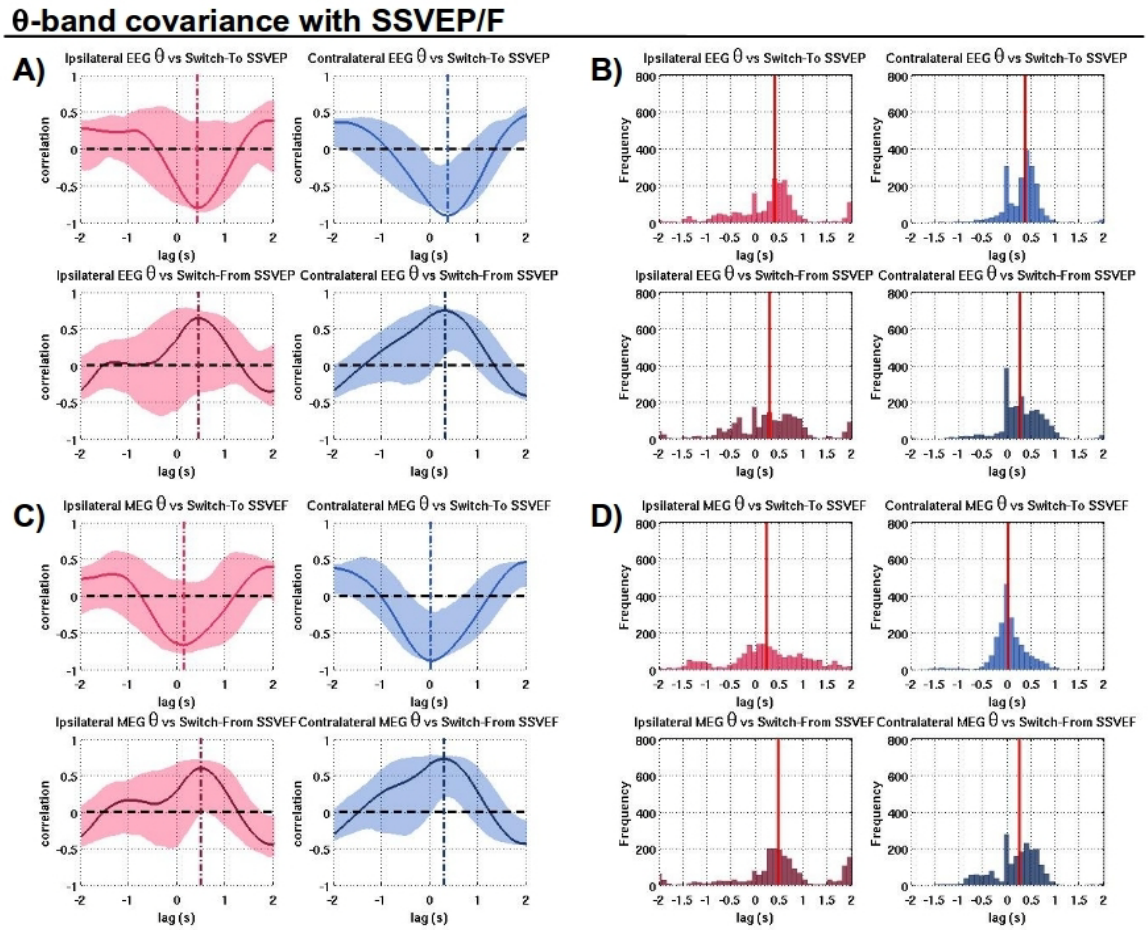

Figure 15. Covariance between contra/ipsilateral theta band signals and the SSVEP/F show a different structure than was observed for the previous two bands. In this band, the ipsilateral and contralateral covariance functions with respect to the SSVEP/F show peaks of the same sign. Both the contralateral and ipsilateral signals covary negatively with the switch-to SSVEP, and positively with the switch-from SSVEP/F. These covariances reach significance primarily for contralateral covariance, but the general pattern is the same for corresponding ipsilateral signals. The lags at which these covariances peak lie between 0-500 ms in all cases, suggesting the the attentional modulation of contra/ipsilateral signals in this band trail that of the SSVEP/F modulations.

ms and 350 ms for EEG/MEG, respectively), but for which the corresponding increase in switch-to data develops later, between 1-2 seconds post-switch. In the RL data, the same trend is clear for the SSVEF. Here we see decreases in switch-from SSVEF reaching significance almost immediately after the switch, whereas the corresponding increase reaches significance around 1100 ms. The one exception to this trend is the RL SSVEP, for which modulations of both signals reach significance in the first half second after the

switch. Still, we felt the SSVEP/F data similar enough between our two switching conditions to pool data across them, and analyze the evoked responses solely in terms of whether it was switched-to or switched-from, but keeping in mind that that now these signals derive from different channel groups. The time course of these averaged switch-to/from SSVEP/F are shown in figure 12, along with bootstrapped confidence intervals based on trials pooled across attention conditions. In both the SSVEP/F, the general pattern remains the same. Decreases in switch-from power reach significance in the first second post-switch (roughly 600 ms for both the SSVEP/F), whereas the corresponding increases in switch-to SSVEP reach significance noticeably later (around 1700, 1200 ms for the SSVEP/F respectively). It is interesting to note that, for both the switch-to and switch-from responses, these modulation latencies fall squarely between those observed for the contra/ipsilateral signals in the alpha and mu-bands, where contralateral decreases occurred within the first half-second, and ipsilateral increases occurred towards the end of the analyzed interval, between 2-3 seconds after the switch.

Alpha-band covariance with the SSVEP/F. To further quantify the temporal relationships between our low-frequency signals and steady-state evoked responses, we looked at cross-covariance estimates between the switch-to/from SSVEP/F, and contra/ipsilateral signals in each band. Figure 13 shows cross-covariance as a function of lag for each combination of signals (14a, and c for EEG/MEG respectively). Lags represents the relative time shift between the two signals, positive or negative, at which covariance is computed. By convention, in these and the plots that follow, negative lags indicate the low-frequency signal leading the SSVEP/F, and vice versa for positive lags. Also shown for each case are bootstrapped confidence intervals,

obtained by computing cross-covariance between signals for each of our 1000 bootstrap samples. For both the EEG and the MEG, a general pattern is clear. Contralateral alpha signals (blue) show strong, significant negative covariance with the switch-to SSVEP/F, and likewise show significant positive covariance with the switch-from SSVEP/F. Conversely, ipsilateral alpha signals show significant positive correlations with the switch-to SSVEP/F. These ipsilateral signals also show corresponding negative covariance with the switch-from SSVEP/F although these are weaker and fail to reach significance in the EEG or MEG. This general pattern reflects the simple trend we have already described- that after the switch, contralateral alpha and switch-from SSVEP/F decrease, whereas ipsilateral alpha and switch-to SSVEP/F increase.

A pattern with respect to the relative timing of these covariances is also apparent. Indicated by dashed lines in these plots are the lag values at which covariance magnitude obtains it maximum. Contralateral covariance with both SSVEP/F signals peaks at or before zero- a trend that is especially obvious in the MEG- whereas ipsilateral covariance with the SSVEP/F generally peaks much later. The only case in which this is not so is the covariance between the ipsilateral EEG and the switch-from SSVEP, for which our covariance never reach significance to begin with. To further quantify this effect, in figure 13 b, and d we show histograms of the lags for which each bootstrap sample obtains its maximum covariance. For the contralateral EEG (fig 13b) these distributions are centered on zero (medians indicated in red), whereas for the contralateral MEG they are centered at roughly -350 and -500 ms for covariance with respect to the switch-to and switch-from SSVEF, respectively. In contrast,

distributions for ipsilateral alpha are centered on larger positive lags. Taken together, these results tell a simple story- contralateral decreases in alpha band power precede attentional modulation of our gamma-band SSVEP/F, whereas the corresponding ipsilateral increases trail them.

Mu-band covariance with the SSVEP/F. The patterns apparent in the covariance between the SSVEP/F and our mu-band attention signals are precisely the same as those noted above for the alpha-band. Still, to be thorough we have included them in figure 14. The primary difference observed between the mu and alpha band is that covariance rarely reaches significance. It does, however, reach significance between the contralateral EEG and both SSVEP/F responses. For the contralateral mu and switch-to SSVEP, covariance peaks at zero, whereas for the contralateral mu and switch-from SSVEP it peaks just before. Histograms of lags corresponding to maximal covariance for the bootstrap samples confirms these timings. Again, these data would seem to suggest that atttentional modulations of contralateral mu precede those of the stimulus evoked response.

Theta-band covariance with the SSVEP/F. Covariance between contra/ipsilateral theta band signals and the SSVEP/F show an altogether different structure than was observed for the previous two bands (Figure 15). In clear contrast to the alpha and mu bands, the ipsilateral and contralateral covariance functions with respect to the SSVEP/F show peaks of the same sign. Thus we see that both the contralateral and ipsilateral signals covary negatively with the switch-to SSVEP, and positively with the switch-from SSVEP/F. There is sufficient variance in the data in this band so that these covariances reach significance primarily for contralateral covariance, but the general pattern is the same for corresponding ipsilateral signals. The lags at which these covariances peak lie

between 0-500 ms in all cases, suggesting the the attentional modulation of contra/ipsilateral signals in this band trail that of the SSVEP/F modulations.

4. Discussion

The results of our experiment concern the dynamic structure of covert visual spatial attention. These results bear on the time course of attentional gains/losses afforded to the responses evoked by attended/unattended visual stimuli. In addition, they bear on the dynamic structure of attentional modulation of endogenous low-frequency activity, and the differences within this structure observable across frequency bands, and cerebral hemispheres. Finally, the most novel aspect of our results concern the *relative* timing of attentional modulations of these endogenous, and stimulus evoked signals.

The interpretation of the time course of attentional gain is complicated by the variability observed in our data. Gains in switched-to SSVEP/F did not reach significance until much later after the switch (1200 ms for MEG, 1700 ms for EEG), than the 600-800 which was reported by Müller et al. (1998). However, we note that the average SSVEP waveform we observed showed a rise from pre-switch levels which reached its plateau precisely within this 600-800 ms interval. Moreover, the latency with which the differences between switch-to and switch from SSVEP/F power became significant (652 ms for EEG, 569 ms for MEG) also suggest an earlier facilitation of attention than the latency to significance we observed. This figure is also in agreement with another more recently conducted study by Anderson & Müller which showed the latency of the peak increase in switched-to SSVEP occurred just before 600 ms. However, in this same paper the authors suggest that the time course of the increase in switch-to SSVEP precedes that of the decay of the switch-from SSVEP- a finding which is not explicityly

supported by our results. Interestingly, the corresponding plateau in the MEG waveform was observed to occur later (around the time of significance at 1200 ms). One possible explanation for this is that the SSVEP and SSVEF were being driven by spatially proximate sources with distinct dynamics. This could be the case if, say, the source configuration underlying the response to the flicker was situated within visual cortex primarily upon a gyral surface but extended across and into a sulcal fold as well. If attentional modulation of this source was maximal at the center of this source distribution, and fell off with distance, then the MEG, being maximally sensitive to the sulcal component, could pick up a substantially delayed time course such as the one we observed.

The directionality of the modulation observed for our contra/ipsilateral alpha-band signals is in agreement with numerous previous studied which have demonstrated similar patterns of relative contralateral suppression (Sauseng et al. 2005; Thut et al. 2006; Yamagishi et al. 2005), and ipsilateral rise (Worden et al. 2000; Kelly et al. 2006; Rihs et al. 2007). In these experiments, two general interpretations of results have dominated, both of which are relevant to our findings. Firstly, studies in which ipsilateral alpha increases were reported argue that such alpha signals represent an active inhibitory mechanism which suppresses behaviorally irrelevant components of the visual scene. This idea is in agreement with evidence obtained from studies of attention in cross-modal paradigms, where global alpha increases (not specific to a particular cerebral hemisphere) observed in response to cueing towards auditory stimuli were interpreted as evidence for the anticipatory gating of expected competing visual information (Foxe et al. 1998; Fu et al. 2001). This notion of an active inhibitory mechanism at work in spatial attention is

consistent with fMRI studies which suggest that anticipatory BOLD suppression of areas mapped to competing unattended visual field locations predicts whether subjects will accurately detect difficult targets at attended locations. (Sylvester et al, 2007). Conversely, studies in which contralateral decreases have been reported argue this reflects enhanced excitability of cortical areas processing attended stimuli. Compellingly, these interpretations are consistent with studies in monkeys which show that low-frequency desynchronization in anticipation of visual stimuli at an attended location accompanies increased gamma-band synchrony in response to the stimulus when it arrives (Fries et al 2001).

Our results shed light on both these interpretations, due to our novel framework which allows for the examination of the temporal evolution of both contra/ipsilateral alpha signals in conjunction with those evoked by the attended/unattended stimuli. Our results clearly indicate that increases in alpha (and related mu) band activity over ipsilateral parietal areas occurs only after the response to the switched-from stimulus has already decayed. It would seem then that this activity cannot represent an active inhibitory mechanism of the type suggested by previous authors. Rather, this phenomenon is more parsimoniously explained as the gradual emergence, within relatively idle visual areas, of passive synchronization with global alpha-rhythm. With this interpretation, previous studies which have shown a topographic specificity for the origins of these increased alpha rhythms- focused over ipsilateral parietal cortex with position dependent upon the attended location (Rhis et al. 2007)- *may still suggest focused, active inhibition of these areas*, just not by means of the ipsilateral alpha rhythm itself.

In contrast, the timing of the contralateral desynchronization, which was observed to precede the gain in the response to the attended stimulus, is entirely consistent with an active role for these rhythms in facilitating the increased neural responses associated with attention. However, a few critical questions for this picture remain. Firstly, if such low frequency desynchronization truly underlies attentional gains in all cases, then why is this phenomenon not readily observed in all cases? Two aspects of our methodology may be relevant here. Our comparison of post-switch signals with respect to a baseline *in which attention was directed to the opposite hemisphere* may have enhanced our ability to detect these effects. Also, as previous authors have noted, alpha decreases may be more subtle due simply to the fact that alpha power cannot inherently decrease below zero. Our log normalization may thus have had the effect of putting these subtle decreases on the same scale as complimentary high amplitude increases associated with inattention.

Finally, the question as to origins of the alpha desynchronization itself must be addressed. One possible mechanism may be that top-down synchronization of areas working in concert at the top of the spatial attention hierarchy with sensory cortical areas processing environmental stimuli, may functionally decouple the distributed network from globally generated alpha-rhythm. Recent studies have suggested a role for theta rhythms in the mediation of this type of synchrony between distal neural populations (Schak et al. 2002; Conolty et al. 2006). With regards to spatial attention, Sauseng and colleagues (2008) provided evidence that attentional shifts to a cued hemifield facilitate theta/gamma- band phase synchronization in response to validly cued targets over posterior scalp areas contralateral to the cue. Similarly, lateralized gamma-band synchrony, between widespread cortical areas and posterior sites contralateral to the

attended hemifield, was shown to increase in punctuated bursts whose timing coincided with activity in the theta band (Doesburg et al. 2008). These results have been interpreted as indicating that such timing reflects the maintenance or refinement of spatial attention networks by distributed theta-band activity. The patterns of ipsilateral/contralateral theta activity we observed suggest endogenous theta-rhythms increase simultaneously over both hemispheres in response to the switch. This pattern is consistent with this interpretation that such rhythms may reflect top-down signals which mediate the formation and maintenance of transitory attentional networks via the modulation of high frequency synchrony. Future work should endeavor to test this these ideas explicitly.

Conclusions. We have herein presented evidence that the effects of attention on responses evoked by a visual stimulus are preceded by desynchronization of alpha and mu-band activity over the hemisphere contralateral to the switch, consistent with a picture in which such desynchronization actively facilitates gains in the attended response. Complimentary increases in these same low-frequency signals over ipsilateral areas occur only after the attentional modulations of stimulus evoked activity have unfolded, suggesting theories which treat these signals as a mechanism for active suppression may need to be reconsidered.

References

Andersen, S. K., & Müller, M. M. (2010). Behavioral performance follows the time course of neural facilitation and suppression during cued shifts of feature-selective attention. *Proceedings of the National Academy of Sciences of the United States of America*, *107*(31), 13878-82. doi:10.1073/pnas.1002436107

Basar, E., Basar-Eroglu, C., Karakas, S., & Schürmann, M. (1999). Oscillatory brain theory: a new trend in neuroscience. *IEEE engineering in medicine and biology magazine : the quarterly magazine of the Engineering in Medicine & Biology*

Society, *18*(3), 56-66. Retrieved from http://www.ncbi.nlm.nih.gov/pubmed/10337564

Bauer, M., Oostenveld, R., Peeters, M., & Fries, P. (2006). Tactile spatial attention enhances gamma-band activity in somatosensory cortex and reduces low-frequency activity in parieto-occipital areas. *The Journal of neuroscience : the official journal of the Society for Neuroscience*, *26*(2), 490-501. doi:10.1523/JNEUROSCI.5228-04.2006

Bush, P., & Sejnowski, T. (1996). Inhibition synchronizes sparsely connected cortical neurons within and between columns in realistic network models. *Journal of computational neuroscience*, *3*(2), 91-110. Retrieved from http://www.ncbi.nlm.nih.gov/pubmed/8840227

Canolty, R. T., Edwards, E., Dalal, S. S., Soltani, M., Nagarajan, S. S., Kirsch, H. E., Berger, M. S., et al. (2006). High gamma power is phase-locked to theta oscillations in human neocortex. *Science (New York, N.Y.)*, *313*(5793), 1626-8. doi:10.1126/science.1128115

Doesburg, S. M., Roggeveen, A. B., Kitajo, K., & Ward, L. M. (2008). Large-scale gamma-band phase synchronization and selective attention. *Cerebral cortex (New York, N.Y. : 1991)*, *18*(2), 386-96. doi:10.1093/cercor/bhm073

Eckhorn, R., Bauer, R., Jordan, W., Brosch, M., Kruse, W., Munk, M., & Reitboeck, H. J. (1988). Coherent oscillations: A mechanism of feature linking in the visual cortex? *Biological Cybernetics*, *60*(2), 121-130. doi:10.1007/BF00202899

Engel, a K., Fries, P., & Singer, W. (2001). Dynamic predictions: oscillations and synchrony in top-down processing. *Nature reviews. Neuroscience*, *2*(10), 704-16. doi:10.1038/35094565

Foxe, John J, Ca, G. V. S., & Ahlfors, S. P. (1998). Parieto-occipitial ~10 Hz activity reflects anticipatory state of visual attention mechanisms. *NeuroReport*, *9*(17), 3929-3933.

Fries, P. (2001). Modulation of Oscillatory Neuronal Synchronization by Selective Visual Attention. *Science*, *291*(5508), 1560-1563. doi:10.1126/science.1055465

Fu, K. M., Foxe, J. J., Murray, M. M., Higgins, B. a, Javitt, D. C., & Schroeder, C. E. (2001). Attention-dependent suppression of distracter visual input can be cross-modally cued as indexed by anticipatory parieto-occipital alpha-band oscillations. *Brain research. Cognitive brain research*, *12*(1), 145-52. Retrieved from http://www.ncbi.nlm.nih.gov/pubmed/11489617

Gruber, T., Müller, M. M., Keil, a, & Elbert, T. (1999). Selective visual-spatial attention alters induced gamma band responses in the human EEG. *Clinical neurophysiology : official journal of the International Federation of Clinical Neurophysiology*, *110*(12), 2074-85. Retrieved from http://www.ncbi.nlm.nih.gov/pubmed/10616112

Izhikevich, E. M. (2006). Polychronization: computation with spikes. *Neural computation*, *18*(2), 245-82. doi:10.1162/089976606775093882

Izhikevich, E. M., Desai, N. S., Walcott, E. C., & Hoppensteadt, F. C. (2003). Bursts as a unit of neural information: selective communication via resonance. *Trends in Neurosciences*, *26*(3), 161-167. doi:10.1016/S0166-2236(03)00034-1

Kelly, S. P., Lalor, E. C., Reilly, R. B., & Foxe, J. J. (2006). Increases in alpha oscillatory power reflect an active retinotopic mechanism for distracter suppression during sustained visuospatial attention. *Journal of neurophysiology*, *95*(6), 3844-51. doi:10.1152/jn.01234.2005

Lumer, E. D., Edelman, G. M., & Tononi, G. (1997). Neural dynamics in a model of the thalamocortical system. I. Layers, loops and the emergence of fast synchronous rhythms. *Cerebral cortex (New York, N.Y. : 1991)*, *7*(3), 207-27. Retrieved from http://www.ncbi.nlm.nih.gov/pubmed/9143442

Müller, M. M., Gruber, T., & Keil, a. (2000). Modulation of induced gamma band activity in the human EEG by attention and visual information processing. *International journal of psychophysiology : official journal of the International Organization of Psychophysiology*, *38*(3), 283-99. Retrieved from http://www.ncbi.nlm.nih.gov/pubmed/11102668

Müller, M. M., Teder-Sälejärvi, W., & Hillyard, S. a. (1998). The time course of cortical facilitation during cued shifts of spatial attention. *Nature neuroscience*, *1*(7), 631-4. doi:10.1038/2865

Nunez, P. L. (1995). *Neocortical dynamics and human EEG rhythms.* Oxford University Press.

Nunez, P., & Srinivasan, R. (2005). *Electric Fields of the Brain: The Neurophysics of EEG, 2nd Edition* (2nd ed.). Oxford University Press, USA. Retrieved from http://www.citeulike.org/group/1104/article/106318

Regan, D. (1989). Human Brain Electrophysiology: Evoked Potentials and Evoked Magnetic Fields in Science and Medicine. Retrieved from http://www.citeulike.org/group/8861/article/4033861

Regan, David. (1977). Steady-state evoked potentials. *Journal of the Optical Society of America*, *67*(11), 1475. OSA. doi:10.1364/JOSA.67.001475

Rihs, T. a, Michel, C. M., & Thut, G. (2007). Mechanisms of selective inhibition in visual spatial attention are indexed by alpha-band EEG synchronization. *The European journal of neuroscience*, *25*(2), 603-10. doi:10.1111/j.1460-9568.2007.05278.x

Sauseng, P, Klimesch, W., Stadler, W., Schabus, M., Doppelmayr, M., Hanslmayr, S., Gruber, W. R., et al. (2005). A shift of visual spatial attention is selectively associated with human EEG alpha activity. *The European journal of neuroscience*, *22*(11), 2917-26. doi:10.1111/j.1460-9568.2005.04482.x

Sauseng, Paul, Klimesch, W., Gruber, W. R., & Birbaumer, N. (2008). Cross-frequency phase synchronization: a brain mechanism of memory matching and attention. *NeuroImage*, *40*(1), 308-17. doi:10.1016/j.neuroimage.2007.11.032

Schack, B., Vath, N., Petsche, H., Geissler, H., & Moller, E. (2002). Phase-coupling of theta gamma EEG rhythms during short-term memory processing. *International Journal of Psychophysiology*.

Singer, W. (1993). Synchronization of cortical activity and its putative role in information processing and learning. *Annual review of physiology*, *55*, 349-74. doi:10.1146/annurev.ph.55.030193.002025

Singer, W., & Gray, C. M. (1995). Visual feature integration and the temporal correlation hypothesis. *Annual review of neuroscience*, *18*, 555-86. doi:10.1146/annurev.ne.18.030195.003011

Srinivasan, R., Russell, D. P., Edelman, G. M., & Tononi, G. (1999). Increased synchronization of neuromagnetic responses during conscious perception. *The Journal of neuroscience : the official journal of the Society for Neuroscience*, *19*(13), 5435-48. Retrieved from http://www.ncbi.nlm.nih.gov/pubmed/10377353

Sylvester, C. M., Jack, A. I., Corbetta, M., & Shulman, G. L. (2008). Anticipatory suppression of nonattended locations in visual cortex marks target location and predicts perception. *The Journal of neuroscience : the official journal of the Society for Neuroscience*, *28*(26), 6549-56. doi:10.1523/JNEUROSCI.0275-08.2008

Sylvester, C. M., Shulman, G. L., Jack, A. I., & Corbetta, M. (2007). Asymmetry of anticipatory activity in visual cortex predicts the locus of attention and perception. *The Journal of neuroscience : the official journal of the Society for Neuroscience*, *27*(52), 14424-33. doi:10.1523/JNEUROSCI.3759-07.2007

Tallon-Baudry, C., Bertrand, O., Delpuech, C., & Pernier, J. (1997). Oscillatory gamma - Band (30-70 Hz) Activity Induced by a Visual Search Task in Humans. *J. Neurosci.*, *17*(2), 722-734. Retrieved from http://www.jneurosci.org/cgi/content/abstract/17/2/722

Thorpe, S., D'Zmura, M., & Srinivasan, R. (2012). Lateralization of frequency-specific networks for covert spatial attention to auditory stimuli. *Brain topography*, *25*(1), 39-54. Springer New York. doi:10.1007/s10548-011-0186-x

Thut, G., Nietzel, A., Brandt, S. a, & Pascual-Leone, A. (2006). Alpha-band electroencephalographic activity over occipital cortex indexes visuospatial attention bias and predicts visual target detection. *The Journal of neuroscience : the official journal of the Society for Neuroscience*, *26*(37), 9494-502. doi:10.1523/JNEUROSCI.0875-06.2006

Tiitinen, H., Sinkkonen, J., Reinikainen, K., Alho, K., Lavikainen, J., & Näätänen, R. (1993). Selective attention enhances the auditory 40-Hz transient response in humans. *Nature*, *364*(6432), 59-60. doi:10.1038/364059a0

Traub, R. D., Bibbig, A., LeBeau, F. E. N., Cunningham, M. O., & Whittington, M. A. (2005). Persistent gamma oscillations in superficial layers of rat auditory neocortex: experiment and model. *The Journal of physiology*, *562*(Pt 1), 3-8. doi:10.1113/jphysiol.2004.074641

Whitham, E. M., Pope, K. J., Fitzgibbon, S. P., Lewis, T., Clark, C. R., Loveless, S., Broberg, M., et al. (2007). Scalp electrical recording during paralysis: quantitative

evidence that EEG frequencies above 20 Hz are contaminated by EMG. *Clinical neurophysiology : official journal of the International Federation of Clinical Neurophysiology*, *118*(8), 1877-88. doi:10.1016/j.clinph.2007.04.027

Whittington, M. A., & Traub, R. D. (2003). Interneuron Diversity series: Inhibitory interneurons and network oscillations in vitro. *Trends in Neurosciences*, *26*(12), 676-682. doi:10.1016/j.tins.2003.09.016

Worden, M. S., Foxe, J. J., Wang, N., & Simpson, G. V. (2000). Anticipatory biasing of visuospatial attention indexed by retinotopically specific alpha-band electroencephalography increases over occipital cortex. *The Journal of neuroscience : the official journal of the Society for Neuroscience*, *20*(6), RC63. Retrieved from http://www.ncbi.nlm.nih.gov/pubmed/10704517

Yamagishi, N., Goda, N., Callan, D. E., Anderson, S. J., & Kawato, M. (2005). Attentional shifts towards an expected visual target alter the level of alpha-band oscillatory activity in the human calcarine cortex. *Brain research. Cognitive brain research*, *25*(3), 799-809. doi:10.1016/j.cogbrainres.2005.09.006

Yuval-Greenberg, S., Tomer, O., Keren, A. S., Nelken, I., & Deouell, L. Y. (2008). Transient induced gamma-band response in EEG as a manifestation of miniature saccades. *Neuron*, *58*(3), 429-41. doi:10.1016/j.neuron.2008.03.027

von Stein, a, Chiang, C., & König, P. (2000). Top-down processing mediated by interareal synchronization. *Proceedings of the National Academy of Sciences of the United States of America*, *97*(26), 14748-53. doi:10.1073/pnas.97.26.14748

Chapter 4. A Wilson-Cowan based cortical model for treating the effects of spatial attention on local sensory populations.

Abstract. *In this study we model the effects of endogenous spatial attention signals on steady-state evoked responses in visual cortex. For this aim we have developed a cortical population model based on a modification of the framework originally developed by Wilson & Cowan. We use this model in conjunction with simultaneously recorded EEG/MEG data to simulate effects of attention on steady-state responses evoked in the context of a previous spatial attention experiment. The local sensory responses driven by our visual stimuli are modeled by Wilson-Cowan (WC) populations driven by gamma-band sinusoids, representing steady-state gamma-band flicker. These populations are embedded in a global environment of characteristic EEG rhythms, which are then modulated by functional forms of the attention signals observed in our previous experiment. Functional forms for these attention signals were parameterized as a distribution of fitted logistic functions (sigmoids), which then influence the background state of activity about which the local populations oscillate. Our results show that attention-related decreases in ongoing modulation result in increases in simulated steady-state responses. Likewise, increases in ongoing modulation in response to the switch have the effect of suppressing the local steady-state response. Together, these results suggest that mechanism of interaction between local and global networks posited by our model may have experimental relevance to neural phenomenon at the scale of EEG/MEG.*

1. Background and Significance

Behavioral benefits of attention to a visual stimulus, including increased performance at stimulus detection (Shaw & Shaw 1977), and decreased response time (Eriksen & Hoffman 1972), have been argued to occur through a number of neural mechanisms. These mechanisms include enhanced efficacy of the neural response to a stimulus (Spitzer et al. 1988, Spitzer & Richmond 1991), suppression of neural activity coding unattended distractor information (Reynolds et al. 1999, Kastner et al. 1998, Sylvester, 2008), and increased baseline neural activity even in the absence of visual stimulation (Kastner et al. 2000; Luck et al. 1997). All of these mechanisms are thought to have their anatomical basis in feedback projections to areas at various positions in the

visual cortical hierarchy from frontal and parietal areas operating in dedicated attention networks (Kastner & Ungerleider, 2000, Corbetta et al, 2002).

Experimental studies in humans and animals suggest that the top-down influences of these attention networks most likely involve the modulation of low-frequency oscillations in the alpha or theta bands (Engel et al, 2001). For instance, Fries et al. (2001) showed that cells in the receptive fields of attending monkeys exhibited low frequency desynchronization during an interval in which the monkeys anticipated a visual stimulus. This low-frequency desynchronization was then accompanied by an increase in gamma-band synchrony in response to the stimulus once it appeared. This lead the authors to argue that low-frequency desynchronization via attention might act to enhance the efficacy of the subsequent response of the sensory neurons. In the EEG literature, numerous spatial cueing experiments have shown that attention to a region of space in anticipation of a visual stimulus results in the modulation of occipito-parietal alpha rhythms (Worden et al, 2000, Kelly et al. 2006; Rihs et al. 2007). In these and other similar experiments, alpha-band EEG activity is always either enhanced over the cerebral hemisphere ipsilateral to the attended visual hemifield, or decreased over the contralateral hemisphere (Sauseng et al. 2005; Thut et al. 2006; Yamagishi et al. 2005), leading the former authors to propose parieto-occipital alpha rhythms may act to suppress unattended visual information, and the latter to suggest that low-frequency desynchronization may serve to enhance sensory neural responses.

We recently conducted an experiment which explored how top-down attentional effects on responses in sensory populations unfold in time (see chapter 2). In this study subjects were asked to maintain center fixation while detecting targets embedded in one

of two flickering peripheral stimuli located in left/right sides of visual space. At random intervals, the subjects were prompted to switch attention to detect the targets embedded in the opposite stimulus. Wavelet analysis of simultaneously recorded EEG/MEG data demonstrated that modulation of alpha-band activity over parieto-occipital areas in response to the attentional shifts accompanied modulations of steady-state responses evoked by attended/unattended visual stimuli. In particular, when attention was switched to a new spatial location, alpha-band power over contralateral occipito-parietal electrodes decayed quickly, preceding the rise/decay in the steady-state responses evoked by the newly attended/unattended stimuli. Only significantly later did we observe the eventual rise of alpha band power over ipsilateral parieto-occipital electrodes. The timing of these effect suggest that attention-dependent decreases in contralateral power may actively facilitate gains in the attended response, whereas complimentary increases in ipsilateral activity do likewise play an active role in suppression.

Because the signals observed in our experiment describe the temporal evolution of attentional modulation, these data provide a unique input-output relationship for testing the modeling framework we have recently developed for treating the interaction of top-down signals with local cortical populations (Srinivasan et al. in press). At the heart of the model is the issue of local/global interaction- the idea that there is a specific "local" circuit of neurons processing stimuli with dynamics governed by intrinsic connectivity and local physiology, and that this circuit is subject to top-down influences from one or more global systems defined by long-range connectivity, such as a fronto-parietal attention network. Numerous models have attempted to combine local/global cortical dynamics into a single framework (Nunez 1981, 1995, 2000; Jirsa & Haken

1996, 1997; Wright & Liley 1995; Robinson et al. 1997). However, to our knowledge, ours is the first to make the mechanism of their interaction explicit.

Whereas the *global* theories advanced by Nunez predict spatially coherent theta and alpha band oscillations over the surface of the cortex, physiologically realistic models of *local* populations in sensory cortex tend to give rise to faster oscillations in the gamma band (Bush and Sejnowski, 1995; Traub et al. 1997, 2005). Both predictions mesh well with the results of our experiment- our attentional manipulation elicited widespread alpha lateralization, whereas our gamma-band flicker evoked responses which were constrained to early visual areas, and so appear to reflect local visual processes. However, for the purposes of drawing comparisons to EEG, MEG, and SSVEPs, we require models which are developed in macroscopic variables that describe synaptic mass action. One of the most often cited and well studied models of this type is that of Wilson and Cowan (1972, 1973). In general, this model produces free, damped oscillations over a broad range of physiologically realistic parameter space in response to a step function input to the excitatory population. The oscillations in all parts of the network are highly correlated, as there is no independent noise in each population. The rate of damping of the oscillations is largely determined by the ratio of excitatory to inhibitory weights to each population with higher inhibition leading to overdamped oscillations. The frequency of the oscillation is determined primarily by the membrane time constants and connectivity strength.

In this paper, we make use of a modified Wilson-Cowan model developed to account for the effects of a background brain state on the local dynamics of a population. In this framework the effects of attention are modeled as dynamic modulation of the

background state of the local population, whereas the steady-state responses are driven via explicit periodic input to the population itself (figure 1). We use this formulation to examine the modulation of model generated gamma band steady-state responses by attention signals derived from the actual data we previously observed. We are thus able to simulate the time-course of steady-state responses for comparison with those observed in our experiment. In doing so we show that the proposed mechanism of interaction action between local and global networks results in modulations of population activity similar to those measurable in our SSVEP/F, thereby showing this simple model to be relevant to the dynamics of attentional effects on local oscillations in EEG/MEG studies.

2. Materials and Methods

The modified Wilson-Cowan framework. Wilson & Cowan (1972) derived a model neural population containing both excitatory and inhibitory neurons with dynamics described by a set of coupled, nonlinear differential equations, herein labeled *WC*. The solution of these equations gives the proportion of cells in each subpopulation (excitatory/inhibitory) that become active per unit time. The cells comprising the population are assumed to be in close spatial proximity, with interconnections dense enough so that any two cells within it are path-connected. Furthermore, the model assumes that local interactions between neurons within the population are largely random, but that this local randomness gives rise to precise structure at larger spatial scales. The situation is analogous to an example taken from thermodynamics, in which a fluid with a macroscopically structured flow can be observed to be undergoing stochastic Brownian motion at the molecular level. The same framework set forth by Wilson &

Cowan has been extended in a number of straightforward ways to models with more general connectivity, and an arbitrary number of spatially distinct neural populations (Campbell & Wang 1996; Borisyuk & Denham, 2000; Frank et al. 2000). Yousif & Denham (2005) extended the *WC* framework to model interacting thalamic (reticular formation) and cortical structures involved in the generation of spindle oscillations (7 – 14 Hz) in early sleep stages. Jirsa&Haken (1997), used a *WC* model interacting with a global model to interpret MEG data in a syncopated tapping audio-motor task (the so-called Julliard experiment).

Here we adopt a modified version of *WC* to make it more physiologically realistic. Specifically, this treatment fixes an inconsistency in WC's original expression for the *proportion of sensitive cells,* which is not dimensionally correct, and leads to these proportions having the capacity to exceed 1 (see Appendix A), which is physiologically impossible. The basic dependent variables are the *fractions of excitatory and inhibitory active cells* (action potential densities) $E(t), I(t)$, which can evidently exhibit high frequency jitter not treated in this analysis. Rather, the original *WC* equations are written in terms of coarse grained excitatory $\langle E(t) \rangle$ and inhibitory $\langle I(t) \rangle$ action potential densities. The basic model is illustrated in Fig. 1. We introduce the new dependent variables $X_E(t), X_I(t)$, which provide perturbations about the critical point (E_0, I_0), which may be interpreted as a global background brain state. Thus, we express

$$\begin{aligned} \langle E(t) \rangle &= E_0 + X_E(t) \\ \langle I(t) \rangle &= I_0 + X_I(t) \end{aligned} \qquad \textbf{(1)}$$

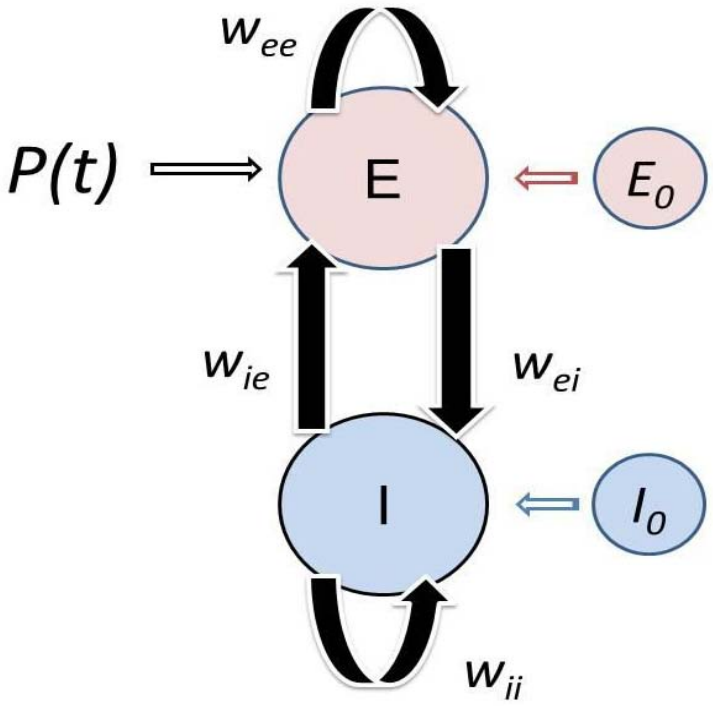

Figure 1. The modified Wilson-Cowan model. Reciprocally connected excitatory and Inhibitory subpopulations interact with each other with weighted connections ($w_{ee,}w_{ei},w_{ie}$, and w_{ii}), which determine the type of oscillations (damped vs. limit cycle) exhibited by the model. P(t) represents external stimulation whereas top-down signals are modeled as modulations of the background state (E0,I0) about which the population oscillates. For the simulations which follow, we have chosen the weights of w_{ei} = 50, $_{wie}$ = 15, w_{ii} = 0, and w_{ee} = 15, which represent a point in parameter space for which the model exhibits damped oscillatory behavior, as opposed to less physiologically realistic limit cycle behavior.

Since the excitatory action potential densities are defined as fractions of the total cell populations, we require:

$$\begin{aligned} 0 \le E_0 + X_E(t) \le 1 \\ 0 \le I_0 + X_I(t) \le 1 \end{aligned} \quad \textbf{(2)}$$

The basic WC equations then become

$$\begin{aligned} \frac{dX_E}{dt} &= -E_0 - X_E + \left(1 - E_0 - X_E\right) S_E\left(X_E, X_I, P\right) \\ A\frac{dX_I}{dt} &= -I_0 - X_I + \left(1 - I_0 - X_I\right) S_I\left(X_E, X_I\right) \end{aligned} \quad \textbf{(3)}$$

Here $A = \frac{\tau_I}{\tau_E}$ is the ratio of inhibitory to excitatory time constants, and $P(t)$ is an excitatory external (driving) input, for example sensory input to the population from the thalamus. The set of parameters $\{w_{EE}, w_{IE}, w_{EI}, w_{II}\}$ are gain parameters that give the strength of connections between the excitatory and inhibitory populations as indicated in Fig. 1. As shown in Appendix B for the special case $P(t) = 0$, the sigmoid functions S_E, S_I in Eqs (3) then take the forms

$$S_E = \frac{1}{1 + \left(\frac{1}{E_0} - 2\right)\exp\left(-w_{EE}X_E + w_{IE}X_I - P\right)} \quad E_0 < \frac{1}{2} \tag{4}$$

$$S_I = \frac{1}{1 + \left(\frac{1}{I_0} - 2\right)\exp\left(-w_{EI}X_E + w_{II}X_I\right)} \quad I_0 < \frac{1}{2} \tag{5}$$

Parameter Choices. For our simulations the main parameters of interest are the background state variables E_0 and I_0, which we will vary as described in the following sections. The free parameters were the set of connection weights $\{w_{EE}, w_{EI}, w_{IE}, w_{II}\}$ which were determined by the following physiological considerations:

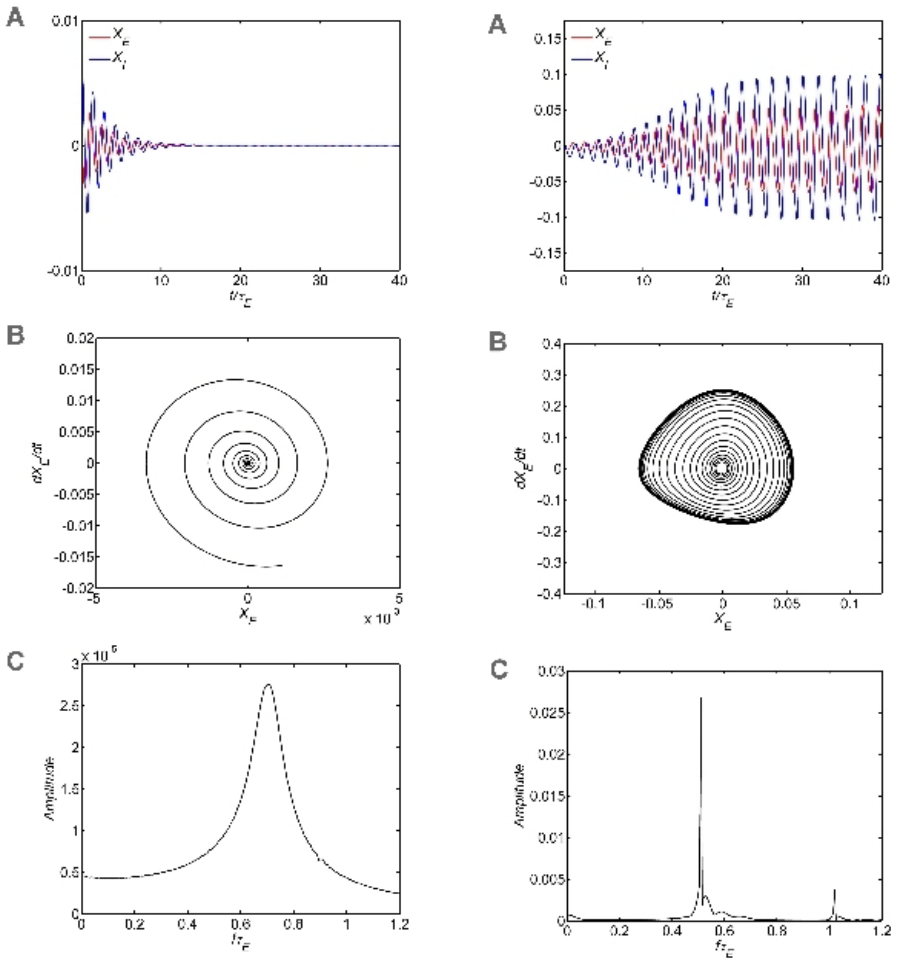

Figure 2 (left). Two regimes of the model. In all of the simulations, the following parameters are fixed: (1) The ratio of time constants , (2) the background state , (3) the connection weights are and (4) the input P(t) = 0.1 is a step function at time 0. Plots 2a-c show the results for the damped oscillation observed with self-excitation w_{ee} = 15.
Figure 3 (right). show the results for the limit cycle oscillation observed with self-excitation w_{ee} = 20. The time series of the excitatory and inhibitory subpopulations are shown in plots 2,3a. In these plots time is normalized by excitatory membrane time constant. Phase-plane plots for the excitatory subpopulation are shown in plots 2,3b. Amplitude spectra obtained by the FFT are shown in plots 2,3c. Normalized frequency is $f\tau_E$. If τ_E = 20 ms, normalized frequency of 1 is 50 Hz**.**

(1) In the cortex, excitatory connections are estimated to be 4-5 times more common than inhibitory connections (Bush & Sejnowski, 1996), and (2) Inhibitory connections are more typically found on the cell body possibly increasing their effectiveness in comparison to excitatory connections on dendritic trees (Mountcastle, 1997). Taking these two points into consideration we first fixed the two parameters w_{EI} = 50 and w_{IE} =

15. We set the self-inhibition w_{II} = 0, as we found little practical effect for the small values of this parameter, other than to increase damping in the system, and shift the critical point for transition from a damped oscillation to a limit cycle regime.

These equations (3) produce stable limit cycle solutions about the critical point (E_0, I_0) for a wide range of the parameters. For example, setting $A = 1$ and $E_0 = I_0$ the necessary condition for oscillatory solutions about (E_0, I_0) is

$$w_{EE} < 2\sqrt{w_{IE} w_{EI}} \qquad \textbf{(6)}$$

This oscillatory solution is an unstable limit cycle if:

$$w_{EE} > \frac{2}{E_0 (1 - 2E_0)} \qquad \textbf{(7)}$$

From Equation (7) we were always able to find the critical value of w_{EE} below which the system produced damped oscillations (figure 2a,b,c), while above this value the system produced limit cycle

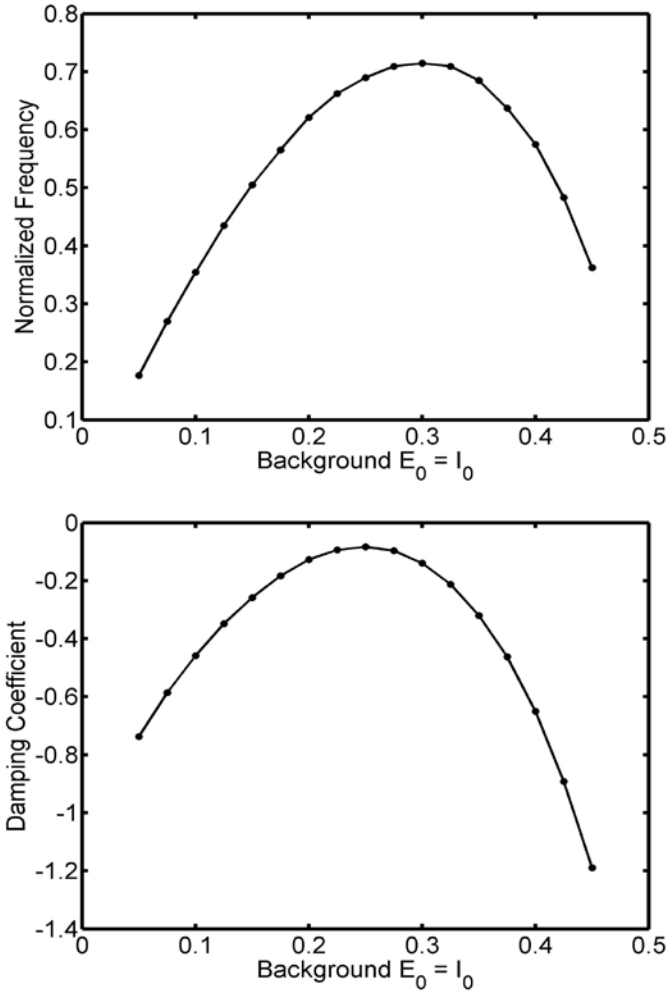

Figure 4. Dependence of frequency (top) and damping (bottom) on background state for the damped oscillations. System connection weights are fixed as wEE = 15, wIE = 15; wEI = 50; wII = 0. Input is a step function of magnitude 0.1. Verified that the curves are the same for step functions up to 0.3 Frequency was estimated by analyzing zero crossings. Damping was estimated by fitting an exponential decay to the peaks of a rectified (absolute value) of the time series. Normalized frequency is $f\tau_E$. If τ_E = 20 ms, normalized frequency of 1 is a 50 Hz oscillation.

oscillations in response to a step function input (figure 3a,b,c). For our choice of w_{EI} = 50 and w_{IE} = 15, this critical value corresponds to w_{EE} = 16. Since we suspect true sustained limit cycle activity is improbable in physiological systems such as the brain, we chose to set w_{EE} = 15 for our simulations, thus examining the model in the regime for which it produces damped oscillations. In a separate exploratory analysis in which we fixed E0 = I0, and the ratio of excitatory to inhibitory time constants at 1, we have shown that frequency and damping of oscillations in this regime depend strongly on the background state. When these condition holds, oscillations are least damped, and oscillation frequency is at its peak, for the values E0 = I0 = 0.25 (see figure 4). Thus for our purposes we chose to fix these as the background state for our model.

Parameterization of experimental attention signals. Recall from chapter 2 that we obtained a set of signals which described the modulation by attention of endogenous low-frequency activity, as well as the neural response to the visual stimulus. In this experiment we characterized the temporal evolution of these signals by analyzing wavelet spectra. Our general findings were that attentional switches results in swift desynchronization of alpha, and mu-band power over scalp areas contralateral to the switch. A complimentary increase in alpha and mu-band power was also seen over ipsilateral areas. We postulated that the contralateral signals, in particular, may have an active role in facilitating observed increases in the attended SSVEP/F signals. This was primarily because the modulation of these signals preceded the corresponding modulations of the stimulus evoked SSVEP/F. Because the observed low-frequency modulations were most significant in the alpha-band, we chose them as the basis for our top-down signal in this set of simulations. The bootstrapping procedure we used for our analyses provided us a distribution of 1000 contralateral and ipsilateral alpha-band modulation signals. The same procedure gave us a similar distribution of SSVEP/F which we can compare to model outputs.

In order to parameterize the rise and decay characteristics of the alpha-band and SSVEP/F signals for use in the model, we opted to approximate these data as sigmoids of the form:

$$S(t) = \mathrm{A} + \frac{\mathrm{K} - \mathrm{A}}{\left(1 + e^{-b(t-m)}\right)} \qquad \textbf{(8)}$$

where K and A represent upper and lower asymptotes of the sigmoid, the parameter m represents the inflection point (time of maximal growth), and the parameter b the slope at inflection. When b is negative the function describes nonlinear decay from K to A,

whereas positive b values indicate nonlinear growth from A to K. In order to constrain and simplify the optimization problem, the parameters A and K were fixed from the data itself. The choice of these parameters depended on the nature of the signals. For our contralateral alpha signals, as well as for our switch-*from* SSVEP/F, which both show decreases after the switch, the upper asymptote K was fixed as the mean value of the signal in the interval immediately preceding the switch (t = [-0.5, 0]). For these same signals the lower asymptote was set as the mean value at the end of the three second switch interval (t = [2, 3]). Conversely, for ipsilateral alpha, and switch-to SSVEP/F, which show increases after the switch, the upper asymptote K was fixed as the mean at the end of the post-switch interval, and A as the pre-switch mean. In order to fit these sigmoids we used the MATLAB built-in function *fminsearch.m* (optimization toolbox) to find the minimum of the Error function:

$$Error(\mathrm{b}, \mathrm{m}) = \underset{t\in[-1,3]}{\mathrm{mean}}\left(\left|S(t, \mathrm{A}_n, \mathrm{K}_n, \mathrm{b}, \mathrm{m}) - \mathrm{f}_n(\mathrm{t})\right|^2\right) \quad \textbf{(9)}$$

where $f_n(t)$ above denotes nth bootstrap sample of the fitted signal f(t). By fitting sigmoids in this manner to each of our 1000 bootstrapped signals, we obtained distributions for the slope and inflection parameters which characterized the modulation observed in our experiment.

Top-down influences of attention networks on a local WC population. Recall that we seek to understand the effects of dynamic modulation of the local population background state by oscillations in global attention network. The studies described above, including our previous experiment, suggest that these networks operate in low-frequency bands characteristic of human EEG. In our own experiment, we found the strongest attention-dependent modulations in the alpha-band, spanning 8-12 Hz. Thus for simplicity of

analysis we presume that the larger scale network generates oscillations at a characteristic frequency at the center of this band, that is:

$$E_0 \to E_0 + B_\alpha \alpha_E(t)\cos\left(2\pi\omega_\alpha t\right)$$
$$I_0 \to I_0 + B_\alpha \alpha_I(t)\cos\left(2\pi\omega_\alpha t\right) \qquad \textbf{(10),(11)}$$

where ω_α = 10 Hz, and the amplitudes $(\alpha_E(t), \alpha(t)_I)$ represent attention-dependent changes in the magnitude of the 10-Hz modulation about the background state (E_0, I_0). In order to incorporate the attentional effects observed in our data, we assumed there to be a baseline alpha modulation present at the start of each trial with amplitude set at $B_\alpha/2$. The functional forms for $\alpha(t)$, obtained from our logistic fitting procedure described above, were then normalized by a factor derived from the data for each type of signal. For each signal, this factor corresponded to the difference between pre-switch and post-switch power on the trial for which the magnitude of this attention dependent change was the greatest. The resulting set of curves had the property that only on the trial corresponding to the maximum decrease in contralateral signal, did $\alpha(t)$ tend towards zero (modulation about (E_0, I_0) decreases to zero), whereas only for the trial corresponding to maximal ipsilateral increase, did $\alpha(t)$ tend towards a value of one (the amplitude of the 10 Hz modulation amplitude about (E_0, I_0) increased towards), and thus baseline modulation increases to B_α). Note that due to the nature of our equations, B_α must be constrained to be less than (E_0, I_0). Having chosen a critical value (E_0, I_0) of (0.25,0.25) about which our population oscillates, we elected to fix our parameter B_α at 0.15. This choice was made in order to examine the case in which the top-down effects of

attention are relatively extreme, such as might be the case for an alert and lucid individual engaged in a demanding attentional task.

Model generated steady-state evoked responses. Within this framework, steady-state responses of the model neural population can be viewed as the output of the model in response to periodic input. Thus the form of the input function, P(t) referred to above, can be chosen as:

$$P(t) = B_\gamma + A_\gamma \cos(2\pi ft) \quad \textbf{(12)}$$

For the purposes of reporting the effects of attention on model generated SSVEP/F, we chose to fix f = 30 Hz, corresponding to the higher of the two flicker frequencies used in our experiment, but noting that the qualitative behavior of the system remains the exact same when run at the other flicker frequency (20 Hz).

It is a general property of linear systems that a system responds maximally to periodic input with frequencies which match the oscillator's natural resonance frequency. In order to investigate whether our model exhibits this same kind of tuning behavior, we examined model outputs for a range of values of the driving frequency. Since we have previously seen that the natural frequency of our population is primarily dependent on the choice of membrane time constants τ_E, and τ_I, we chose to fix these at the physiologically realistic value of 20 ms for these simulations. At these values, the resultant natural frequency of the population then falls between 25 - 30 Hz (figure 3), so we elected to sweep a range of values for f from 1 – 50 Hz in order to encompass this resonance. In order to ascertain whether the presence top-down modulation might effect the tuning behavior of the system, we ran these simulations for a pair of values of our

baseline modulation- once at B_α = 0.15 (high backround state modulation), and once for B_α = 0 (no modulation).

Simulations and Data Analysis. All of the simulations carried out here were performed using the built in ode solver in MATLAB (Natick, MA), *ode23.m*. For simulations of tuning behavior, the model was solved for a time interval spanning 0 – 10 seconds. The solution for this interval was then transformed via FFT, and the resulting power was analyzed at the frequency bin corresponding to that of the frequency of stimulation (driving frequency). For simulations of the effects of attentional modulation on steady-state responses, the model was run for a time interval spanning -2 – 4 seconds, where the value zero corresponding to the time of the attentional switch. The resultant outputs were

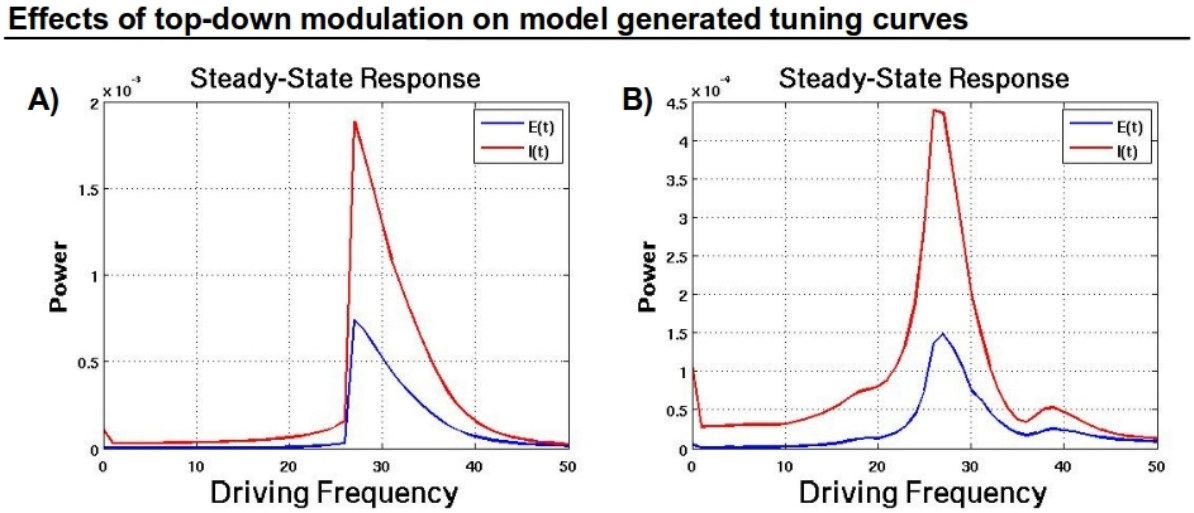

Figure 5 shows the results of our simulation where the model is driven with sinusoidal input across a range of driving frequencies (0 – 50 Hz), analogous to probing tuning behavior in SSVEP/F experiments. On the left (a), the background state of the population is not subject to modulation, and thus remains constant at (E_0,I_0) = (0.25,0.25), whereas on the right (b), the background state is modulated about (E_0,I_0) at 10 Hz (the amplitude of this 10 Hz modulation was set at 0.15). In both modulated, and non-modulated cases, the model exhibits classic tuning behavior in which oscillatory output peaks in amplitude as the driving frequency approaches the natural frequency of the oscillator. However, peak amplitude is much larger in the non-modulated case (on the order of 10e-3) than when background state is modulated (on the order of 10e-4).

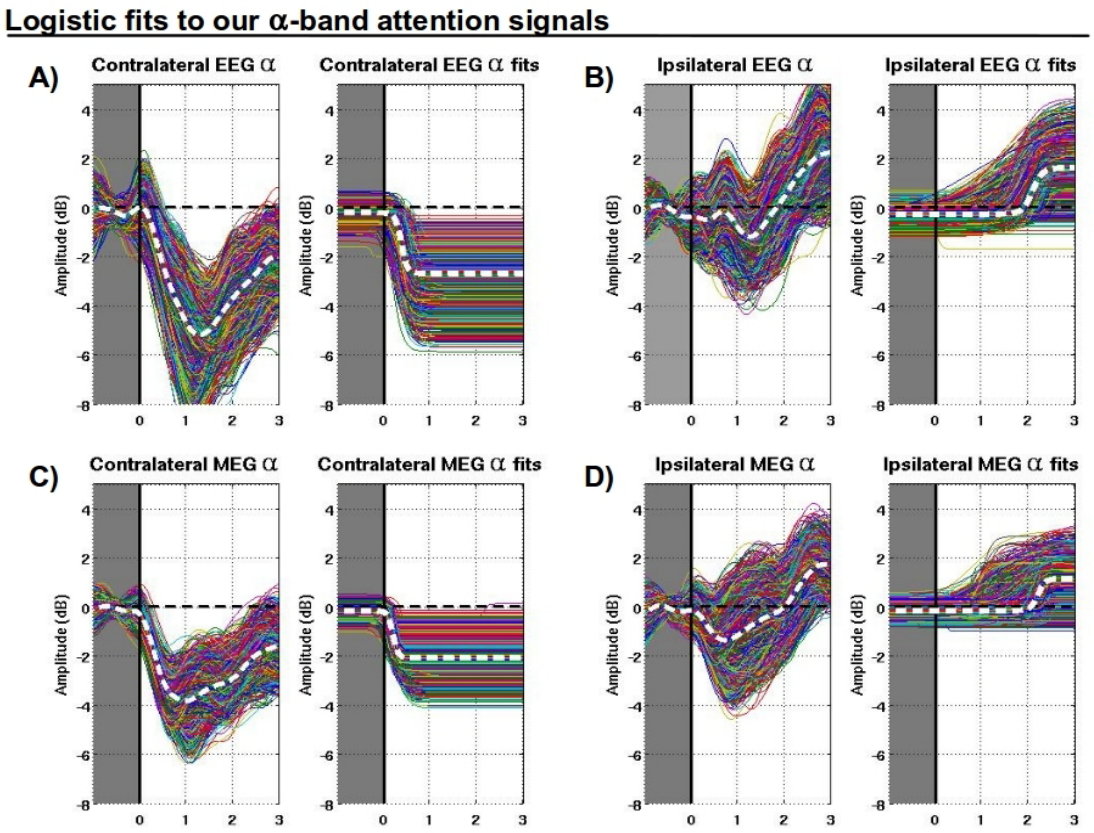

Figure 6. Shows the results of our logistic function fitting procedure for our 2000 bootstrap samples for each signal- contra/ipsilateral (a,c/b,d) alpha-band EEG/MEG (a,b/c,d). In each case we see that the gross characteristics of each family of curves are retained. Specifically, the late onset of the ipsilateral rise, as compared to the early onset contralateral decay. Overlayed on top of each set of bootstrap samples (left), in white dashed lines, are the average signal for each condition. Overlayed on top of each set of fits (right), in white dashed lines, are the corresponding fits of the mean signal

then transformed via complex Morlet wavelet with frequency centered on the stimulation frequency (30 Hz). To facilitate comparison to the SSVEP/F signals recorded in our experiment, wavelet power for these model outputs was then normalized by the mean power in the pre-switch (-0.5 – 0) interval, and a 20*log (dB) transform applied, so that the resulting outputs are expressed as decibel power difference

between post and pre-switch wavelet power.

3. Results

Model Generated SSVEP. Figure 4 illustrates the tuning behavior of the model for zero modulation (a), and high baseline modulation (b) conditions. In both cases steady-state responses exhibit maximal power when driven at frequencies corresponding to the natural frequency of the system. The primary difference between the two conditions is that when the model is driven without any top-down modulation, steady-state evoked responses at the peak frequency are nearly an order of magnitude larger, demonstrating that the modulation has the effect of suppressing SSVEP output. Also, for this condition tuning peaks more sharply at the natural resonance relative to when modulation is introduced. The modulated pattern seen in fig 4b is more reminiscent of the frequency response subsystems, first characterized by Reagan (1977), which are observable in human steady-state responses. Noticeably absent from figure 4b is any semblance of a peak response at the modulation frequency (10 Hz). However, the presence of the modulation is discernible as sidebands roughly +/- 10 Hz relative to the primary peak. Thus our model has already made at least one testable prediction. The detection of such sidebands in human gamma-band SSVEP/F could lend compelling support for the mechanism of top-down interaction specified in our model.

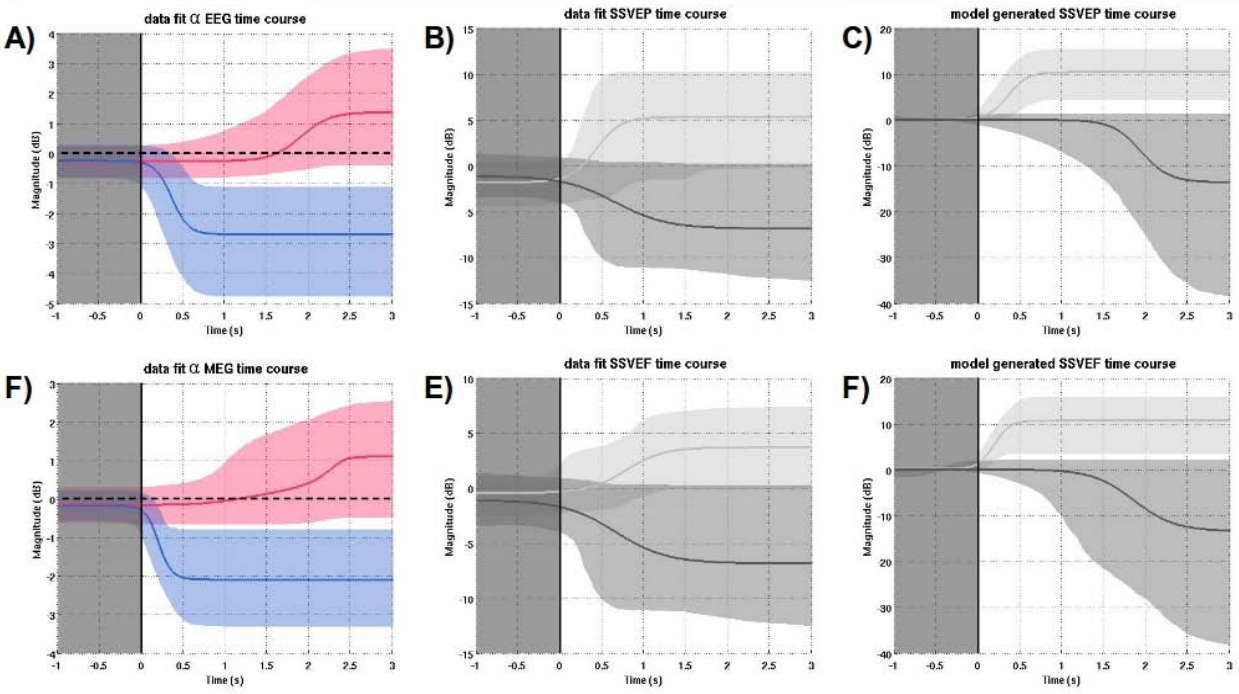

Effects of attentional modulation. Figure 5 shows the fits for our experimental alpha-band attention signals obtained by our sigmoid fitting procedure. The fits appear to preserve all the gross characteristics reported in our experiment (see chapter 2 results). Specifically, contralateral signals are generally diminished, and ipsilateral signals generally increased, due to this trend being present in the data. Moreover, rise/decay latencies (indicated by sigmoid inflection points) for contralateral signals occur within the first second of the post-switch interval, whereas for ipsilateral signals these generally **Figure 7.** Shows the results of our simulation using our fitted attention signals as modulation functions to vary the background state of the local WC population. On the left are shown logistic fits to the mean contralateral (blue) and ipsilateral (red) signals for both the EEG (top) and MEG (bottom), along with 95% confidence intervals obtained from fitting the corresponding distributions of bootstrap samples. In the center are shown the fits obtained for our experimental SSVEP/F responses. SSVEP/F corresponding to SSVEP which were "switched-to" are shown in light gray, whereas SSVEP/F which were "switched-from" are shown in dark grey. Finally, on the right are shown the corresponding "switch-to/from" model generated SSVEP/F outputs. In the time course of these plots, time zero represents the time at which a subject switches the locus of their attention from one stimulus to another located in the opposite visual hemifield. We see that the model does an excellent job reconstructing the directionality of effects after the switch (i.e. the rise of the switched-to SSVEP/F, and the corresponding fall in switched-from SSVEP/F). However, in our model, the rise/decay of the SSVEP/F happen contemporaneously with the decay/rise of the conta/ipsilateral alpha-band signals- a result which was not reflected in our data.

occur much later. Overlayed on top of each distribution of curves (dashed white lines) are sshown the trial averaged signal (left), and our logistic fit of this curve (right).

Figure 6 shows the results of our simulation using these fitted attention signals as modulation functions to vary the background state of the local WC population. On the left are shown logistic fits to the mean contralateral (blue) and ipsilateral (red) signals for both the EEG (top) and MEG (bottom), along with 95% confidence intervals obtained from fitting the corresponding distributions of bootstrap samples. In the center are shown the fits obtained for our experimental SSVEP/F responses. Finally, on the right are shown the model generated SSVEP/F outputs. A few aspects of these simulations are worth noting. First, it is clear that post-switch suppressions/increases of alpha-band modulation via contralateral/ipsilateral signals elicit contemporaneous gains/suppressions in the model-generated SSVEP/F. This is a natural consequence of the phenomenon noted above- that low-frequency modulations of the WC population's background state diminish the response of the model to steady state input. Second, while the directionality of these modulations matches nicely those observed for our experimental data, the relative timing of the modulations do not. In our experiment we noted that contralateral decreases in the alpha-band signal precede the corresponding increases observed for the attended SSVEP/F, whereas ipsilateral alpha increases trail the corresponding decrease in the switched-from SSVEP/F signal. In the model outputs these effects are simultaneous.

4. Discussion.

The strength of our model lies primarily in its explicit formulation of the mechanism for top-down interaction of global network activity with a local population. Practically, the strength of the model lies in its predictive ability concerning the disruptive nature of low-frequency modulation on the gamma-band output of the driven

population. However, the failures of the model are equally important. Specifically, the model in its current form cannot account for timing differences between the onset of our contra/ipsilateral top-down modulation signals, and the corresponding modulations of model-generated steady-state responses. One possibility that we explored was that the background state parameter (E_0, I_0) might influence these timings. Exploratory analyses of the model has shown that varying these parameters can influence the phase relationship between the low-frequency modulation signal and the gamma-band response of the population. That is, when the background state is low, the peak amplitude of the modulated gamma-band response are aligned with the positive peaks in the modulation function. The opposite is true when back ground state is high. In that case, gamma-band responses are greatest when the modulation function obtains its negative minima. These slight timing differences are not relative to our findings however, as they are constrained to occur within half the period of the modulation function. In the case where these modulations occur in the alpha band, this means any differences in the timing between the top-down signal and the evoked response would occur within an interval of 50 ms- a window which may be too small to account for the lag between contralateral alpha and mu signals and increased SSVEP/F observed in our experiment, which ranged from 0-300 ms.

These dependency of the phase relationship between modulation signals and the model response on (E_0, I_0) reflect the fact that there is an optimum level of background state arousal about which oscillations of the population are maximal. For our experiment we chose this optimal state as the default. Simulations exploring the effects of varying these parameters have shown that, while the magnitude of the observed modulations may

vary, the direction and relative timing of these effects remain qualitatively similar. This is true even for the case when the symmetry condition $E_0 = I_0$ is broken, and excitatory/inhibitory subpopulations are allowed to oscillate about different background levels of activity.

One possibility for treating these timing differences, for which this simplified top-down model cannot account , is the development of a comprehensive local/global model in which the output of local populations can effect the parameters governing global state dynamics at various locations in the cortex. The need for such a model is illustrated by some of the very first EEG results concerning alpha rhythm which suggest that salient environmental stimuli, such as a loud noise or sudden flash of light, can abolish globally coherent alpha rhythm over large portions of the scalp (references). The development of a functional model of this type is a direction for current and future research which we hope will elucidate the dynamics of top-down interactions with sensory cortical populations, such as those observed in the setting of spatial attention experiments.

Conclusions. We have considered evidence for a cortical population model which explicitly treats the effects of top-down global signaling via the modulation of background state activity about which the population oscillates. We have shown that low-frequency modulation of this background state has the effect of suppressing gamma-band oscillations produced by the model, and that this phenomenon extends to the case of simulated SSVEP/F, where the model is driven with periodic stimulation across a range of frequencies, including the natural resonance of the local oscillator. In response to the attention related changes in levels of top-down modulation observed in our previous experiment, the model reproduces the directionality of observed gains/suppressions of the

steady-state responses to attended/unattended stimuli, but cannot currently account for the observed relative timing of these effects.

References.

Borisyuk, R., Denham, M., Hoppensteadt, F., Kazanovich, Y., & Vinogradova, O. (2000). An oscillatory neural network model of sparse distributed memory and novelty detection. *Bio Systems*, *58*(1-3), 265-72. Retrieved from http://www.ncbi.nlm.nih.gov/pubmed/11164655

Bush, P., & Sejnowski, T. (1996). Inhibition synchronizes sparsely connected cortical neurons within and between columns in realistic network models. *Journal of computational neuroscience*, *3*(2), 91-110. Retrieved from http://www.ncbi.nlm.nih.gov/pubmed/8840227

Campbell, S., & Wang, D. (1996). Synchronization and desynchronization in a network of locally coupled Wilson-Cowan oscillators. *IEEE transactions on neural networks / a publication of the IEEE Neural Networks Council*, *7*(3), 541-54. doi:10.1109/72.501714

Corbetta, M., & Shulman, G. L. (2002). Control of goal-directed and stimulus-driven attention in the brain. *Nature reviews. Neuroscience*, *3*(3), 201-15. doi:10.1038/nrn755

Engel, a K., Fries, P., & Singer, W. (2001). Dynamic predictions: oscillations and synchrony in top-down processing. *Nature reviews. Neuroscience*, *2*(10), 704-16. doi:10.1038/35094565

Eriksen, C. W., & Hoffman, J. E. (1972). Temporal and spatial characteristics of selective encoding from visual displays. *Perception & Psychophysics*, *12*(2), 201-204. doi:10.3758/BF03212870

Frank, T. D., Daffertshofer, A., Peper, C. E., Beek, P. J., & Haken, H. (2000). Towards a comprehensive theory of brain activity : Coupled oscillator systems under external forces. *Physica D*, *144*, 62-86.

Fries, P. (2001). Modulation of Oscillatory Neuronal Synchronization by Selective Visual Attention. *Science*, *291*(5508), 1560-1563. doi:10.1126/science.1055465

Jirsa, V. K., & Haken, H. (1997). A derivation of a macroscopic field theory of the brain from the quasi-microscopic neural dynamics. *Physica D: Nonlinear Phenomena*, *99*(4), 503-526. doi:10.1016/S0167-2789(96)00166-2

Jirsa, V., & Haken, H. (1996). Field Theory of Electromagnetic Brain Activity. *Physical review letters*, *77*(5), 960-963. Retrieved from http://www.ncbi.nlm.nih.gov/pubmed/10062950

Kastner, S. (1998). Mechanisms of Directed Attention in the Human Extrastriate Cortex as Revealed by Functional MRI. *Science*, *282*(5386), 108-111. doi:10.1126/science.282.5386.108

Kastner, Sabine, & Ungerleider, L. G. (2000). Mechanisms of visual attention in the human cortex. *Annual review of neuroscience*, *23*, 315-341.

Kelly, S. P., Lalor, E. C., Reilly, R. B., & Foxe, J. J. (2006). Increases in alpha oscillatory power reflect an active retinotopic mechanism for distracter suppression during sustained visuospatial attention. *Journal of neurophysiology*, *95*(6), 3844-51. doi:10.1152/jn.01234.2005

Luck, S. J., Chelazzi, L., Hillyard, S. A., & Desimone, R. (1997). Neural Mechanisms of Spatial Selective Attention in Areas V1, V2, and V4 of Macaque Visual Cortex. *J Neurophysiol*, *77*(1), 24-42. Retrieved from http://jn.physiology.org/cgi/content/abstract/77/1/24

Mountcastle, V. (1997). The columnar organization of the neocortex. *Brain*, *120*(4), 701-722. doi:10.1093/brain/120.4.701

Nunez, P L. (2000). Toward a quantitative description of large-scale neocortical dynamic function and EEG. *The Behavioral and brain sciences*, *23*(3), 371-98; discussion 399-437. Retrieved from http://www.ncbi.nlm.nih.gov/pubmed/11301576

Nunez, P. (1981). *Electrical fields of the brain*. New York: Oxford University Press.

Nunez, Paul L. (1995). *Neocortical dynamics and human EEG rhythms.* Oxford University Press.

Regan, D. (1977). Steady-state evoked potentials. *Journal of the Optical Society of America*, *67*(11), 1475. OSA. doi:10.1364/JOSA.67.001475

Reynolds, J. H., Chelazzi, L., & Desimone, R. (1999). Competitive mechanisms subserve attention in macaque areas V2 and V4. *The Journal of neuroscience : the official journal of the Society for Neuroscience*, *19*(5), 1736-53. Society for Neuroscience. Retrieved from http://www.jneurosci.org/content/19/5/1736.full

Rihs, T. a, Michel, C. M., & Thut, G. (2007). Mechanisms of selective inhibition in visual spatial attention are indexed by alpha-band EEG synchronization. *The European journal of neuroscience*, *25*(2), 603-10. doi:10.1111/j.1460-9568.2007.05278.x

Sauseng, P., Klimesch, W., Stadler, W., Schabus, M., Doppelmayr, M., Hanslmayr, S., Gruber, W. R., et al. (2005). A shift of visual spatial attention is selectively associated with human EEG alpha activity. *The European journal of neuroscience*, *22*(11), 2917-26. doi:10.1111/j.1460-9568.2005.04482.x

Shaw, M. L., & Shaw, P. (1977). Optimal allocation of cognitive resources to spatial locations. *Journal of Experimental Psychology: Human Perception and Performance,*, *Vol 3*(2), 201-211.

Spitzer, H., & Richmond, B. J. (1991). Task difficulty: ignoring, attending to, and discriminating a visual stimulus yield progressively more activity in inferior temporal neurons. *Experimental Brain Research*, *83*(2). doi:10.1007/BF00231157

Spitzer, H., Desimone, R., & Moran, J. (1988). Increased attention enhances both behavioral and neuronal performance. *Science*, *240*(4850), 338-340. doi:10.1126/science.3353728

Sylvester, C. M., Jack, A. I., Corbetta, M., & Shulman, G. L. (2008). Anticipatory suppression of nonattended locations in visual cortex marks target location and predicts perception. *The Journal of neuroscience : the official journal of the Society for Neuroscience*, *28*(26), 6549-56. doi:10.1523/JNEUROSCI.0275-08.2008

Thorpe, S., D'Zmura, M., & Srinivasan, R. (2012). Lateralization of frequency-specific networks for covert spatial attention to auditory stimuli. *Brain topography*, *25*(1), 39-54. Springer New York. doi:10.1007/s10548-011-0186-x

Thut, G., Nietzel, A., Brandt, S. a, & Pascual-Leone, A. (2006). Alpha-band electroencephalographic activity over occipital cortex indexes visuospatial attention bias and predicts visual target detection. *The Journal of neuroscience : the official journal of the Society for Neuroscience*, *26*(37), 9494-502. doi:10.1523/JNEUROSCI.0875-06.2006

Traub, R D, Jefferys, J. G., & Whittington, M. a. (1997). Simulation of gamma rhythms in networks of interneurons and pyramidal cells. *Journal of computational neuroscience*, *4*(2), 141-50. Retrieved from http://www.ncbi.nlm.nih.gov/pubmed/9154520

Traub, Roger D, Bibbig, A., LeBeau, F. E. N., Cunningham, M. O., & Whittington, M. A. (2005). Persistent gamma oscillations in superficial layers of rat auditory neocortex: experiment and model. *The Journal of physiology*, *562*(Pt 1), 3-8. doi:10.1113/jphysiol.2004.074641

Wilson, H. R., & Cowan, J. D. (1972). Excitatory and inhibitory interactions in localized populations of model neurons. *Biophysical journal*, *12*(1), 1-24. Elsevier. doi:10.1016/S0006-3495(72)86068-5

Wilson, H. R., & Cowan, J. D. (1973). A mathematical theory of the functional dynamics of cortical and thalamic nervous tissue. *Kybernetik*, *13*(2), 55-80. Retrieved from http://www.ncbi.nlm.nih.gov/pubmed/4767470

Worden, M. S., Foxe, J. J., Wang, N., & Simpson, G. V. (2000). Anticipatory biasing of visuospatial attention indexed by retinotopically specific alpha-band electroencephalography increases over occipital cortex. *The Journal of neuroscience : the official journal of the Society for Neuroscience*, *20*(6), RC63. Retrieved from http://www.ncbi.nlm.nih.gov/pubmed/10704517

Yamagishi, N., Goda, N., Callan, D. E., Anderson, S. J., & Kawato, M. (2005). Attentional shifts towards an expected visual target alter the level of alpha-band oscillatory activity in the human calcarine cortex. *Brain research. Cognitive brain research*, *25*(3), 799-809. doi:10.1016/j.cogbrainres.2005.09.006

Yousif, N. a B., & Denham, M. (2005). A population-based model of the nonlinear dynamics of the thalamocortical feedback network displays intrinsic oscillations in the spindling (7-14 Hz) range. *The European journal of neuroscience*, *22*(12), 3179-87. doi:10.1111/j.1460-9568.2005.04496.x

APPENDIX A

I. The Basic WC Analysis

The basic dependent variables in the WC model (Wilson and Cowan 1972; Wilson and Cowan, 1973) are the *fractions of excitatory and inhibitory active cells* (action potential densities) $E(t), I(t)$, which can evidently exhibit very high frequency jitter not treated in the analysis. Rather, the WC equations are written in terms of coarse grained (in time) excitatory $\langle E(t)\rangle$ and inhibitory $\langle I(t)\rangle$ action potential densities, where the critical point $\langle E(t)\rangle, \langle I(t)\rangle = (0,0)$ is considered by WC to be an equilibrium background state occurring when $P(t) = 0$. Thus, the variables $\langle E(t)\rangle, \langle I(t)\rangle$ are allowed to take on negative values by WC, a questionable approximation to their physiological interpretation as fractions of active cells. The WC equations (1.3.1 and 1.3.2 from the 1973 paper) are

$$\begin{aligned}\tau_E \frac{d\langle E(t)\rangle}{dt} &= -\langle E(t)\rangle + \left[1 - r_E \langle E(t)\rangle\right] S_E \left[P(t) + w_{EE}\langle E(t)\rangle - w_{IE} I(t)\right] \\ \tau_I \frac{d\langle I(t)\rangle}{dt} &= -\langle I(t)\rangle + \left[1 - r_I \langle I(t)\rangle\right] S_I \left[w_{EI}\langle E(t)\rangle - w_{II}\langle I(t)\rangle\right]\end{aligned} \tag{1}$$

Here we have dropped the spatial dependence *x* of the variables and distinguished between the excitatory and inhibitory membrane time constants τ_E, τ_I. All axon propagation speeds are assumed to be infinite as in the Wilson and Cowan(1972). In addition,we only allow excitatory afferent input $P(t)$.

II. Some Issues with the original WC analysis

1. WC write*the proportion of sensitive excitatory cells* as $R_E(t) = 1 - \int_{t-r_E}^{t} E(t')dt'$. This is not dimensionally correct and leads to the dimensionally incorrect Eqs (1). The WC equation yields the incorrect result $R_E(t) \to 1$ as the refractory period $r_E \to 0$. The correct expression is

$$R_e(t) = 1 - \frac{1}{r_e}\int_{t-r_e}^{t} E(t')dt' \qquad (2)$$
$$R_e(t) \to 1 - E(t) \text{ when } r_e \to 0$$

The excitatory and inhibitory integrals should have been divided by the refractory times r_e, r_i, equivalent to setting $r_e, r_i = 1$ in Eqs (1) which is commonly done in simulations using this model (Yousif & Denham, 2005).

2. Negative values of $\langle E(t)\rangle, \langle I(t)\rangle$ are also not realistic physiology for essentially the same reason. During times when $E(t), I(t) < 0$, $R_e(t), R_i(t) > 1$, which is not consistent with realistic physiology since the latter are defined as the fraction of total cells that are available to produce new action potentials. In the modified model presented here $\langle E(t)\rangle, \langle I(t)\rangle \geq 0$ for $-\infty < t < +\infty$.

3. WC choose sigmoid response functions such that $S_e(0) = S_i(0) = 0$ to force $(0,0)$ to be an equilibrium point. In so doing, these tissue response functions can become negative, a

physiological impossibility. In the following modified analysis, these conditions are replaced with

$$S_e[P(t),\langle E(t)\rangle,\langle I(t)\rangle]\geq 0$$
$$S_i[\langle E(t)\rangle,\langle I(t)\rangle]\geq 0 \qquad (3)$$

4. WC interpret μ (or τ_e,τ_i) as a single membrane time constant. Based on the classic solution of the cable equation and the distribution of excitatory synapses on dendrites and inhibitory synapses near cell bodies and the increased knowledge of a wide variety of te and ti we must consider cases $\tau_e \neq \tau_i$.

III. A modified version of the WC analysis

Define the nondimensional time $t_1 = \frac{t}{\tau_e}$ and time constant ratio $A = \frac{\tau_i}{\tau_e}$ so that with rescaled variables Eqs (1) become

$$\frac{d\langle E\rangle}{dt_1} = -\langle E\rangle + \left(1-\langle E\rangle\right) S_E\left(P + w_{EE}\langle E\rangle - w_{IE}\langle I\rangle\right)$$
$$A\frac{d\langle I\rangle}{dt_1} = -\langle I\rangle + \left(1-\langle I\rangle\right) S_I\left(w_{EI}\langle E\rangle - w_{II}\langle I\rangle\right)$$

(7)

Here the nondimensional parameter $A = \frac{\tau_i}{\tau_e}$ may range from somewhat less than one to as high as 5. For convenience we drop the subscript 1 on the nondimensional time variable.

Introduce the new dependent variables $X_E(t), X_I(t)$, which provide perturbations about the critical point (E_0, I_0)

$$\begin{aligned} \langle E(t) \rangle &= E_0 + X_E(t) \\ \langle I(t) \rangle &= I_0 + X_I(t) \end{aligned} \tag{8}$$

I will assume here that the input function $P(t)$ is exclusively excitatory such that $P(t) \geq 0$ at all times. The following conditions follow from the variable definitions

$$\begin{aligned} 0 &\leq E_0 + X_E(t) \leq 1 \\ 0 &\leq I_0 + X_I(t) \leq 1 \end{aligned}$$

(9)

Equations (7) then yield

$$\begin{aligned} \frac{dX_E}{dt} &= -E_0 - X_E + (1 - E_0 - X_E) S_E \left[P + w_{EE}(E_0 + X_E) - w_{IE}(I_0 + X_I) \right] \\ A\frac{dX_I}{dt} &= -I_0 - X_I + (1 - I_0 - X_I) S_i \left[w_{EI}(E_0 + X_E) - w_{II}(I_0 + X_I) \right] \end{aligned}$$

(10)

The sigmoid functions are to be chosen such that (E_0, I_0) is a critical point when $P(t) = 0$. Thus, we choose the following sigmoid tissue response functions

$$S_I\left[w_{EI}(E_0+X_E)-w_{II}(I_0+X_I)\right]=\frac{1}{1+\exp\left[-w_{EI}(E_0+X_E)+w_{II}(I_0+X_I)+K_I\right]}$$

(11)

$$S_E\left[w_{EE}(E_0+X)-w_{IE}(I_0+Y)\right]=\frac{1}{1+\exp\left[-w_{EE}(E_0+X_E)+w_{ie}(I_0+X_I)+K_E\right]} \qquad (12)$$

The constants K_E, K_I determine the range of the response functionsduring oscillations about fixed points. This choice of the forms of the sigmoid response functions insures that 1) (E_0, I_0) or $(X,Y)=(0,0)$ is a critical point and 2) $0 \le S_e \le 1$ and $0 \le S_i \le 1$. Substitution of Eqs (11) and (12) into Eqs (10) and setting $X(t)=Y(t)=0$ yields the sigmoid constants in terms of the critical point

$$K_I = w_{EI}E_0 - w_{II}I_0 + Log\left[\frac{1}{I_0}-2\right]$$

(13)

$$K_e = w_{ee}E_0 - w_{ie}I_0 + Log\left[\frac{1}{E_0}-2\right] \qquad (14)$$

Substitution of Eqs (13) and (14) into Eqs (11) and (12) yields

$$S_I\left[w_{EI}(E_0+X_E)-w_{II}(I_0+X_I)\right]=\frac{1}{1+\left(\frac{1}{I_0}-2\right)\exp\left(-w_{EI}X_E+w_{II}X_I\right)} \quad I_0<\frac{1}{2} \qquad (15)$$

$$S_E\left[w_{EE}(E_0+X_E)-w_{IE}(I_0+X_I)\right]=\frac{1}{1+\left(\frac{1}{E_0}-2\right)\exp\left(-w_{EE}X_E+w_{IE}X_I\right)}\quad E_0<\frac{1}{2} \qquad (16)$$

IV. Phase Plane Analysis

We assume $w_{II}\cong 0$ in all of the following analyses. In simulations that include w_{II} the effect is only to set the activity level of the system and has no significant influence on the dynamics. The first step in the analysis of Eqs (10) is to find the nature of the critical point $(0,0)$. To accomplish this we expand the functions $F(X,Y)$ and $G(X,Y)$ about $(0,0)$, where these functions are the expressions on the right sides of Eqs (10), that is

$$\begin{aligned}F(X,Y)&=-E_0-X+\left(1-E_0-X\right)S_e\left[P+w_{ee}(E_0+X)-w_{ie}(I_0+Y)+K_e(E_0,I_0)\right]\\ G(X,Y)&=\frac{1}{A}\left\{-I_0-Y+\left(1-I_0-Y\right)S_i\left[w_{ei}(E_0+X)+K_i(E_0,I_0)\right]\right\}\end{aligned} \qquad (17)$$

Taylor expansion about the critical point $(0,0)$ yields equations of the general form

$$\begin{aligned}\frac{dX}{dt}&=F(X,Y)\cong F(0,0)+\left(\frac{\partial F}{\partial X}\right)_0 X+\left(\frac{\partial F}{\partial Y}\right)_0 Y\equiv aX+bY\\ \frac{dY}{dt}&=G(X,Y)\cong G(0,0)+\left(\frac{\partial G}{\partial X}\right)_0 X+\left(\frac{\partial G}{\partial Y}\right)_0 Y\equiv cX+dY\end{aligned} \qquad (18)$$

But, here we have forced $F(0,0) = G(0,0) = 0$ by proper choice of the constants K_E, K_I in Eqs (13) and (14). The partial derivatives are evaluated at $(0,0)$ yielding the parameters (a,b,c,d). Equations (18) then consist of two first order linear equations governing the dynamic behavior of the nonlinear system close to $(0,0)$. Define the parameters $\beta = a + d$ and $\gamma = ad - bc$; the eigenvalues $\lambda_{1,2}$ of the linear system satisfy $\lambda^2 - \beta\lambda + \gamma = 0$ with solution

$$\lambda_{1,2} = \frac{1}{2}\left(\beta \pm \sqrt{\beta^2 - 4\gamma}\right) \tag{19}$$

We are mainly interested in oscillatory solutions about the critical point $(0,0)$; that is, stable limit cycle solutions These are expected when $(0,0)$ is an *unstable* spiral, which occurs when $\beta > 0$ and $\beta^2 < 4\gamma$. By contrast, stable spirals result in damped oscillations. Saddle points and nodes result in non-oscillatory solutions (stable or unstable).

Consider the following example with $E_0 = I_0$. The critical point (E_0, I_0) is unstable if the following condition is met

$$w_{ee} > \frac{A+1}{AE_0\left(1-2E_0\right)} \quad 0 < E_0 < \frac{1}{2} \tag{20}$$

Note that $A = \frac{\tau_I}{\tau_E}$ so if inhibitory time constants are much shorter than excitatory time constants, larger values of w_{EE} are required to produce linear instability. For the physiologically interesting range $0.1 < E_0 < 0.4$ and $A = 1$, all $w_{EE} > 25$ cause the fixed point to be unstable.

For the case $E_0 = I_0$ and $A = 1$, the fixed point is a spiral if

$$w_{ee} < 2\sqrt{w_{ie} w_{ei}} \tag{21}$$

By combining Eqs (20) and (21) we find the necessary (but possibly not sufficient) conditions for a stable limit cycle about (E_0, E_0) when $A = 1$, that is

$$\frac{2}{E_0(1-2E_0)} < w_{ee} < 2\sqrt{w_{ie} w_{ei}} \tag{22}$$

If this condition is met, the corresponding spiral frequency is

$$\omega_{spiral} = N(E_0)\sqrt{4 w_{ie} w_{ei} - w_{ee}^2} \tag{23}$$

Here the numerical factor lies in the range $0.00790 < N(E_0) < 0.0294$ if $0.1 < E_0 < 0.4$.

An *unstable* spiral point at (E_0, I_0) suggests a likely *stable limit cycle*, but the limit cycle

frequency will not generally equal the (linear) spiral frequency. If w_{ee} exceeds the upper limit in Eq (22) an unstable node or saddle point will occur. In this case the solutions $X(t), Y(t)$ are likely to grow beyond physiologically realistic ranges, implying that the basic equations are no longer valid.

Chapter 5. Summary and Conclusions

In summary of the body of work presented in this document, we have obtained a series of results which bear on the nature of attentional signaling within the brain. Our results touch on multiple related aspects of this signaling, including the spatial organization of attention networks within the brain, the signature frequency bands in which these signals operate, the dynamic evolution of these signals in response to cueing and attentional switching, the nature of the interaction of these signals with sensory cortical populations, and the plausibility of an explicit mechanism for their interactions within a formal mathematical framework. More specifically, our results can be enumerated as follows:

1. Deployment and maintenance of spatial attention in a cued direction reliably induces hemispheric lateralization events in the alpha, mu, beta, and theta frequency bands.

2. The pattern of lateralization events consistently reflects the direction of attentional orientation, with greater levels of activity *in all bands* observed over areas ipsilateral to the cued location (or direction of the switch).

3. The effects of attention on responses evoked by a visual stimulus are preceded by desynchronization of alpha and mu-band activity over the hemisphere contralateral to the switch, consistent with a picture in which such desynchronization actively facilitates gains in the attended response.

4. Complimentary increases in these same alpha and mu band signals over ipsilateral areas occur only after the attentional modulations of stimulus evoked activity have unfolded, suggesting theories which treat these signals as a mechanism for active suppression may need to be reconsidered.

5. With regard to our cortical population model, which explicitly treats the effects of top-down global signaling via the modulation of background state activity about which the population oscillates-

(a) Low-frequency modulation of the background state parameter has the effect of suppressing gamma-band oscillations produced by the model.

(b) In response to attentional modulation similar to that observed in our previous experiment, the model reproduces the directionality of observed gains/suppressions of the steady-state responses, but fails to account for the relative timing of these effects.

Discusssion

Before concluding, some consideration of the theoretical interpretation of our results is warranted. First off, in our initial auditory attention experiment, the patterns of lateralized scalp activity we observed in the alpha, mu, and beta bands, included bilateral foci over both symmetric parietal areas as well as symmetric sensorimotor areas. We speculated that this activity may represent the lateralization of motor signals related to the deployment of attentional orientation, that is, an intended motor program which prepares the subject to orient towards the anticipated stimulus. However, we did not observe this same second pair of foci in our visual attention experiment. One possible reason for this might lie in the nature of our stimulus configurations. In the auditory experiment, the attended/unattended speakers were situated at 45 degrees with respect to the subject's vertical meridian. This was a vastly more peripheral configuration that our visual stimuli, which were only separated by a few degrees of visual angle. Thus the observed difference in patterning of scalp activity could be explained in the context of premotor theory as the

result of the highly peripheral configuration prompting stronger, more coordinated motor plans for intended orientation.

Finally, in both experiments we observed an early significant theta-band effect that preceded in time all other observed effects. We have speculated that this activity may represent a coordinating signal which dynamically updates/reorganizes synchronous oscillations between the attention network and sensory cortices in response to the cue or switch. However, in our first experiment this effect exhibited early lateralization whereas in our second experiment the effect was initially in the same direction over both hemispheres, and only much later did lateralization in the signal develop. We argue this to be a simple consequence of the difference between attentional cueing and attentional switching. In the case of the cue, theta activity showed early lateralization because there were no populations actively processing stimuli which required dynamic reorganization within the functional attention network. In absence of such active signals, early expectancy related low-frequency desynchronization was dominant. In contrast, attentional switching may require both active engagement of the switched-to populations, as well as active disengagement of the switched-from populations, both of which may be expected to occur via theta band signaling. In this case no lateralization patterns would be observed. Rather, initial global increases in theta over both hemispheres would result.

I would like to close with a wildly speculative description of spatial attention signaling which is consistent with the results of this work. In this picture, attentional switches result in dynamic reorganization of synchronous oscillations between the distributed fronto-parietal attention network and sensory populations whose identity is determined by the output of motor computations reflecting intended orientation. This

interareal synchrony, mediated by active theta signals, has the effect of decoupling the newly reorganized network from global endogenous low-frequency activity, thereby resulting in enhanced bottom up efficacy of local activity in the newly incorporated sensory populations. Finally, the interactions suggested by this emerging picture underscore the need for a comprehensive local/global model capable of treating these interactions and making testable predictions within the context of human EEG/MEG studies.